UNITED STATES DEPARTMENT OF COMMERCE
HARRY L. HOPKINS, Secretary
NATIONAL BUREAU OF STANDARDS
Lyman J. Briggs, Director

✦

Journal of Research

of the

National Bureau of Standards

✦

Volume 23, Number 6
December 1939

[Published with approval of the Director of the Budget]

UNITED STATES
GOVERNMENT PRINTING OFFICE
WASHINGTON : 1939

For sale by the Superintendent of Documents, Washington, D. C. - - - - - - Price 30 cents
$3.50 per year on subscription

The prices of the separate Research Papers appearing in this JOURNAL are given on the front cover page. If 100 or more copies of any separate are ordered, a discount of 25 percent is allowed. Those who desire copies of separate Research Papers should send their orders and remittances without delay to the Superintendent of Documents, U. S. Government Printing Office, Washington, D. C. This will aid him to determine the number of copies to be printed for sale. Research Papers are not printed from electrotypes, and usually no more reprints can be had when the first and only printing is exhausted.

U. S. Department of Commerce National Bureau of Standards

RESEARCH PAPER RP1259

Part of Journal of Research of the National Bureau of Standards, Volume 23, December 1939

PHYSICAL PROPERTIES OF PURIFIED 2,2,3-TRIMETHYLPENTANE

By Donald B. Brooks, Frank L. Howard, and Hugh C. Crafton, Jr.

ABSTRACT

A sample of 2,2,3-trimethylpentane prepared synthetically was purified by fractionation in an automatically controlled 6-m helix-packed column. The resulting product was of such purity that a good freezing point could be obtained. The freezing point and melting point were determined in an apparatus in which the rate of cooling or heating could be accurately controlled. Other properties measured included the boiling point and its variation with pressure, and refractive index and density and their variations with temperature.

CONTENTS

		Page
I.	Introduction	637
II.	Preparation of 2,2,3-trimethylpentane	637
III.	Apparatus	638
IV.	Physical properties	639
V.	References	641

I. INTRODUCTION

In connection with an investigation of paraffin hydrocarbons as aviation fuel constituents being conducted at the National Bureau of Standards for the National Advisory Committee for Aeronautics, the Navy Bureau of Aeronautics, and the Army Air Corps, a sample of 2,2,3-trimethylpentane was prepared synthetically, and purified by fractionation in an automatically controlled 6-m helix-packed column. The resulting product was of such purity that a good freezing point could be obtained.

II. PREPARATION OF 2,2,3-TRIMETHYLPENTANE

Methylethyl-*tertiary*-butylcarbinol was prepared from *tertiary*-butyl chloride and methylethylketone, by the Grignard reaction, in yields varying from 21 to 28 percent. *Tertiary*-butyl chloride was obtained from the Eastman Kodak Co., magnesium and ether from the Mallinckrodt Chemical Works, and methylethylketone from Eimer and Amend. All materials were used without further purification. The carbinol distilled at 74° to 76° C at 40-mm Hg pressure.

Methylethyl-*tertiary*-butylcarbinol was refluxed with about 0.5 percent of iodine, and the mixture of resulting olefins was recovered by distillation, dried with calcium chloride, and refluxed with sodium and fractionated in a 100- by 2-cm column packed with Pyrex helices. The portion boiling from 107° to 114° C was collected, and apparently

contained the two isomeric compounds, 2,2,3-trimethylpentene-3, 80 percent, and 2,3,3-trimethylpentene-1, 20 percent, as found by Whitmore and Laughlin [1].[1]

The mixture of olefins was hydrogenated at a hydrogen pressure of 2,000 lb/in.[2] at 130° C in the presence of Raney nickel catalyst. The product was washed with concentrated sulfuric acid, water, 5-percent sodium bicarbonate solution, and then three times with water. It was then dried over calcium chloride, distilled from sodium, and fractionated in a 600- by 4-cm column packed with Pyrex helices. The total charge was 1,700 ml. The still was operated under total reflux until the head temperature, which was measured with a platinum-resistance thermometer, had become constant within 0.01° C. A fraction was then taken by drawing off the 78 ml of liquid in the reflux receiver, and the process was repeated. Distillation data and the refractive indices of the fractions are given in table 1. On the basis of the distillation data, fraction 8 was considered the purest sample of 2,2,3-trimethylpentane, and its physical constants were measured. The residue (530 ml) was saved for future isolation of 2,3,3-trimethylpentane.

TABLE 1.—*Fractionation data*

Fraction number	Reflux time	Head temperature	Barometric pressure	Boiling point at 760 mm Hg	Refractive index at 20°C
	Hours	°C	*mm* Hg	°C	
1	6.7	107.5			1.4017
2	4.0				1.4024
3	7.0	109.57	758.13	109.66	1.4025
4	7.0	109.61	756.98	109.76	1.4030
5	6.0				1.4030
6	6.0				1.4030
7	4.0	109.78	759.25	109.82	1.4030
8	8.0	109.76	759.00	109.81	1.4029
9	6.0				1.4029
10	6.0				1.4029
11	6.0	109.67	757.08	109.81	1.4029
12	0.5				1.4029
13	.5				1.4030
14	.5				1.4029
Residue					1.4050

III. APPARATUS

A glass-stoppered Pyrex flask of somewhat over 50-ml capacity was used in determining density. A portion of the neck of this flask was constricted to 2.5-mm diameter, and a line was etched on the neck at the middle of this constricted portion. In making a density determination, the flask was filled above this line and placed in a bath maintained at a constant temperature within ±0.01° C. When the meniscus of the liquid in the flask showed no further movement under a microscope, the excess liquid was removed, leaving the meniscus a few tenths of a millimeter above the etched line. The neck of the flask was then aerated to remove liquid film, and the final adjustment was made, by removing liquid with a very fine capillary tube while observing the meniscus under a microscope. The flask was then removed from the bath, immersed in dry acetone, dried, and weighed. The liquid was then removed, the flask dried internally, and again

[1] Figures in brackets indicate the literature references at the end of this paper.

weighed. All weighings were made in a dry atmosphere, using calibrated weights, and were corrected to vacuum. The volume of the flask was similarly determined, using air-free distilled water, at 20° C and at 25° C.

The refractive index of the material was determined on an Abbé refractometer (Valentine) graduated to 0.0001. This instrument was immediately calibrated by measuring the index of refraction of a standard sample of 2,2,4-trimethylpentane [2,3], the refractive index of which was 1.39146 at 20° C.

The boiling point was measured while the sample was being distilled through a 10-inch jacketed column, the jacket being externally heated electrically to a temperature such that slight, and only slight, condensation occurred in the column. A jacket temperature about 3° C below the boiling point of the sample was generally found to be satisfactory. A layer of asbestos and a layer of aluminum foil surrounded the heating coil, it having been found by experience to be necessary to eliminate external radiation. A platinum-resistance thermometer inserted in the column was used for the temperature measurements. Atmospheric pressure was measured on a Fortin-type barometer, graduated to 1 mm Hg, and read by vernier to 0.01 mm Hg. The *ensemble* was calibrated each day by measuring the boiling point of distilled water. Earlier work [3] showed that with this procedure the reproducibility averaged about 0.009° C. It is believed that subsequent improvements in technique have materially reduced this error.

The freezing-point determinations were made by means of the apparatus described in a former paper [3], which was modified to facilitate control of the rate of cooling. A Pyrex tube on which had been wound 160 ohms of No. 32 Calido resistance wire was placed inside the Dewar flask, which was immersed in liquid air. The voltage applied to the resistance wire was controlled in the range 15 to 30 volts by a variable transformer and was measured by a voltmeter graduated to 0.2 volt. By this means it was possible to preselect accurately at—110° C any rate of temperature change from 0.8° C per minute cooling to over 1.5° C per minute heating. Tests have shown that with this device a cooling rate of 0.12° C per minute could be maintained with a deviation averaging less than 2 percent and not exceeding 5 percent. Although independently devised, this apparatus is similar in principle and in performance to that described by Roper [5].

A Mueller bridge having coils maintained continuously at 35° C and reading directly to 0.0001 ohm was used in conjunction with the 25-ohm platinum-resistance thermometer on both boiling- and freezing-point tests. Both the bridge and the thermometer were calibrated frequently, the latter in accordance with the procedure specified for the International Temperature Scale.

IV. PHYSICAL PROPERTIES

The distillation data obtained on the sample in one of the two boiling-point determinations, and corrected to a pressure of 760 mm Hg, are shown in figure 1. Taking as the boiling point the average of the temperatures observed in readings from 20 to 80

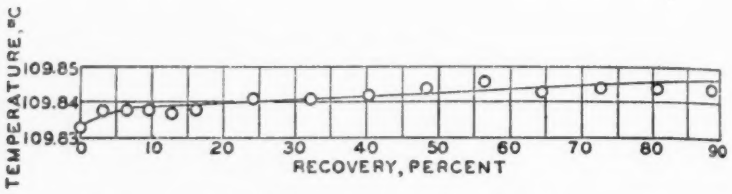

FIGURE 1.—*Distillation of purified 2,2,3-trimethylpentane.*

percent distilled, the values for the two determinations were as follows:

Observed boiling point	Barometric pressure
°C	*mm* Hg
109. 794	758. 99
109. 451	751. 88

The value of dT/dP was computed from the equation

$$\log P = A - B/T,$$

the constants A and B being evaluated from the data given above.

Figure 2 shows one of the freezing and melting curves obtained for the sample of 2,2,3-trimethylpentane. Considerable uncertainty

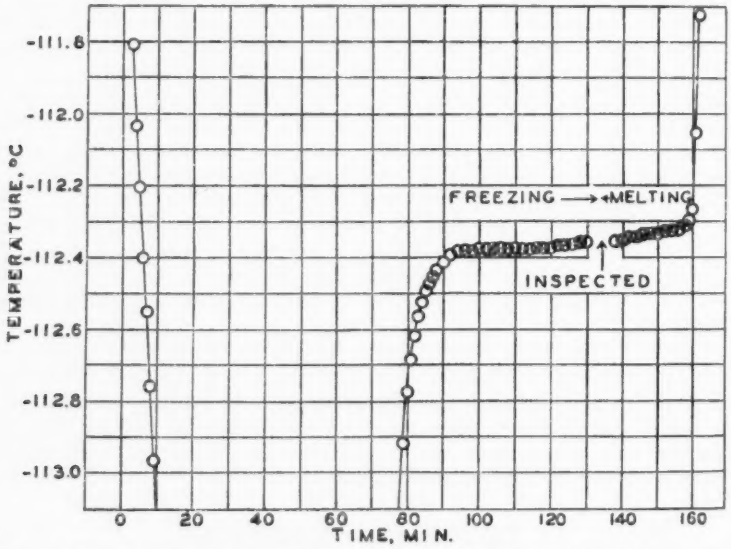

FIGURE 2.—*Freezing and melting curves of purified 2,2,3-trimethylpentane.*

exists as to the freezing point, since it was necessary to undercool the sample several degrees for about 1½ hours before it would freeze. The values obtained for the freezing points were −112.36° and −112.38° C, and for the melting points −112.34° and −112.31° C.

Refractive-index measurements at two temperatures gave 1.40316 at 19.38° C and 1.40005 at 25.67° C. Density measurements were made at 20° C and 25° C.

Properties of 2,2,3-trimethylpentane calculated where necessary to standard conditions are given in table 2, together with values for comparison taken from Egloff's critical review [4] of the literature.

Owing to the fact that the refractometer and the barometer were not calibrated when taking the data shown in table 1, the refractive-index and boiling-point values given in the two tables differ slightly.

TABLE 2.—*Physical properties of 2,2,3-trimethylpentane*

Reference	Melting point	Boiling point at 760 mm Hg	$\frac{dT}{dP}$	Refractive index		$\frac{dn}{dt}$	Density		$\frac{d\rho}{dt}$
				n_D^{20}	n_D^{25}		ρ^{20}	ρ^{25}	
	°C	°C	deg/mm Hg			per deg	g/ml	g/ml	g/ml deg
Present work [a]	−112.32	109.843	0.0480	1.40285	1.400038	−0.000494	0.71617	0.71218	−0.000797
Egloff [4]	"Glassy at low temperatures."	110.3		1.4032			.7162		

[a] The uncertainty of each value is believed not to exceed a few units in the last decimal place given.

V. REFERENCES

[1] F. C. Whitmore and K. C. Laughlin, J. Am. Chem. Soc. **54,** 4011 (1932).
[2] Donald B. Brooks, Robetta B. Cleaton, and Frank R. Carter, J. Research NBS **19,** 319 (1937) RP1027.
[3] Donald B. Brooks, J. Research NBS **21,** 847 (1938) RP1160.
[4] Gustav Egloff, Physical Constants of Hydrocarbons, **1,** 55 (Reinhold Publishing Corporation, New York, N. Y., 1939).
[5] Edwin E. Roper, J. Am. Chem. Soc. **60,** 1693 (1938).

WASHINGTON, October 20, 1939.

U. S. Department of Commerce National Bureau of Standards

RESEARCH PAPER RP1260

Part of Journal of Research of the National Bureau of Standards, Volume 23, December 1939

HEAT OF FUSION OF ICE. A REVISION

By Nathan S. Osborne

ABSTRACT

The results of measurements of the heat of fusion of ice made at the National Bureau of Standards and published in 1913 and 1915 have been revised by one of the original experimenters, usng more recent data for the heat capacity of water, which is involved in the calculations. The revised value, obtained by weighting the results of four independent series of measurements and expressed in terms of the present calorimetric unit of energy, is

333.5 INTERNATIONAL JOULES PER GRAM

with an estimated uncertainty of 0.2 int. j/g.

The heat of fusion of ice was determined at the National Bureau of Standards about twenty-five years ago [1, 2][1]. The reductions of the observations involved the heat capacity of water, for which the values used were chosen from the data then available. Since more accurate values for the heat capacity of water are now available [3], the values for the heat of fusion of ice are subject to revision. It has been suggested that such a revision, having the benefit of the interpretation of the experimenters themselves, would be helpful by combining all of the results into a single definitive value expressed in terms of the present calorimetric unit of energy, the international joule.

The value of heat capacity of water does not enter as a direct factor but affects parts of the calorimetric process depending on which one of the several methods was used in the two original investigations [1, 2]. This work was done at a time when it was not fully appreciated that the use of calories as heat units would complicate not only the original reductions but future revisions as well. For this reason the following description of the revisions is likely to appear complicated.

In these two investigations three essentially different methods were used. In the first investigation, published in 1913, a calorimeter with stirred water as the calorimetric medium was used. A controlled jacket permitted heat leak to be accounted for. Two series of measurements were made by the electric-heating method and one series by the method of mixtures. The samples of ice were precooled, so that initial temperatures were known and accounted for in the reductions. The corrections which can be made now to the data as assembled in tables 3 and 5 of the original paper [1] are to reevaluate the heat supplied to bring the ice to 0° C and to bring the water formed from 0° C to the final temperatures of the various experiments.

[1] Figures in brackets indicate the literature references at the end of this paper.

For the ice correction a tentative value of 0.52 cal/g-° C was taken at the time as an approximation to the specific heat of ice in the range from 0° to −3.78° C. In the second investigation, published in 1915 [2], the heat capacity of ice was measured in international joules per gram degree and was finally expressed by the equation

$$C_p = 0.5057 + 0.001863t \text{ cal}_{20}/\text{g-° C},$$

where C_p is specific heat at 1-atm pressure, t is centigrade temperature, and the calorie$_{20}$ was taken as equal to 4.183 int. j. For use in the present revision, this equation is now converted back to international joules thus

$$C_p = 2.1153 + 0.00779t \text{ int. j/g-° C}.$$

For recomputing the water correction, the table given in a recent publication by Osborne, Stimson, and Ginnings [3] is used (table 6, page 238).

The heat supplied in these two series by the electric method was furnished by current in an electric-heating coil, and was measured by use of a potentiometer, a standard cell, and a standard resistor, thus obtaining the power, which, with the observed time, gave the heat added in international joules. This energy per gram of ice as originally corrected for heat leak, temperature change of calorimeter, stirring energy, and heat capacity of the ice holder is given in column 2 of tables 1 and 2, expressed in a nominal 15-degree calorie of 4.187 int. j. In column 3 these data are converted back to international joules per gram. The heat per gram absorbed by the melted ice, as revised by the new heat-capacity data, is given in column 4, and the heat absorbed by the ice from the initial temperature to 0° C is given in column 5. The corrections of −1.52 and −7.94 int. j/g for −0.72° and −3.78°, respectively, in tables 1 and 2 are next applied giving the final values for heat of fusion in column 6.

TABLE 1.—*Revision of table 3 (1918)*

Final temperature, t_2	Ice at −0.72 to water at t_2		Water 0 to t_2	Ice at −0.72 to water at 0	Ice at 0 to water at 0
°C	cal_{15}/g	*Int. j/g*	*Int. j/g*	*Int. j/g*	*Int. j/g*
15.12	95.15	398.39	63.57	334.82	333.30
14.83	94.92	397.43	62.36	335.07	333.55
14.60	94.67	396.38	61.40	334.98	333.46
15.79	95.88	401.45	66.37	335.08	333.56
15.59	95.67	400.57	65.54	335.03	333.51
14.89	94.97	397.64	62.61	335.03	333.51
14.87	94.96	397.60	62.53	335.07	333.55
14.96	94.98	397.68	62.90	334.78	333.26
23.81	103.91	435.07	99.91	335.16	333.64
23.67	103.75	434.40	99.32	335.08	333.56
15.53	95.60	400.28	65.29	334.99	333.47
15.76	95.81	401.16	66.25	334.91	333.39
15.65	95.72	400.78	65.79	334.99	333.47
Mean of group •					333.48

• In obtaining the final mean, this value was given a weight of 4.

TABLE 2.—*Revision of table 5 (1913)*

Final temperature, t_2	Ice at −0.72 to water at t_2		Water 0 to t_2	Ice at −0.72 to water at 0	Ice at 0 to water at 0
°C	cal_{15}/g	*Int. j/g*	*Int. j/g*	*Int. j/g*	*Int. j/g*
15.36	97.00	406.14	64.58	341.56	333.62
14.81	96.49	404.00	62.27	341.73	333.79
14.88	96.54	404.21	62.57	341.64	333.70
15.09	96.75	405.09	63.44	341.65	333.71
15.86	97.50	408.23	66.66	341.57	333.63
14.80	96.45	403.84	62.23	341.61	333.67
14.81	96.47	403.92	62.28	341.64	333.70
14.90	96.60	404.46	62.65	341.81	333.87
14.93	96.61	404.51	62.77	341.74	333.80
14.82	96.46	403.88	62.32	341.56	333.62
14.76	96.43	403.75	62.06	341.69	333.75
14.71	96.35	403.42	61.86	341.56	333.62
Mean of group *					333.71

* In obtaining the final mean, this value was given a weight of 4.

TABLE 3.—*Revision of table 4 (1913)*

Final temperature t_2	Δt	Ice at −0.72 to water at t_2	$\left(\frac{C_p(NBS)}{C_p(HLC)}\right)_{t_m}$	Ice at −0.72 to water at t_2		Water 0 to t_2	Ice at −0.72 to water at 0	Ice at 0 to water at 0
°C	°C	$cal_{15}/g(HLC)$		$cal_{15}/g(NBS)$	*Int. j/g*	*Int. j/g*	*Int. j/g*	*Int. j/g*
12.02	3.110	92.09	0.9999	92.08	385.35	50.59	334.76	333.24
16.57	3.447	96.56	1.0002	96.58	404.19	69.64	.55	.03
17.02	2.946	97.05	1.0002	97.07	406.24	71.52	.72	.20
17.47	5.994	97.49	1.0003	97.52	408.12	73.40	.72	.20
18.18	5.732	98.20	1.0003	98.23	411.09	76.37	.72	.20
18.48	5.281	98.51	1.0003	98.54	412.39	77.42	.97	.51
17.88	5.759	97.88	1.0003	97.91	409.75	75.12	.63	.11
18.19	5.301	98.21	1.0003	98.24	411.18	76.41	.77	.25
Mean of groups (*)								333.21

(*) In obtaining the final mean, this value was given a weight of 4.

TABLE 4.—*Revision of table 10 (1915)*

[Anerold calorimeter]

Initial temperature, t_1	Final temperature, t_2	Water 0 to t_2			Mass of ice	Correction per gram	Correction for premelting	Heat of fusion	Revised heat of fusion (*)
		Old value	New value	New−old					
°C	°C	*Int. j*	*Int. j*	*Int. j*	*g*	*Int. j/g*	*Int. j/g*	*Int. j/g*	*Int. j/g*
−3.622	+4.746	9367.8	9410.2	42.4	468.7	−0.09	+0.11	333.14	333.16
−0.240	+4.7549	8005.1	8042.3	37.2	399.8	−.09	+1.67	332.34	333.92
−1.635	+3.602	6993.6	7035.6	42.0	460.7	−.09	+0.01	333.59	333.51

(*) In obtaining the final mean, these values were given weights of 1, 1, and 2, respectively.

In revising the data obtained by the method of mixtures, given in table 4 of the 1913 report, the first step is to reevaluate the heat taken up by the ice from its initial temperature to the final temperature of the calorimeter. This was measured by the observed change of temperature of the calorimeter when the ice was added, and was evaluated in 15-degree calories according to the table of heat capaci-

ties given by H. L. Callendar [4] in 1912. These values, as originally given, with corrections applied for heat leak, stirring energy, etc., are shown in column 3 of table 3. In column 4 the ratio is shown of the heat capacity of water according to the new NBS data to the heat capacity given by Callendar, at the mean temperature of the experiment, both in 15-degree calories.

These factors are applied to the figures in column 3, giving the figures in column 5, which are then converted in column 6 to international joules per gram by use of the equivalent from the NBS data, i. e., the heat capacity at 15° C is equal to 4.1850 int. j/g-°C. The remainder of the revision is similar to that of table 1.

In connection with the later investigation [2], three measurements of heat of fusion were made in the electrically heated heavy-copper calorimeter (aneroid). The main revision of these calculations is the revaluation of the heat taken up by the water from 0° C to t_2. The old and new values for the entire mass of water are given in columns 3 and 4 of table 4 and their differences in column 5. The corresponding corrections per unit mass of ice are given in column 7. The corrections for premelting of part of the ice, as determined in the specific-heat measurements, are given in column 8. The sum of the two corrections is applied to the original value, as given in column 9, taken directly from column 15 of the original publication. The revised values are found in column 10.

In order to deduce a single figure for the heat of fusion representing an interpretation of the entire amount of experimental data, some relative weighting of experiments or groups must be adopted. This is an arbitrary choice, based on the combined judgment of two of the original authors. Each of the first three groups of measurements in the first investigation is taken as an independent unit with a relative weight of 4. In the second investigation the first two experiments are each given a weight of one and the last a weight of two. According to this weighting, the general weighted mean is 333.48 int. j/g.

The revised figure can therefore be taken as 333.5 int. j/g, with an uncertainty of 0.2 int. j/g, which has been estimated to include both accidental and systematic errors.

---

[1] D. R. Harper 3d, and N. S. Osborne, *Latent heat of fusion of ice*, H. C. Dickinson, Bul. BS **10,** 235 (1914) S209.
[2] H. C. Dickinson and N. S. Osborne, *Specific heat and heat of fusion of ice*, Bul. BS **12,** 49 (1915–16) S 248.
[3] Nathan S. Osborne, Harold F. Stimson, and Defoe C. Ginnings, *Measurements of heat capacity and heat of vaporization of water in the range 0° to 100° C*, J. Research NBS **23,** 197 (1939) RP1228.
[4] H. L. Callendar, *On the variation of the specific heat of water with experiments by a new method.* Phil. Trans. Roy. Soc. (London) [A] **212,** 1 (1912).

Washington, October 17, 1939.

U. S. Department of Commerce National Bureau of Standards

RESEARCH PAPER RP1261

Part of Journal of Research of the National Bureau of Standards, Volume 23, December 1939

POTENTIOMETRIC METHOD FOR THE ACCURATE MEASUREMENT OF HYDROGEN-ION ACTIVITY

By Walter J. Hamer and S. F. Acree

ABSTRACT

A potentiometric method is described for measurements of hydrogen-ion activities in aqueous solutions.

Galvanic cells without liquid junctions are used. In this method hydrogen and silver-silver chloride electrodes are placed in solutions to which known amounts of either sodium or potassium chloride have been added. A detailed description is given of the equipment and experimental procedures which are necessary for precise measurements of hydrogen-ion activities. The electromotive force of the galvanic cell, on the average, is reproducible to 0.02 mv which is equivalent to 0.0003 pH unit. It is found that the electrodes function reversibly and exhibit no aging, hysteresis, or polarization effects.

It is shown how the hydrogen-ion activity may be calculated from the electromotive force by thermodynamic methods, using the Nernst equation, in which the concepts of activity and interionic attraction are incorporated.

CONTENTS

	Page
I. Introduction	647
II. Discussion of method	649
III. Description of equipment and experimental procedures	651
1. Assembly of equipment	651
2. Procedure for filling cells and bubble tubes	653
3. Preparation of solutions	654
4. Hydrogen electrodes and purification of hydrogen gas	654
5. Silver-silver chloride electrodes	655
6. Thermostat and temperature regulation	656
7. Instruments for measuring electromotive force	657
IV. Data illustrating precision of measurements	658
V. References	662

I. INTRODUCTION

The importance of the measurement and control of hydrogen-ion activities in industrial, biological, and scientific work is now firmly established. The two principal means for determining hydrogen-ion activities are the potentiometric and colorimetric methods.[1] The

[1] The conductometric and catalytic methods are supplementary. The conductance of a solution depends upon the concentration and mobility of all the ions in the solution. Therefore, it is necessary to have some detailed knowledge of the constituents of a solution and of the properties of each before any information on the hydrogen- or hydroxyl-ion activity can be obtained by the conductivity method. Likewise, in the catalytic method, it is necessary to know whether the hydrogen or hydroxyl-ion catalyzes a reaction, and if so, the relationship between the activity of the hydrogen or hydroxyl-ion and the rate of the reaction. These facts must be determined for every case and the method, therefore, is not a general or a fundamental one. In the case of other physical methods, such as the use of refractive indices of a solution, the relationship between the hydrogen- or hydroxyl-ion activity and the physical quantity measured must also be determined for each special case.

former is the basic method. In the colorimetric method, the color changes of an indicator must be correlated with a definite change in hydrogen-ion activity, and the latter change must be determined by potentiometric methods.

The potentiometric methods depend upon the use of various types of electrodes. Of these, the hydrogen electrode has been arbitrarily chosen as the standard and the potentials of all other electrodes are referred to its potential. It is assumed to give a correct measurement of hydrogen-ion activity, and has been chosen for accurate determinations of pH, which has been defined as the negative of the common logarithm of the hydrogen-ion activity [2] and is so used in this paper.

The galvanic cell which has been used for accurate determinations of pH and for standardization of the pH scale [1, 3, 4, 5, 6, 14] [3] consists of a hydrogen electrode, a buffer solution, and a calomel half-cell. This type of cell is one with a liquid junction formed by the contact of the KCl solution of the calomel half-cell and the buffer solution.

Although extensive investigations have been made and numerous papers have been written on the applications of this type of galvanic cell to the determinations of pH, considerable diversity still persists in the results obtained. For example, the pH of 0.05 molar potassium acid phthalate, most commonly employed as a standard solution having a definite pH value, has been reported to be 3.94 [2], 3.974 [3], 4.005 [4], 4.008 [5], and 4.010 [6] at 25° C, the maximum difference corresponding to 0.0042 v in the emf of the galvanic cell. The pH values reported for other solutions show similar differences. Although for many industrial processes the differences in pH values reported for potassium acid phthalate are well within the pH tolerance, these variations introduce misconceptions as to the accuracy and reproducibility obtainable with an individual pH assembly and are significant for many types of work. Furthermore, these differences indicate the lack of an establishment of a definite reference point on the pH scale or a lack of an accurate standardization of this scale. This lack of agreement is due in part to the use, by some workers, of the exact laws of thermodynamics and by others of nonthermodynamic or empirical methods of calculation; to differences in experimental technique; to the use of different values for the potential of the calomel half-cell; and to the use of different definitions for pH (footnote 2). The lack of agreement is due in larger part to use of galvanic cells with liquid junctions, which introduce into the total emf a potential whose magnitude depends upon the manner in which the junction is formed and can only be approximately calculated for any type of junction [7].

It is the purpose of this paper to describe an accurate potentiometric method for determinations of pH in which galvanic cells without liquid junctions are employed and to describe equipment and experimental

[2] pH has also been defined (1) as the negative of the common logarithm of the hydrogen-ion concentration, (2) as some value between the negative of the common logarithms of the hydrogen-ion concentration and activity, and (3) as a quantity proportional to the emf of a galvanic cell with liquid junction and termed "pH number" without regard to physical interpretation. It is generally believed that the hydrogen-ion activity is the important quantity in industrial, biological, and chemical reactions, and is, therefore, employed in this paper as the basis for the definition of pH. These other definitions have been proposed because a differentiation between activity and concentration cannot be clearly made on a thermodynamic basis. It is, however, not a question of making this differentiation but of the degree in which it can be made. Sørensen and Linderstrøm-Lang, Compt. rend. trav. lab. Carlsberg, **15**, 40 (1924) suggested using p_H for the negative of the common logarithm of the hydrogen-ion activity. Although introduction of this symbol has some justifications, its use is confusing, and it appears more logical to redefine the symbol pH than to propose new symbols.

[3] Figures in brackets indicate the literature references at the end of this paper.

technique by which measurements may be made with high precision at temperatures from 0° to 60° C. In principle, the method is similar to the one employed in recent years by Harned and associates [8] in determinations of the thermodynamic ionization constants of weak electrolytes. Although galvanic cells without liquid junctions have been used for various purposes, they have not been used for determinations of pH values,[4] or for a standardization of the pH scale. Measurements are made at the different temperatures in order to obtain information about the variation of hydrogen-ion activity values with temperature.

II. DISCUSSION OF METHOD

A silver-silver chloride and a hydrogen electrode are placed in an aqueous solution, and a known amount of either sodium or potassium chloride is added to the solution. It is necessary to add the chloride so that the silver-silver chloride electrode will function reversibly and give a reproducible potential. The silver-silver chloride electrode is chosen as the reference electrode, because it is only slightly soluble in most dilute solutions, is attacked by few materials, exhibits very little temperature hysteresis, recovers quickly from accidental concentration polarization, and its potential relative to the "normal hydrogen electrode" is known for a wide temperature range with a precision of about 0.02 to 0.05 mv [9].

This galvanic cell without liquid junction may be represented by

$$\mathrm{Pt} \mid \mathrm{H_2(g)} \mid \text{solution} + \mathrm{NaCl(or\ KCl)} \mid \mathrm{AgCl(s)} \mid \mathrm{Ag(s)},$$

in which g=gas, s=solid, and the vertical lines indicate the junction of two phases, as in the convention adopted in the International Critical Tables [10]. The emf of this cell is proportional to the activities of the hydrogen and chloride ions and is represented for 1 atmosphere of hydrogen pressure by the equation

$$E = E^\circ - \frac{RT}{F} \ln (\mathrm{H^+})(\mathrm{Cl^-}), \tag{1}$$

where E represents the measured emf; E° the "normal" electrode potential of the silver-silver chloride electrode; $(\mathrm{H^+})$ the hydrogen-ion activity; $(\mathrm{Cl^-})$ the chloride-ion activity; and R, T, and F have their usual significance. Rearranging and converting to common logarithms gives

$$\frac{(E-E^\circ)F}{2.3026\,RT} + \log (\mathrm{Cl^-}) = -\log (\mathrm{H^+}) = \mathrm{pH}, \tag{2}$$

by which the pH of the solution may be calculated, provided the activity of the chloride ion in solution is known. When the activity of the chloride ion is not known, it may be calculated by using the known concentrations of the solution, added chloride, and the theoretical equation of Debye and Hückel [11] in the form suggested by Hückel [12]. Hückel's equation is valid for a considerably wider range of concentration than is the original equation of Debye and Hückel. For example, Harned and Ehlers [9] have shown that the activity

[4] Guggenheim, J. Phys. Chem. **34**, 1758 (1930) and Hitchcock, J. Am. Chem. Soc. **58**, 855 (1936) have suggested their use in determining a quantity proportional to the hydrogen-ion "concentration"; and Hamer, Trans. Electrochem. Soc. **72**, 45 (1937) showed how galvanic cells without liquid junctions may be used in routine measurements of hydrogen-ion "concentrations."

coefficients of HCl may be represented successfully by the Hückel equation over the concentration range of 0 to 4 molal. The activity of an ion is a function of the concentration, and the ratio of the activity to the concentration is termed the activity coefficient,[5] represented by f_i.

Hence the activity of the chloride ion (Cl^-) is equal to the product of the chloride-ion concentration [Cl^-] and the activity coefficient of the chloride ion, f_{Cl}. Hückel [12], from theoretical considerations of the electrostatic forces between positive and negative ions in concentrated solutions, found that the activity coefficient of an ion is given as a function of the concentration in moles per liter by the equation

$$\log f_i = \frac{-Az_i^2\sqrt{\mu}}{1+Ba_i\sqrt{\mu}} + \beta\mu, \tag{3}$$

where A and B are general constants applying to all aqueous solutions; a_i and β are constants characteristic of the solution studied; μ is the ionic strength of the solution in moles per liter and defined as half the sum of the concentration of each ion multiplied by the square of its valence, and z_i is the valence of the ion. In this method z_i always has a value of one, since only the activity coefficient of HCl, a uniunivalent electrolyte, is involved, as indicated in the emf equation. Substituting [Cl^-]f_{Cl} for (Cl^-) in eq 2, and eq 3 for f_{Cl} gives

$$\frac{(E-E^\circ)F}{2.3026RT} + \log [Cl^-] - \frac{A\sqrt{\mu}}{1+Ba_i\sqrt{\mu}} + \beta\mu = -\log (H^+) = \text{pH}. \tag{4}$$

It is now possible by means of this equation to calculate the pH of a solution from the measured emf, the ionic strength, and the known concentration of the sodium or potassium chloride added to the solution.[6] Numerical values of E°, A and B at temperatures from 0° to 60° C, inclusive, are given in a paper by Harned and Ehlers [9]. Values of a_i and β are known for a few electrolytes and electrolytic mixtures. If values of a_i and β are not known for the electrolyte or electrolytic mixture studied, it is well to employ solutions as dilute as is practical. For dilute solutions, the $Ba_i\sqrt{\mu}$ and $\beta\sqrt{\mu}$ terms are of less

[5] The concentration of a solution may be expressed in one of three ways, namely, (1) moles of solute per liter of solution (volume concentration, c), (2) moles of solute per 1,000 g of solvent (molality, m), or (3) mole fraction=N. Corresponding to these units for the concentration of a solution there are three units for activity coefficients, represented, respectively, by f, γ, and f; the first two termed the practical activity coefficients and the last one termed the rational activity coefficient. For a relation between these, see MacInnes, The Principles of Electrochemistry, chap. 6, p. 131 (Reinhold Publishing Corp., New York, 1939). For illustration, only c and f will be employed in this paper. It should be pointed out that c, m, and N will approach the same numerical value as the solution is made more dilute. For approximate results, these may be used interchangeably. For precise work and for standardization purposes, the units of concentration should be stated clearly.

[6] In this method it is assumed that sodium and potassium chloride in aqueous solutions are completely dissociated into ions. Ample justification of this assumption has been reported in the literature from results obtained from experiment and conclusions deduced from theory. See Falkenhagen, Electrolytes, translation by Bell, p. 51 (Claredon Press, Oxford, London, 1934), also MacInnes, The Principles of Electrochemistry, chap. 8. (Reinhold Publishing Corporation, New York, N. Y., 1939). It is also assumed that the activity coefficient of an individual ion can be determined. Actually, only the mean activity coefficient of the ions of a solute can be determined experimentally. It is necessary, therefore, to make some assumption in order to arrive at a value for the activity coefficient of an individual ion. See MacInnes, J. Am. Chem. Soc. **41**, 1086 (1919); Scatchard, J. Am. Chem. Soc. **47**, 696 (1925), and Guggenheim, J. Phys. Chem. **34**, 1758 (1930) for discussions of assumptions which may be used to calculate values of the activity coefficients of individual ions. Mean activity coefficients are employed to test the Debye-Hückel equation. Therefore, the constants, β and a_i, are characteristic of a solute and not of individual ions. Hence, in using this equation to calculate the activity coefficient of an individual ion, it must be assumed that the activity coefficient of the ion is equal to the mean activity coefficient of a solute (in this case, HCl) composed in part of this ion. The hydrogen-ion activity may also be converted to hydrogen-ion concentration, using a similar assumption.

significance in the calculations of values for $\log f_{Cl}$ or pH. Hence the method herein described is better adapted to solutions of a concentration of 0.1 *M* or less. For accurate work and for standardization purposes, it is necessary to know these values. They may be determined from studies of the thermodynamics of solutions, considerations of interactions of ions, or by other means, the details of which are beyond the scope of this paper.

It will be noted that the method herein described may also be used for routine determinations of the pH of aqueous solutions of unknown composition. The concentration of the sodium or potassium chloride added to the solution is employed in eq 2 instead of the activity of the chloride ion, in calculations of pH. Unless the solution is extremely acid or contains large quantities of salts, the pH thus calculated will be the correct value within ± 0.1 pH unit for most solutions.

III. DESCRIPTION OF EQUIPMENT AND EXPERIMENTAL PROCEDURES

For precise measurements of hydrogen-ion activity it is necessary (a) that the galvanic cells be maintained at constant temperature within 0.02° C; (b) that the electrodes behave reversibly, or are not subject to appreciable polarization, overvoltage, or passivity; (c) that the electrodes exhibit no temperature hysteresis, do not change in potential with time and are not "poisoned"; and (d), that the solution studied be as free as possible from soluble impurities, particularly carbon dioxide, and undergo no reduction or catalytic change by the electrodes, heat, light, or other conditions to which they are exposed. When these conditions are attained, the galvanic cell is said to be in a state of equilibrium. For the hydrogen electrode, it is essential that the hydrogen gas and solutions contain no oxygen and be in gaseous and vapor equilibrium, and that a good surface for adsorption of hydrogen gas be used in its construction.

Descriptions of equipment and experimental procedures which have been used for precise measurements of the galvanic cell described above are given in the following sections.

1. ASSEMBLY OF EQUIPMENT

Figure 1 is a schematic diagram of the principal parts of the assembly of the cell designed for precise measurements without liquid junction. The cell and bubble tube are designed (1) so that they may be filled in the absence of air and will exclude air, (2) so that different solutions may be studied under similar conditions which may be easily and accurately reproduced, and (3) so that they may be conveniently filled with solution and drained and cleaned after a series of measurements.

The Pyrex-glass cell, *AB*, of about 140-ml capacity, has a compartment, *A*, for the silver-silver chloride electrodes and a compartment, *B*, for the hydrogen electrodes. The electrodes are supported in rubber stoppers inserted in the openings of the compartments. In all measurements two pairs of electrodes are employed in the solution. Electrodes which do not agree better than 0.05 mv are not considered to be functioning properly. The hydrogen inlet tube of compartment *B* is

sealed to the outlet tube of a Pyrex-glass bubble tube, *D*, of about 40-ml capacity, which consists of an outer glass tube and an inner glass rod around which is sealed a glass spiral of six turns. The bubble tube serves to equilibrate the hydrogen gas with water vapor prior to its entrance into the solution in compartment *B*, thus preventing changes in the concentration of the solution and errors in the emf. The efficiency of the bubble tube was tested by filling it with distilled

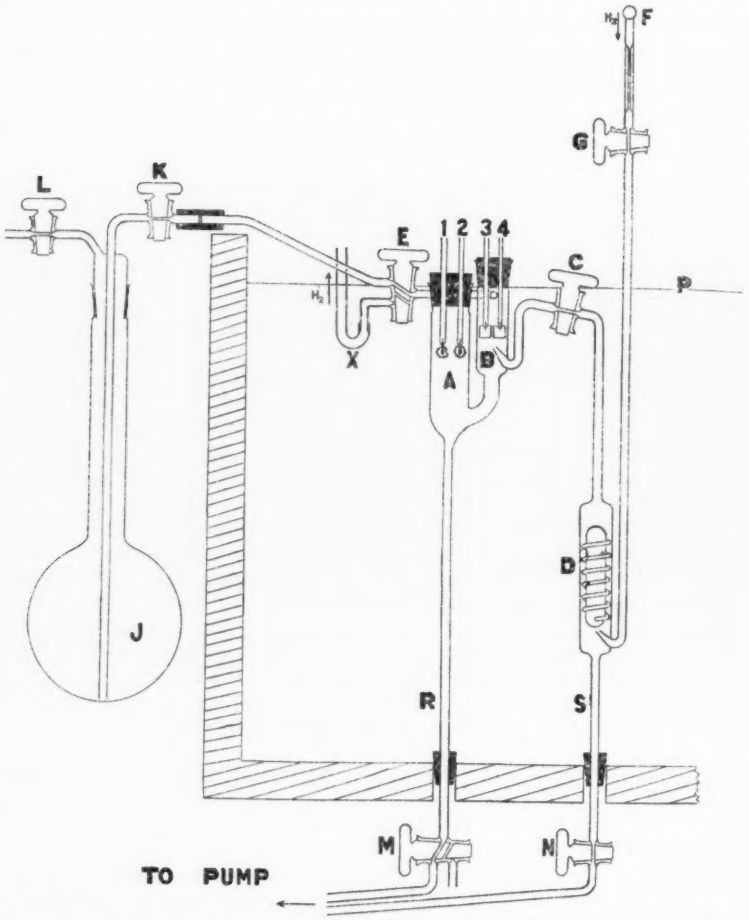

FIGURE 1.—*Schematic diagram of principal parts of apparatus employed for accurate measurements of hydrogen-ion activities in solutions.*

water and passing hydrogen through it and then through 50 g of water contained in a weighed Erlenmeyer flask completely immersed in a constant-temperature bath. After 10 hours of flow, no change in the weight of the water in the flask was found. Stopcock *C* is inserted between the bubble tube and compartment *B* to aid in filling the cell and bubble tube with solution. The cell and bubble tube are installed in the thermostat, *P*, as indicated schematically in figure 1, and, in

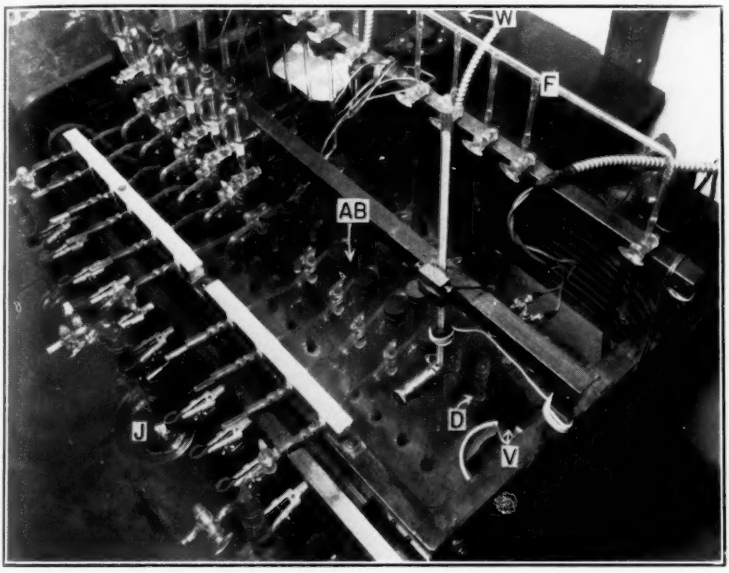

FIGURE 2.—*Assembly of 10 cells and 10 hydrogen-gas bubble tubes in a water thermostat and the interior arrangement of the water thermostat.*

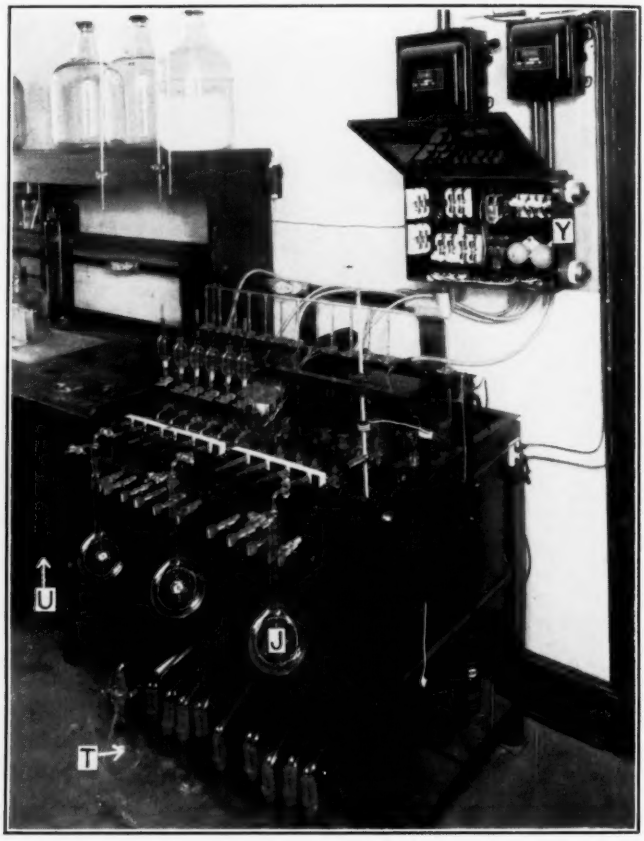

FIGURE 3.—*Complete apparatus, including the drainage flasks, vacuum line and pump, shielded emf leads, vacuum-tube-relay box, supports for the solution flasks, and accessories employed in the accurate measurements of hydrogen-ion activities in solutions.*

figure 2, with the drainage tubes, *R* and *S*, protruding through rubber stoppers inserted into ½-in. holes in the bottom of the thermostat. The hydrogen inlet tube is sealed to a glass manifold, *F*, through which the hydrogen gas enters the apparatus. Stopcock *G* is inserted between the manifold and the bubble tube to aid in regulating the rate of flow of the gas.

The tube leading from the rear of compartment *B* to flask *J*, containing the solution to be studied, serves two purposes: (1) To convey the solution from flask *J* to *A*, *B*, and *D* when stopcock *E* is in the position shown, and (2) as the outlet tube for hydrogen gas from *B* when stopcock *E* is turned through an angle of 180°. This tube is connected to the delivery tube of flask *J* by rubber tubing. The hydrogen outlet tube and stopcock *E* are nearly completely immersed in the bath to prevent water condensing in them and running back into the cell, which would dilute the solution and cause errors in the emf measurements. A rubber tube extending over the edge of the thermostat is connected to the hydrogen outlet tube at position *X*.

The apparatus is a single glass unit from stopcock *G* to stopcock *K* and to stopcocks *M* and *N*, except for the small portion of rubber tubing joining flask *J* to the apparatus proper. All stopcocks are cleaned and greased before each series of measurements. Stopcock *C* is in the bath to prevent condensation of water vapor from the hydrogen gas as it passes from the bubble tube to the cell. The tube bearing the stopcock has a 5° slope toward the bubble tube, so that if any water does leak through the stopcock from the thermostat it will drain into the bubble tube and not the cell.

Ten assemblies[7] of this type are mounted in the thermostat shown in figure 2. They are supplied simultaneously with hydrogen from a cylinder through the manifold, *F*. The 3 inches of capillary tubing inserted between manifold *F* and stopcock *G* aid in equalizing the flow of hydrogen gas in the 10 assemblies. The tubes *R* and *S* of each assembly are connected to a drainage flask, *T*, shown in figure 3. The apparatus and the drainage flask are evacuated by means of a Hyvac pump, *U*, shown at the left in figure 3, which is protected from water vapor by a glass tower containing calcium chloride and a second tower filled with potassium hydroxide sticks. The pressure is indicated by a mercury manometer inserted between the glass towers and the pump. The apparatus when dry can be evacuated to a pressure of about 0.1 mm of mercury and has been found to hold this pressure overnight.

2. PROCEDURE FOR FILLING CELLS AND BUBBLE TUBES

The apparatus is rinsed and filled with solution in the absence of air as follows. Immediately after the rubber stoppers supporting the electrodes are inserted into compartments *A* and *B*, the entire apparatus from stopcock *G* to stopcock *K* is evacuated through stopcocks *M* and *N*. The stopcocks are then closed and the apparatus gradually filled with hydrogen by opening stopcock *G*. This procedure of evacuating and filling the apparatus with hydrogen is repeated twice and the apparatus finally evacuated. Stopcock *K* is then opened slightly and the apparatus filled with solution, hydrogen

[7] The six cells shown on the left in figures 2 and 3 are designed for studies of galvanic cells with liquid junctions, the details of which will not be considered in this paper.

gas being admitted through stopcock L to flask J to maintain constant pressure within it and to avoid contamination of the solution with air and carbon dioxide. The solution is allowed to remain in the apparatus from 15 to 20 minutes in order to wash it and the electrodes thoroughly. The apparatus is then drained through M and N by evacuation and simultaneously filled with hydrogen, reevacuated, and refilled with solution. This second solution is also kept in the apparatus for 15 to 20 minutes and then withdrawn as above. Finally, the apparatus is evacuated for a third time and completely filled with solution. For efficient flow of the hydrogen, part of the solution in the bubble tube is forced out through stopcock N by means of hydrogen. Since the hydrogen electrode functions best when only partially immersed in solution and the gas must escape through stopcock E, part of the solution in compartment B is likewise forced out through stopcock M by hydrogen. The flow of hydrogen is then regulated at a rate of about two bubbles per second. The gas passes around the spiral in the bubble tube and over the hydrogen electrodes in compartment B and escapes through stopcock E and tube X.

3. PREPARATION OF SOLUTIONS

Conductivity water employed for the preparation of all solutions is obtained by oxidation of the organic matter in distilled water with alkaline permanganate, distillation in an all-glass still, and subsequent redistillation in a tin still [13]. The specific conductance of the water in the present work was 1.0×10^{-6} mho. Dissolved air and carbon dioxide are then removed by boiling the water under reduced pressure for 3 to 4 hours and by cooling it in a steady stream of hydrogen gas. This water is then stored under an atmosphere of hydrogen. The dissolved gases in the solutions studied are also removed by boiling them under reduced pressure and then cooling them in a stream of hydrogen gas. For those solutions which decompose when heated, even under reduced pressure, the dissolved gases are removed by bubbling hydrogen through the solution at room temperature for 2 to 3 hours. In all cases, corrections for loss of water from the solutions by evaporation during these operations are made by determining the weight of the solutions before and after deaeration. Purified salts are always used in preparations of the solutions. Weighings are made in a constant temperature room ($25° \pm 0.2°$ C) of about 50-percent relative humidity. All weights are corrected to the "vacuum" basis. The weights used were calibrated by the Mass Section of the Bureau.

4. HYDROGEN ELECTRODES AND PURIFICATION OF HYDROGEN GAS

The bases of the hydrogen electrodes are constructed of platinum foil (10 by 15 by 0.2 mm) welded to a platinum wire sealed in the end of a glass tube. The foil is cleaned for about 3 minutes in aqua regia diluted with an equal volume of water and washed in distilled water. A chloroplatinic acid solution is prepared by dissolving 3 g of platinum in aqua regia, evaporating it to dryness on a water bath, moistening the residue with concentrated hydrochloric acid, reevaporating and dissolving the residue in 100 ml of 0.25 N hydrochloric acid. One milliliter of 5-percent lead acetate solution is added.

The solution must be perfectly clear. The foil is then plated with a thin coat of platinum black by electrolysis in the chloroplatinic acid solution for three minutes at a current density of 250 ma per cm^2 of electrode surface. After the electrodes are coated with platinum black they are thoroughly washed and stored in distilled water. Newly plated electrodes are always used for each experiment. They are not previously saturated with hydrogen gas by electrolysis in sulfuric acid, as is often done in practice, since in the procedure described above, they are dried by evacuation, thus making any presaturation valueless. Furthermore, Loomis and Acree [14] found that it was unnecessary to saturate a hydrogen electrode in this way. Possible changes in the pH of dilute solutions by contamination with H_2SO_4 from the sponge are also avoided. Electrodes prepared in this manner have been found to be reproducible and to function reversibly within 0.02 mv, when used in solutions which are not reduced by the hydrogen electrode. The preparation of electrodes for use in solutions which may be reduced by the hydrogen electrode is not considered in this paper.

Commercial electrolytic hydrogen gas stored in cylinders is used for the hydrogen electrodes and deaeration of the solutions. It is important that the last traces of oxygen be removed from the hydrogen gas. MacInnes and Cowperthwaite [15] observed differences as large as 50 mv between the potentials of two hydrogen electrodes when commercial hydrogen gas is used without purification. Lorch [16] showed that 0.92 percent of oxygen in hydrogen gas will cause a chemical polarization of the hydrogen electrode displacing the potential 0.78 mv from the equilibrium value. The hydrogen gas is therefore purified by passing it through a soda-lime scrubber to remove carbon dioxide, through a Chamberland filter to remove soda-lime dust, and finally over palladinized asbestos contained in a Pyrex-glass tube, 30 cm in length and 1 cm in diameter, heated to 220° C to remove oxygen, as recommended by Loomis and Acree [14]. It is conducted to manifold *F* (fig. 1) through a copper tube of 0.5-mm bore. The tube is joined to the manifold with de Khotinsky cement.

5. SILVER-SILVER CHLORIDE ELECTRODES

Several types of silver-silver chloride electrodes are in common use. They are the electrolytic, thermal-electrolytic, and thermal types. Smith and Taylor have recently shown that if sufficient time is allowed, all three types will give the same potential within 0.02 mv with respect to the same solution containing chloride ion and that the thermal-electrolytic type attains a state of equilibrium sooner than the other two types. Since the thermal-electrolytic type may be more easily prepared in a state of high purity than the other two,[8] and because its potential relative to the "normal hydrogen electrode" is accurately known, it was used in this work. It is considered the best type for use in precise measurements.

The method of preparation proposed by Harned [18] was followed with slight modifications. The base of the silver-silver chloride electrode consists of a helix (4 turns) of platinum wire of about 0.3-mm

[8] In the preparation of the electrolytic type, the silver is deposited by electrolysis from a solution of potassium silver cyanide and complete removal of the cyanide is bothersome. In the thermal type, silver-oxide and silver-chlorate pastes are heated in an oven at 700° C, and care must be taken to avoid explosions. Furthermore, it is difficult to ascertain if all the silver chlorate has been reduced to silver chloride.

diameter. A glass tube sealed to the helix serves as the electrode support. Silver-oxide paste is prepared from hot solutions of silver nitrate and sodium hydroxide, thoroughly washed in distilled water, inserted in the helix, and is then converted to metallic silver by heating to 450° C in an electric furnace. The helix with the metallic silver is then cooled, and the silver partially converted to silver chloride by electrolysis in a normal solution of purified hydrochloric acid for 2 hours at a current density of 8 ma per cm² of electrode surface.

Güntelberg [19] observed that traces of bromide ion produce appreciable changes in the potential of silver-silver chloride electrodes. For example, he found that the equilibrium potential for the silver-silver chloride electrode in a solution of 0.0968 *M* KCl, 0.001 *M* $PbCl_2$ and 0.002 *M* HCl was lowered 0.53 mv and 2.68 mv by the addition, respectively, of 0.01 mole percent and 0.05 mole percent of KBr. The hydrochloric acid used in the preparation of the silver-silver chloride electrodes was prepared by the method of Brunel and Acree [20], which should give a solution of hydrochloric acid containing no bromide ion. Hydrogen chloride gas, generated in a Kipp generator by the action of concentrated sulfuric acid on pure fused ammonium chloride, is passed into conductivity water. After leaving the generator, the gas is passed at a rate of two bubbles per second through a wash bottle containing concentrated sulfuric acid. The hydrochloric acid was tested for sulfate ion and the test was negative.

The electrodes are about 7 mm in diameter. They are thoroughly washed and soaked overnight in distilled water, before being used in experiments. Smith and Taylor find that electrodes should be aged in the solution to be studied to prevent concentration polarization (due to differences between the concentration in the pores of the electrode and the bulk solution) which may produce errors of the order of 0.1 mv in the emf if the electrodes are used prior to 10 hours of aging. It will be evident from the data given in table 1 that soaking the electrodes overnight in distilled water and the procedure of evacuation described above greatly reduce, if they do not entirely eliminate the concentration difference which gives rise to polarization.

6. THERMOSTAT AND TEMPERATURE REGULATION

The thermostat shown in figures 2 and 3 consists, in part, of a thermally insulated copper tank, 16 by 36 by 24 inches, filled with water. It is supported 16 inches above the floor, as shown in figure 3. The temperature of the water is controlled by means of a mercury regulator, *V*, (fig. 2), sensitive to 0.001° C. It is included in an electric circuit with a vacuum tube, a light-duty relay, and a heavy-duty relay, housed in a metal box, *Y* (fig. 3), and a 1,500-watt immersion heater on the bottom of the bath. The mercury regulator was designed so that it can be adjusted quickly for use at temperatures from 0° to 60° C, or higher. A cross section is shown in figure 4. While the temperature of the bath is being raised or lowered, the ground-glass stopper, *A*, is lifted from its seat, so that the mercury remains at approximately the same level in bulb, *B*, and capillary tube, *C*. The stopper is seated when the desired temperature is reached and is held in place by rubber bands. The fixed terminal, *D*, and the adjustable terminal, *E*, are both of platinum wire. A glass

bead, *F*, is sealed on the platinum wire used in the capillary tube to keep the wire in position.

The temperature of the bath is measured by means of a thermometer, graduated in tenths of a degree from −10° to 102° C, calibrated by the Thermometry Section of the National Bureau of Standards. The ice point is redetermined at frequent intervals. The temperature of the bath was constant to about 0.01° C at all the temperatures employed. For temperatures below that of the room, the bath is cooled by means of a ½-hp refrigerator unit with 10 coils of ½-inch copper tubing serving as the expansion coil placed at the inside wall of the bath (fig. 2). To control the temperature of the bath at or below room temperature, the refrigerator is operated continuously and heat supplied by electric immersion heaters and the temperature regulated in the same manner as for higher temperatures. The water of the bath is stirred by means of a 10-inch, 6-blade propeller, making 108 rpm, driven by a motor, *W*, (fig. 2), with built-in reduction gear. The effectiveness of the stirring was tested by exploring the bath at 0° and 25° C with a Beckmano thermometer. The temperature was found to be uniform within ±0.002° C. Two auxiliary 1,000-watt immersion heaters are employed independently of the vacuum tube-relay circuit so that rapid changes in the temperature of the bath may be made when desired. Other features of the thermostat and assembly, such as the manner in which the solution flasks are held in position and the support for the tubes leading from the flasks to the cells, are shown in figures 2 and 3.

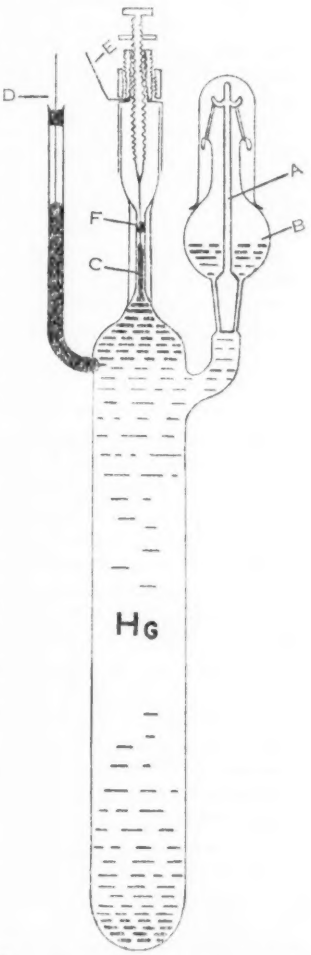

FIGURE 4.—*Cross section of the mercury regulator for control of temperatures of a water bath from 0° to 60° C, or higher.*

7. INSTRUMENTS FOR MEASURING ELECTROMOTIVE FORCE

The measurements of the emf of the galvanic cells are made with a Leeds & Northrup type *K* potentiometer, calibrated by the Resistance Measurements Section of the Bureau, with a Leeds & Northrup type *R* galvanometer and an unsaturated Weston cell. Contact between the potentiometer leads and all electrodes is made with mercury contained in the electrode supports.

IV. DATA ILLUSTRATING PRECISION OF MEASUREMENTS

To illustrate the reproducibility of the results and the precision obtainable, two assemblies were filled with the same solution (table 1) at 25° C, cooled to 0° C, and the emf recorded at intervals until constant readings of the emf or equilibria of the cells were attained. After the measurements of the emf at 0° C were recorded, the temperature of the bath was raised from 0° to 60° C in 5-degree steps and measurements of the emf made at each temperature. In each cell, two silver-silver chloride electrodes, Nos. 1 and 2 (fig. 1) and two hydrogen electrodes, Nos. 3 and 4, were employed, thus making possible measurements of six pairs of electrodes and a total of four checks on the emf of the cell.

Illustrative data are given in table 1 for a galvanic cell containing a solution of malonate salts and sodium chloride.[9] These emf values have been corrected to 1 atmosphere of hydrogen pressure in the usual manner by means of the equation [21]

$$\Delta E=\frac{2.3026RT}{2F}\log\frac{760}{(p_b-p_s)}, \tag{5}$$

in which ΔE is the correction to be applied to the measured emf; p_b, the observed barometric pressure in millimeters of mercury at 0° C; and p_s, the vapor pressure of the solution in millimeters of mercury. The vapor pressure of pure water was used for p_s in this work and may be used for dilute solutions with negligible error. The vapor pressures of pure water used for the various temperatures were those obtained in this Bureau by Osborne, Stimson, and Ginnings [22].

In column 1 of table 1, the time in minutes after the flow of hydrogen gas was started is given for 0° C. For the other temperatures, the time refers to the interval after the temperature of the bath had been changed. Inspection of this table shows that approximately 4 hours is required at 0° C before equilibrium of the cells is attained and that after a change in temperature only half an hour or less is required. The lag at 0° C is due primarily to the time required to saturate the hydrogen electrodes with hydrogen. At the other temperatures it is due primarily to the time required to obtain constant temperature within the cells. Columns 3 and 4 give the values of the emf of the galvanic cell, using different pairs of hydrogen and silver-silver chloride electrodes for cell 1; and columns 7 and 8 give similar data for cell 2. The average of the four readings is given in column 11. In columns 12 and 13, the maximum and average deviations of the individual emf from the average, respectively, are given. The maximum deviation ranges from 0.02 to 0.04 mv for different cells, which is equivalent, respectively to 0.0004 and to 0.0007 pH unit at 25° C. The average deviation is between 0.01 and 0.02 mv, equivalent, respectively, to 0.0002 and 0.0004 pH unit at 25° C. Further inspection of the data of this table shows that the emf obtained for cell 1 is in close agreement with the emf obtained for cell 2, thus affording a good check upon the reproducibility of the results obtained with the method employed in filling the cells and in preparing the electrodes.

[9] Acknowledgment is made to John O. Burton, formerly of this Bureau and now Chief Research Engineer of the Minnesota and Ontario Paper Co., International Falls, Minn., for the purification of the malonic acid, hydrochloric acid, and sodium hydroxide used in the preparation of these solutions and for aid in obtaining some of the data.

After the final measurements of the emf were made at 60° C, the temperature of the bath was lowered to 45° C in order to learn whether the emf of the cells would agree with the first values obtained at 45° C and to determine if there was a temperature hysteresis. The value of 652.87 mv agrees closely with the 652.84 mv value previously obtained. The bath was then cooled to 25° C to obtain a further check. The value of 635.44 mv agrees closely with the 635.40 mv value previously obtained at 25° C. Data obtained at duplicate temperatures generally agree to within 0.04 mv, showing that proper equilibria can be obtained at all the temperatures; and that the electrodes function properly and exhibit no temperature hysteresis or aging effects. Inspection of the data of table 1 shows that a change of 0.01° C produces a change of about 0.009 mv in the emf, which is slightly less than the experimental error of the electrical measurements.

In columns 5 and 9 the differences observed in the potential between the two silver-silver chloride electrodes are given. It will be seen that this difference is only 0.01 to 0.03 mv at equilibrium. Similar observations with hydrogen electrodes are given in columns 6 and 10. These data also show that the electrodes exhibit no appreciable temperature hysteresis. Furthermore, no aging effects were observed over a period of 15 hours, which is the time that elapsed between the first and second set of readings at 25° C. The differences between duplicate electrodes account almost entirely for the deviations found for the emf of the galvanic cells, indicating that the method of filling the cells and making the measurements is better than stated above and that the limiting factor is the reproducibility of the electrodes. Similar precision was obtained for other galvanic cells containing aqueous solutions of various concentrations of malonate salts [23] and solutions prepared from other organic aliphatic materials.

Only estimates can be made of the accuracy obtainable by the method and procedures described in this paper. The uncertainty in $E°$ is estimated as 0.05 mv from a consideration of the work of Harned and Ehlers [9]. On the basis of an uncertainty of 0.1 percent in the dielectric constant of water [10] and the uncertainties in R, T_0, F, ϵ, and k given by Wensel [24], the uncertainties in $2.3026RT/F$, A, and B are respectively, 0.02 mv, 0.003, and 0.001 reciprocal angstrom. The uncertainty in the concentration is taken as 0.1 percent, even though, in many cases, it may be only 0.01 percent. An error of 0.05 mv in $E°$ and an error of 0.02 mv in $2.3026RT/F$ are equivalent, respectively, to errors of 0.0008 and 0.0006 pH unit. An error of 0.003 in A at 25° C, combined with an error of 0.001 reciprocal angstrom in B, produces an error of 0.0012 pH unit at a concentration of 1 molar and an error of about 0.0003 pH unit at 0.01 molar—a value of 3 angstroms was used for a_i in these calculations. Finally, an error of 0.1 percent in the concentration at 1 molar results in an error of only 0.0005 pH unit. The experimental error in E is less than half the uncertainty which has been assigned to $E°$, while the error in t is of the same order as the uncertainty in T_0.

[10] The general constants A and B used in eq 4 are defined by

$$A=\frac{\sqrt{2\pi}}{2.3026}\left(\frac{\epsilon}{\sqrt{Dk(t+T_0)}}\right)^3\left(\frac{N}{1000}\right)^{1/2}$$

and

$$B=\frac{4.6052\ Dk(t+T_0)}{\epsilon^2}A,$$

where ϵ is the electronic charge, N the Avogadro number, D the dielectric constant of water, k the Boltzmann constant, t the centigrade temperature, and T_0 the Kelvin temperature of the ice point.

TABLE 1.—*Data for the galvanic cell* Pt | $H_2(g)$ | *sodium malonate (0.029535 M), sodium acid malonate (0.029535 M), sodium chloride (0.029535 M)* | AgCl(s) | Ag(s) *illustrating the precision obtainable from 0° to 60° C with galvanic cells without liquid junction*

Time after starting the hydrogen flow or after a change in temperature	Temperature	Data for cell 1 containing the malonate solution and using electrode combinations—				Data for cell 2 containing the malonate solution and using electrode combinations—				Average emf	Maximum deviation from the average emf	Average deviation from the average emf	Average pH values [3]	Average pH values [4]
		1-3	2-4	1-2 [1]	3-4 [1]	1-3	2-4	1-2 [1]	3-4 [1]					
1	2	3	4	5	6	7	8	9	10	11	12	13	14	15
Minutes	°C	*mv*	*mv*	*mv*	*mv*	*mv*	*mv*	*mv*	*mv*	*mv*	*mv*	*mv*		
60	0	613.33	613.26	+0.04	−0.03	613.24	613.23	+0.04	+0.03					
90	0	613.49	613.44	+.06	+.01	613.44	613.41	+.04	+.01					
120	0	613.61	613.58	+.03	.00	613.57	613.59	−.04	−.02					
150	0	613.71	613.69	.00	−.02	613.69	613.68	+.04	+.03					
180	0	613.78	613.79	−.02	−.01	613.74	613.77	−.03	.00					
210	0	613.85	613.88	−.02	+.01	613.82	613.85	−.04	−.01					
240	0	613.89	613.94	−.03	+.02	613.88	613.93	−.03	+.02					
270	0	613.93	613.95	−.01	+.01	613.87	613.93	−.03	+.03					
300	0	613.93	613.96	−.01	+.02	613.89	613.93	−.02	+.02					
330	0	613.93	613.95	−.01	+.01	613.90	613.93	−.02	+.01					
360	0	613.93	613.95	−.01	+.01	613.90	613.93	−.02	+.01					
Equilibrium value		613.93	613.95	−0.01	+0.01	613.90	613.93	−0.02	+0.01	613.93	0.03	0.01	5.323	5.251
10	20	630.87	630.93	−.04	+.02	630.91	630.96	−.02	+.03					
30	20	630.97	631.03	−.03	+.02	630.96	631.00	−.02	+.02					
45	20	631.01	331.03	−.01	+.01	630.99	631.00	.00	+.01					
60	20	631.01	631.03	−.01	+.01	630.99	631.00	.00	+.01					
Equilibrium value		631.01	631.03	−0.01	+0.01	630.99	631.00	0.00	+0.01	613.01	0.02	0.01	5.323	5.250
10	25	635.21	635.27	−.04	+.02	635.27	635.31	−.05	−.01					
30	25	635.29	635.33	−.01	+.02	635.41	635.42	−.01	.00					
45	25	635.39	635.43	−.03	+.01	635.39	635.41	−.01	+.01					
60	25	635.39	635.42	−.02	+.01	635.39	635.41	−.01	+.01					
90	25	635.39	635.42	−.02	+.01	635.39	635.41	−.01	+.01					
Equilibrium value		635.39	635.42	−0.02	+0.01	635.39	635.41	−0.01	+0.01	635.40	0.02	0.01	5.331	5.258
10	45	652.71	652.77	−.04	+.02	652.68	652.73	−.02	+.03					
30	45	652.85	652.86	.00	+.01	652.79	652.82	−.02	+.01					
45	45	652.85	652.86	+.01	+.02	652.80	652.82	−.01	+.01					
60	45	652.85	652.86	.00	+.01	652.80	652.82	−.01	+.01					
Equilibrium value		652.85	652.86	0.00	+0.01	652.80	652.82	−0.01	+0.01	652.84	0.04	0.02	5.384	5.312
10	60	666.14	666.17	−.02	+.01	666.16	666.19	−.04	−.01					
30	60	666.21	666.23	.00	+.02	666.20	666.23	−.02	+.01					
45	60	666.25	666.21	+.03	−.01	666.22	666.26	−.06	−.02					
60	60	666.25	666.21	+.03	−.01	666.22	666.27	−.03	+.02					
75	60	666.25	666.21	+.03	−.01	666.22	666.27	−.03	+.02					
Equilibrium value		666.25	666.21	+0.03	−0.01	666.22	666.27	−0.03	+0.02	666.24	0.03	0.02	5.440	5.372

10	45	653.07	653.05	+.03	+.01	653.14	653.15	−.03	−.02					
30	45	652.91	652.90	+.01	.00	652.99	653.03	−.05	−.01					
45	45	652.87	652.86	+.01	.00	652.89	652.91	−.01	+.01					
60	45	652.87	652.86	+.01	.00	652.85	652.89	−.02	+.02					
90	45	652.87	652.86	+.01	.00	652.85	652.89	−.02	+.02					
Equilibrium value		652.87	652.86	+0.01	0.00	652.85	652.89	−0.02	+0.02	652.87	0.02	0.01	5.384	5.312
10	25	635.47	635.56	−.04	+.05	635.74	635.69	+.03	−.02					
30	25	635.44	635.48	−.02	+.02	635.53	635.57	−.04	.00					
45	25	635.42	635.46	−.02	+.02	635.44	635.48	−.02	+.01					
60	25	635.42	635.46	−.02	+.02	635.43	635.45	−.01	+.01					
90	25	635.42	635.46	−.02	+.02	635.43	635.45	−.01	+.01					
Equilibrium value		635.42	635.46	−0.02	+0.02	635.43	635.45	−0.01	+0.01	635.44	0.02	0.02	5.332	5.259

[1] A plus sign indicates that the electrode named first in the heading is the anode.
[2] The maximum deviations from the average emf obtained at 5, 10, 15, 30, 35, 40, 50, and 55° C were, respectively, 0.03, 0.03, 0.02, 0.02, 0.02, 0.03, 0.02, and 0.03 mv, and the average deviations were, respectively, 0.02, 0.02, 0.01, 0.01, 0.01, 0.02, 0.02, and 0.02 mv.
[3] Values obtained by using the numerical values of a_4 and β given on page 662 of this paper.
[4] Values obtained by assuming the numerical values of a_1 and β in eq 4 are zero.

It is not possible to give values of the hydrogen-ion activity of the solution here employed until values of a_i and β are known for HCl solutions containing malonate salts. However, it has been found [11] that β has a value of zero for this solution, and that a_i has a value of 4.99, 4.82, 4.75, 4.29, and 3.76 A for the temperatures of 0°, 20°, 25°, 45°, and 60° C, respectively. In column 14 of table 1, the pH values obtained by using these constants and the values of R, T_o and F reported by Wensel [24] are given. In column 15, the pH values obtained on the assumption that both a_i and β are zero are listed. It is evident from comparison of these two sets of values, that for this solution, the two sets of pH values differ by a constant amount of about 0.07 pH unit, which is small for routine measurements. However, for standardization purposes, this difference emphasizes the need for accurate evaluation of the constants a_i and β.

A consideration of the various sources of error and the fact that the uncertainties were assigned magnitudes which the actual errors are not likely to exceed lead to the conclusion that pH measurements can be made with an accuracy of about 0.001 pH unit.

V. REFERENCES

[1] Clark, The Determination of Hydrogen Ions, chap. 23 (Williams & Wilkin Co., Baltimore, Md., 1928).
[2] Kolthoff and Tekelenburg, Rec. trav. chim. **46,** 33 (1927).
[3] Clark and Lubs, J. Biol. Chem. **25,** 479 (1916).
[4] MacInnes, Belcher, and Shedlovsky, J. Am. Chem. Soc. **60,** 1094 (1938).
[5] Hitchcock and Taylor, J. Am. Chem. Soc. **59,** 1812 (1937).
[6] Hitchcock and Taylor, J. Am. Chem. Soc. **60,** 2710 (1938).
[7] Hamer, Trans. Electrochem. Soc. **72,** 45 (1937) [a review].
[8] Harned and Ehlers, J. Am. Chem. Soc. **55,** 2179 (1933); Harned, J. Franklin Inst. **225,** No. 6, 623 (1938) [a review].
[9] Harned and Ehlers, J. Am. Chem. Soc. **54,** 1350 (1932).
[10] Int. Critical Tables **6,** 321 (1930).
[11] Debye and Hückel, Physik. Z. **24,** 185, 305, 334 (1923).
[12] Hückel, Physik. Z. **26,** 93 (1925).
[13] Fawcett and Acree, Ind. Eng. Chem., Anal. Ed. **2,** 78 (1930).
[14] Loomis and Acree, Am. Chem. J. **46,** 585 (1911).
[15] MacInnes and Cowperthwaite, J. Am. Chem. Soc. **53,** 555 (1931).
[16] Lorch, Trans. Electrochem. Soc. **55,** 2194 (1933).
[17] Smith and Taylor, J. Research NBS **20,** 837 (1938) RP1108 [a review].
[18] Harned, J. Am. Chem. Soc. **51,** 416 (1929).
[19] Güntelberg, Studier over Elektrolyt-Aktiviteter. I-Vandige Oplösninger, G. E. C. Gads Forlag-Köbenhavn. [Dissertation] (1938).
[20] Brunel and Acree, Am. Chem. J. **36,** 117 (1906).
[21] Loomis and Acree, J. Am. Chem. Soc. **38,** 2391 (1916); Lewis and Randall, J. Am. Chem. Soc. **36,** 1969 (1914); Ellis, J. Am. Chem. Soc. **38,** 737 (1916).
[22] Osborne, Stimson, and Ginnings, J. Research NBS **23,** 261 (1939) RP1229.
[23] Burton, Univ. Maryland, College Park, Md., [Dissertation] (June 1937.)
[24] Wensel, J. Research NBS **22,** 375 (1939) RP1189.

WASHINGTON, October 13, 1939.

[11] Hamer, Burton, and Acree, publication pending.

U. S. Department of Commerce National Bureau of Standards

RESEARCH PAPER RP1262

Part of Journal of Research of the National Bureau of Standards, Volume 23, December 1939

RETENTION OF ALUMINUM ION AND HYDROGEN ION IN PAPERS

By Herbert F. Launer

ABSTRACT

The decrease in pH, observed when paper-water mixtures are heated and then cooled, was found to be ascribable to the increased hydrolysis of the aluminum salts in the papers. Studies of fiber-alum-water mixtures showed that aluminum ion is selectively retained by the fibers, and that the amount of aluminum salts in papers is thus much larger than that calculated solely from the concentrations involved in the manufacture of papers. It was found that the fibers raise the pH of alum solutions to which they have been added by an amount which is characteristic of the type of fiber and of the concentration of the alum, aluminum sulfate. It is also shown that the change in pH upon heating such mixtures is likewise determined by the type of fiber and the concentration of the alum. Hydrogen ion is also strongly retained by fibers in an amount shown to be unchanged after heating and cooling. The effect of rosin upon pH relationships in papers is also discussed.

CONTENTS

		Page
I.	Introduction	663
II.	Relationship between changes in pH by hot extraction and amounts of alum used in paper manufacture	664
III.	Effect of acids from sources other than hydrolysis of aluminum salts	665
IV.	Behavior of alum solutions in the presence of fibers	666
V.	Retention phenomena under papermaking conditions	671
VI.	Effect of rosin upon pH relationships	673
VII.	Fudamental basis for choosing between hot extraction and cold extraction	674

I. INTRODUCTION

In a recent publication [1] dealing with the determination of the pH values of papers by the method of cold extraction, it was found that these values were usually higher, by 0.6 pH, on the average, than those obtained when extraction was made at 100° C, as in the TAPPI [2] standard method. An explanation for the cause of this difference was not given at that time, as the main efforts were devoted to finding whether the simpler method of cold extraction was preferable from a practical standpoint. In the present article a study of the underlying causes of this difference is presented.

Investigators have previously studied the effects of hot extraction. Browning and Ulm [3] have shown that hot extraction gives lower pH values than cold extraction and ascribe this in part to the increased

[1] Herbert F. Launer, *The determination of the* pH *value of papers*, J. Research NBS **22**, 553 (1939) RP1205.
[2] Technical Association of the Pulp and Paper Industry—T435m, Hydrogen ion concentration (pH) of paper extracts, September 6, 1934. Copies may be obtained from the Association, 122 East 42d Street, New York, N. Y.
[3] B. L. Browning and R. W. K. Ulm, Paper Trade J. **102**, 89 (Feb. 20, 1936).

hydrolysis of alum, $Al_2(SO_4)_2.18H_2O$, added in the course of papermaking. Kullgren [4] found that the hydrolysis of $AlCl_3$ in a 0.002 *N* solution increased tenfold upon raising the temperature from 25° to 100° C. Furthermore, Heyrovsky [5] found that the reversal of this hydrolysis reaction takes place slowly, and that $AlCl_3$, the hydrolysis of which had been increased by heating, remained in that condition long after cooling.

In discussing another possible explanation of the effect of heating, Browning and Ulm point out the possibility that sulfuric acid, which arises from the hydrolysis of alum, and which acid they assume is adsorbed by the fibers in the cold, may be released upon heating, thus lowering the pH. It has not yet been conclusively shown, however, that sulfuric acid is adsorbed under the conditions of extraction, that is, under the same conditions of concentration and temperature. They also give titration curves which show that weak organic acids are present in the extract. No evidence has been presented, however, as to what extent organic acids formed during the hot extraction contribute to the measured pH. Since the pH may be affected by liberation of adsorbed sulfuric acid, if any, or formation of organic acids, or both, by heating, it is necessary to determine the magnitude of these effects before dealing with any other possible effects of heating.

Furthermore, Browning and Ulm observed that a solution of alum did not change in pH upon heating when sulfite fibers were present, although large pH changes occurred in the absence of the fibers. This points to a complexity which is greater than the behavior of simple alum solutions, and an explanation for this apparent discrepancy is offered herein.

Finally, it is important to decide whether the amount of hydrolyzable aluminum salt in the finished paper is simply the amount in the paper-machine solution held by the fibers (1 g of fibers holds 1.5 g of paper-machine solution before entering the machine dryers), or whether the amount of aluminum is actually much larger than this, by virtue of its selective retention by the fibers in the beater and chest.

It was believed that a study of these points would not only provide a fundamental basis for choosing between the two methods of extraction, but would also add to existing information concerning the chemistry of paper.

II. RELATIONSHIP BETWEEN CHANGES IN pH BY HOT EXTRACTION AND AMOUNTS OF ALUM USED IN PAPER MANUFACTURE

For the sake of clarity, a part of the experimental results presented in the previous publication (see footnote 1) is shown in table 1. As was previously pointed out, the similarity of changes in pH, column 7, is misleading in that it shows little with regard to acidity changes. When these are expressed as changes in hydrogen-ion concentration, column 8, the correlation with the amounts of alum, column 4, indicates strongly that the acidity changes occurring upon heating the paper-water extracts are dependent upon the amounts of alum used in making the papers, except for smaller effects such as amount of alkaline rosin size and type of fiber. This correlation and the factors affecting it were discussed in the previous publication.

[4] Carl Kullgren, Z. physik. Chem. **85**, 466 (1913).
[5] Jaroslav Heyrovsky, J. Chem. Soc. **117**, 11. 29 (1920).

TABLE 1.—*Relations between the acidity values and other characteristics of the papers*

1	2	3	4	5	6	7	8	9	10
Sample [a] number	Fibers	Resin found	Alum [b] used in paper-making	pH, using cold extraction	pH, using hot extraction	pH, change upon heating	(H^+) change upon heating	(H^+), using cold extraction	pH, change upon heating filtrates
		Percent	*Percent*				*Equiv/liter* ($\times 10^{-7}$)	*Equiv/liter* ($\times 10^{-7}$)	
1	New rags	0.9	4.0	4.9	4.3	0.6	376	126	0.6
2	do	1.7	4.0	5.1	4.4	.7	321	79	.0
3	do	0.9	2.0	5.2	4.5	.7	253	63	.4
4	do	1.7	2.0	5.4	4.7	.7	160	40	.2
5	do	0.2	1.5	5.5	4.9	.6	94	32	.1
6	do	1.8	1.2	5.6	5.0	.6	75	25	.0
7	do	0.9	1.1	5.6	5.0	.6	75	25	.0
8	do	1.6	0.9	6.4	5.9	.5	9	4	.0
9	do	0.3	.8	6.4	6.0	.4	6	4	
10	do	.8	.7	6.3	6.0	.3	5	5	
11	do	.3	.5	7.2	7.3			0.6	
12	Soda-sulfite (1:1)	1.2	2.4	5.2	4.6	0.6	188	63	0.3
13	do	0.2	2.1	4.9	4.3	.6	376	126	.6
14	do	.2	1.5	5.3	4.8	.5	108	50	.2
15	do	1.6	1.4	5.5	4.9	.6	94	32	.0
16 [c]	do	0.9	1.3	5.8	5.1	.7	63	16	.0
17	do	1.0	1.3	5.9	5.1	.8	66	13	.0
18	do	1.2	1.1	6.0	5.3	.7	40	10	
19	do	0.3	1.0	6.4	5.7	.7	16	4	.0
20	do	.9	0.8	6.2	5.5	.7	26	6	
21	do	.3	.5	6.6	6.2	.4	4	2.5	
22 [c]	do	.3	0	6.9	6.4	.5	3	1.3	.0
23	Special sulfite [d]	1.9	2.3	5.2	4.9	0.3	63	63	0.1
24	do	1.7	1.1	5.6	5.3	.3	25	25	.0
25	do	1.1	0.8	5.6	5.0	.6	75	25	
26	do	1.6	.8	6.1	5.7	.4	12	8	
27	do	1.1	.6	6.0	5.7	.3	10	10	
28	do	0.2	0	6.9	7.2			1	
29	Bleached sulfate [d]	1.0	2.3	5.2	4.9	0.3	63	63	0.2
30	do	0.9	1.0	5.8	5.0	.8	84	16	.0
31	do	.9	0.7	6.4	6.0	.4	6	4	
32	do	.1	0	6.8	7.0			2	

[a] These papers were made in the paper mill of the National Bureau of Standards.
[b] Percentage of alum was based on dry weight of solid materials in the chest.
[c] These papers contained no clay, all others listed contained 8 to 13 percent of clay.
[d] Pulps subjected to special purifying process by the manufacturers.

III. EFFECT OF ACIDS FROM SOURCES OTHER THAN HYDROLYSIS OF ALUMINUM SALTS

The correlation between the amounts of alum and the change in acidity upon heating may be interpreted in another manner—namely, that the amounts of any organic acids from cellulose, produced during heating by the action of the hydrogen ion resulting from hydrolysis, may increase with increasing proportions of alum. Although any organic acids produced would probably be weak, and their ionization would, therefore, as Browning and Ulm point out, be repressed by the strong acid, it has not yet been shown conclusively that they do not contribute to the measured pH when papers are extracted by heating.

The possibility must also be considered that hydrogen-ion retained by the fibers in the cold may be released during heating, since it will be shown that fibers extensively reduce the acidity of hydrolyzed alum solutions.

These points were investigated [6] as follows. A solution of alum having a pH=4.7, containing 0.0031 g per 70 ml, was heated as in the

[6] The experimental technique was the same as that previously described. See footnote 1.

method of hot extraction for 1 hour at 100° C. Upon cooling, the pH was found to be 3.7. Continued heating produced no further appreciable change in pH. To 70-ml portions of this hydrolyzed alum solution 1-g portions of fibers from samples 11, 22, 28, and 32 were added; and after 1 hour at room temperature, the pH of the mixtures was determined. The pH in every case was found to be much higher after than before the addition of the fibers to the previously heated solution, which showed that extensive decreases in the concentration of hydrogen ion had occurred. The results are given in table 2, column 2. It should be pointed out that this hydrolyzed alum solution remained at pH=3.7 for several days when no fibers were added. Samples 11, 22, 28, and 32 were in the neutral region, as shown by the values for pH-cold in column 5, table 1.

TABLE 2.—*The behavior of a previously heated alum solution in the presence of neutral paper fibers*

Sample [c]	pH [a] of mixtures of 1 g of fibers with 70 ml of previously heated alum solution (0.0031 g of alum per 70 ml). pH before addition of fibers=3.7.[b]	
	Before heating the mixtures	After heating the mixtures
11. Rag	4.6	4.5
22. Soda sulfite	5.2	5.3
28. Special sulfite	4.7	4.7
32. Bleached sulfate	5.0	5.0

[a] All pH measurements were made at 25° C.
[b] This solution had a pH=4.7 before heating, and was further hydrolyzed to pH=3.7 by heating for 1 hour at 100° C, after which further heating caused no appreciable change in pH.
[c] The numbers are the same as in table 1, in which the samples are more fully described.

The four mixtures of hydrolyzed alum solution and fibers were then heated for 1 hour at 100° C, cooled, and their pH values determined. The results, listed in column 3 of table 2, reveal that little or no change in pH had occurred upon heating. Thus, since the hydrolyzed alum solution was known to contain relatively large amounts of hydrogen ion, as shown by the pH=3.7, and since the fibers added were found to remove relatively large quantities of hydrogen ion from solution, the fact that subsequent heating of these mixtures resulted in no decrease in pH shows that no appreciable hydrogen ion was released by the fibers during the process. It appears, therefore, that such a release of hydrogen ion, if it occurs, cannot explain the pH changes encountered in the method of hot extraction.

Although the mixtures of hydrolyzed alum solution and fibers were even more acidic than usual, these higher concentrations of strong acid were not effective in producing organic acids during the heating process in amounts large enough to affect the measured pH appreciably.

IV. BEHAVIOR OF ALUM SOLUTIONS IN THE PRESENCE OF FIBERS

Although the simple fact that alum solutions undergo decreases in pH upon heating makes it appear reasonable that the alum used in the manufacture of paper is responsible for the observed pH changes occurring when paper-water mixtures are heated, it remains to be

shown that pH changes of the expected order of magnitude occur in alum solutions when fibers are present.

That the presence of fibers affects the hydrolytic process is shown by the following. From the details of a typical papermaking run,[7] for example, paper 13, table 1, in which 2.1 percent of alum was used, it can be calculated that 1 g of this finished paper would contain aluminum corresponding to 0.00091 g of alum, if selective retention of aluminum ion by the fibers in the beater and chest were neglected. The pH-cold of a mixture of 1 g of paper sample 13 with 70 ml of distilled water was 4.9, and the pH changed to 4.3 upon heating. When, however, 1-g portions of sample 22, containing the same fibers as paper 13, and samples 11, 28, and 32 (all largely free of alum) were added to 70-ml portions of distilled water containing 0.00091 g of alum, the pH of the mixtures was much higher than 4.9 and the change in pH, if any, upon heating was small. In the absence of fibers, an alum solution containing 0.00091 g per 70 ml changed in pH from 4.9 to 4.1 upon heating. These results, given in table 3, columns 2 and 3, and footnote a, indicate that the reactions involved in the pH changes upon heating alum solutions differ in the presence and absence of fibers. The results also indicate that the paper-water mixtures of table 1 behaved differently upon heating than the mixtures represented in table 3, which consisted of the same kind and amount of fibers, plus an amount of alum calculated upon the basis of no selective retention of aluminum. When the amount of alum was increased to 10 times the calculated amount, the pH changes upon heating, shown in columns 6 and 7, table 3, became similar to those in table 1. Such a large increase in the amount of alum, however, resulted in pH values which, even before heating, were abnormally low when contrasted with the values for pH-cold of table 1. Use of an intermediate amount of alum, columns 4 and 5, resulted in initial pH values which were normal, but gave pH changes upon heating which were smaller than those usually found in papers of this pH range.

TABLE 3.—*Behavior of previously unheated alum solutions in the presence of neutral paper fibers*

Sample	pH of mixtures of 1 g of fibers with 70 ml of alum solutions					
	0.00091 g of alum per 70 ml. pH before addition of fibers=4.9 [a]		0.0031 g of alum per 70 ml. pH before addition of fibers=4.7 [a]		0.0091 g of alum per 70 ml. pH before addition of fibers=4.5 [a]	
	Before heating mixtures	After heating [b] mixtures	Before heating mixtures	After heating [b] mixtures	Before heating mixtures	After heating [b] mixtures
11. Rag	5.9	6.1	4.9	4.6	4.5	3.7
22. Sulfite-soda	6.1	5.9	5.6	5.3	4.6	4.2
28. Special sulfite	5.8	6.0	5.0	4.7	4.5	3.8
32. Bleached sulfate	6.0	6.0	5.2	4.9	4.5	3.9

[a] The three solutions containing 0.00091, 0.0031, and 0.0091 g of alum per 70 ml had pH values upon cooling of 4.1, 3.7, and 3.4, respectively, after heating for 1 hour at 100° C without fibers present at any time.
[b] All pH determinations were made at 25° C.

[7] In this run the proportions were 32 cu ft of water to 1.2 lb of papermakers' alum and 58 lb of fibers and clay. 1.5 parts by weight of machine water remain with each part of solid material until evaporated in the dryers.

It is evident that the paper-alum-water mixtures just discussed differ in an important manner from the paper-water mixtures of table 1, in that, in the former, the pH changes upon heating are too small if the pH-cold is normal, or the pH-cold is too low if the changes in pH upon heating are normal. The cause of this difference will be considered in section V. The data presented thus far, however, allow some deductions to be made concerning the nature of the reactions occurring in the fiber-alum-water mixtures.

The data of table 3 raise three important questions: (1) Do fibers raise the pH of alum solutions by taking up only hydrogen ion, or is aluminum ion also retained and the acidity thus indirectly reduced? (2) Why is the rise in pH brought about by the addition of fibers large in the weak and hardly noticeable in the stronger solution of alum? (3) Why is the change in pH upon heating alum solutions much less in the presence of fibers than in their absence? A consideration of these three question follows.

In answer to question (1), relatively large amounts of unhydrolyzed aluminum ion are in the alum solutions before heating, at the three concentrations described in table 3. This was shown by the fact that heating greatly changed the pH. The approximate amount of unhydrolyzed aluminum ion can be calculated from the data at hand. If the hydrolysis reaction is simply written as

$$Al^{+++}+3HOH=Al(OH)_3+3H^+,^6 \quad (1)$$

the degree of hydrolysis is represented by the expression [measured concentration of hydrogen ion]÷[concentration of hydrogen ion at complete hydrolysis.]

For the weakest of the three solutions the degree of hydrolysis is 11 percent, as calculated from the pH=4.9, and the concentration of alum=0.00091 g/70 ml=0.000117 equivalent of alum or aluminum ion per liter. This shows that 89 percent of the aluminum ion was not hydrolyzed in the unheated solution. In the two stronger alum solutions the proportion of unhydrolyzed aluminum ion was, of course, still greater.

The simplest expression for the hydrolysis constant for equation (1) as written is

$$K_{hydrolysis}=\frac{(H^+)^3}{(Al^{+++})}.$$

Substituting the three independent sets of data, for the three solutions, into this expression, the values obtained are 0.6×10^{-10}, 0.7×10^{-10} and 0.6×10^{-10}, in the order of increasing concentration of the three alum solutions of table 3. The agreement may be considered as a measure of substantiation of the correctness of the hydrolysis equation as written.

Inasmuch as the removal of aluminum ion by the fibers would cause the reversal of the hydrolysis reaction, thus reducing the hydrogen ion concentration and raising the pH, it is desirable to know if such a removal occurs.

[6] It is recognized that aluminum ion may hydrolyze in steps, but the equation as written represents the sum of these steps.

Schwalbe [9] showed that a sulfite pulp reduced the concentration of aluminum in an alum solution. His results were confirmed in the present work by the following experiments.

Samples of the basic materials, from which the papers listed in table 1 were made, were added in 1-g portions to 70-ml portions of alum solution containing 0.0031 g of $Al_2(SO_4)_3.18H_2O$ per 70 ml. The basic materials, rather than the papers, were used, with the exception of sample 22 (see footnote c, table 1), in order to avoid large amounts of aluminum, present as clay in samples 11, 28, and 32. These basic materials were found to have the same pH as the corresponding papers, with the exception of the special sulfite pulp, which was alkaline, but which became neutral upon washing twice with distilled water. They were found, furthermore, to have essentially the same effect upon the pH of alum solutions as the corresponding neutral papers, samples 11, 28, and 32. The aluminum in solution was determined with the sensitive colorimetric aurintricarboxylic acid method before and after the addition of the fibers. The sulfate was determined in the same solutions by precipitation with barium.[10] The results given in table 4 show that extensive retention of aluminum ion occurred in all cases, since the changes shown are much larger than the indicated probable experimental error. The conclusions regarding the retention of sulfate ion are less definite, for these experimentally determined changes are as large as the experimental uncertainty; and it is not possible to decide from these data whether or not selective retention of sulfate ion occurs to a small extent. The data show, however, that aluminum sulfate is not retained as $Al_2(SO_4)_3$, since one part by weight of aluminum would therein be associated with over 5 parts by weight of sulfate. The slight gains, if real, in sulfate ion by the solutions are apparently due to the presence of sulfate, 0.05 to 0.15 mg, known[11] to be present per gram of the usual fibers used in papermaking. The fact that aluminum ion is selectively retained is of major importance, since the amount of aluminum in paper, calculated solely upon the basis of concentrations in the beater, would not be large enough to explain the observed pH changes upon heating.

TABLE 4.—*Retention of aluminum by fibers in an unheated alum solution* [a]

Fibers (1 g per 70 ml of solution)	Aluminum concentration		Sulfate concentration	
	Before addition of fibers	After addition of fibers [b]	Before addition of fibers	After addition of fibers [b]
	mg per 70 ml	*mg per 70 ml*	*mg per 70 ml*	*mg per 70 ml*
A. New rags (half stuff)	0.27 ±0.02	0.17 ±0.02	1.3 ±0.2	1.6 ±0.2
B. Soda-sulfite (sample 22)	.27 ±0.02	.10 ±0.02	1.3 ±0.2	1.6 ±0.2
C. Special sulfite pulp	.27 ±0.02	.03 ±0.02	1.3 ±0.2	1.2 ±0.2
D. Bleached sulfate pulp	.27 ±0.02	.02 ±0.02	1.3 ±0.2	1.4 ±0.2

[a] The alum solution was made by dissolving 0.0031 g of cp $Al_2(SO_4)_3.18H_2O$ per 70 ml. Upon analysis, the salt was found to have lost water and was better represented by the formula $Al_2(SO)_3.16H_2O$.

[b] All fibers were removed by filtration and dissolved organic matter was removed before the analyses. All $Al(OH)_3$, not retained by the fibers but removed in the filtering process would constitute a small correction of the values of column 3. The correction would probably be negligible, since not more than 5 percent of the aluminum would be present as $Al(OH)_3$, as shown by the value for the degree of hydrolysis for this concentration of aluminum sulfate.

[9] Carl G. Schwalbe, Z. angew. Chem. **37**, 125 (1924).

[10] The author thanks W. D. Mogerman and W. W. Walton of the Chemistry Division for cooperation in making these analyses.

[11] R. C. Griffin, Paper Trade J. **90**, 63 (May 1, 1930).

The experiments just described do not, by themselves, indicate the form in which the aluminum is retained. It may be retained either (a) as completely hydrolyzed $Al(OH)_3$ or (b) as unhydrolyzed Al^{+++} or as partially hydrolyzed $Al(OH)^{++}$, for example, or both. In any case, the substances may be either physically adsorbed as such, or in some chemical combination with the organic or inorganic constituents of the fibers. Since physical adsorption would require that the sum of the ions, positive and negative, be zero, and since the concurrent removal of $SO_4^{=}$ has not been shown, the retention of Al^{+++} as such, or its partially hydrolyzed forms, would be explainable by an ion exchange with the inorganic fiber constituents, calcium, for example. The mechanism of retention was not investigated.

If the aluminum were retained only as $Al(OH)_3$, however, then practically all of the aluminum in the system, at least in the cases of *C* and *D*, table 4, would be in a completely hydrolyzed condition before heating. The amount of unhydrolyzed aluminum, Al^{+++}, would be then insufficient to explain the pH changes upon heating, as shown in table 3, columns 4 and 5. It appears, therefore, that the retention of hydrolyzable aluminum must occur.

These conclusions are necessary according to the theory which requires that the activity or mass-action effect of "solid" substances, in equilibrium with a solution, is unity, and that the amount of the solid phase present does not affect the ionic equilibrium. This means that $Al(OH)_3$ may be taken up by the fibers without upsetting the ionic equilibrium and without consequent formation of more $Al(OH)_3$. Thus, only 11 percent or less of the aluminum in the three solutions under consideration could be removed from solution, if removed only as $Al(OH)_3$. Table 4 shows this value to be greatly exceeded in all cases.

Additional evidence of the removal of aluminum ion by fibers is given in table 5. After fibers had been in contact with an alum solution for 1 hour, they were removed completely and the filtrates were heated for one hour at 100° C, as usual, and cooled. Measurement of the final pH showed that the pH changes, and especially the changes in hydrogen-ion concentration of the filtrates upon heating, were much smaller than in the original solution, showing that hydrolyzable aluminum ion had been removed from solution. It should be stated that filtrates from mixtures of the fibers with distilled water alone, containing no alum, did not change in pH upon heating.

TABLE 5.—*Changes in* pH *of the filtrates from fiber-alum-water mixtures*

Sample	pH of mixtures of 1 g of fibers +70 ml water +0.0031 g of alum. pH before addition of fibers=4.7[a]	pH of filtrate before heating	pH[b] of filtrate after heating	Change in H^+-concentration upon heating filtrates
				$\times 10^{-7}$
11. Rag	4.9	4.7	4.1	600
22. Soda-sulfite	5.6	5.6	5.3	25
28. Special sulfite	5.0	4.8	4.5	155
32. Bleached sulfate	5.2	5.2	4.7	140

[a] The solution after heating alone had a pH=3.7. The change in pH from 4.7 to 3.7 represents a change in hydrogen ion concentration of 1800×10^{-7} equivalents per liter.
[b] All pH measurements were made at 25° C.

In answer to question (1), therefore experimental evidence shows that fibers selectively retain aluminum ion in alum solutions, thereby indirectly lowering the acidity. This occurs concurrently with the direct retention of hydrogen ion and the consequent direct lowering of acidity.

In answer to question (2), why fibers raise the pH of strong alum solutions less than that of weak solutions, it may be pointed out that the percentage of aluminum ion left in solution after retention by the fibers becomes larger with an increase in concentration of aluminum ion, inasmuch as retention cannot be expected to increase indefinitely with concentration in a strict proportion; that is, the fibers approach "saturation." As the total amount of alum was increased, table 3, the proportion left in solution after retention became larger, until, in the strongest solution, sufficient aluminum ion remained in solution to maintain the pH at the original value, except in the case of the soda-sulfite fibers. Even in the strongest solution as much as one-fourth of the aluminum ion may have been retained by the fibers, since the hydrolysis relationship $(H^+)=K\sqrt[3]{(Al^{+++})}$ shows that large changes in the concentration of aluminum ion must occur before the pH changes become appreciable. Thus, in the more concentrated solutions of alum, the selective retention of aluminum ion may be considerable without affecting appreciably the cube root of the aluminum-ion concentration.

In answer to question (3), why pH changes upon heating alum solutions are larger in the absence than in the presence of fibers, there are two mechanisms which may be considered. Either the aluminum ion taken up by the fibers is not hydrolyzed by heating and only the aluminum in solution is, or else all, or most, of the aluminum ion hydrolyzes, but the hydrogen ion produced is subsequently taken up by the fibers. The latter appears more likely, however, for the values in table 2, column 2, which were obtained by first hydrolyzing the aluminum ion and then reducing the acidity by adding fibers, are in good agreement with the values in table 3, column 5, which were obtained by heating the alum in the presence of fibers. This speaks in favor of the mechanism that all or most of the aluminum ion in the system is hydrolyzed upon heating, and the hydrogen ion produced is retained to an extent depending upon the nature of the fiber and upon the concentration of the acid.

V. RETENTION PHENOMENA UNDER PAPERMAKING CONDITIONS

The conditions of the experiments thus far described simulated conditions of paper extraction and were useful in showing the behavior of acid and alum occurring therein. The concentrations of materials during papermaking conditions are much different, however, than during extraction conditions. In a typical papermaking run, for a paper made with a medium amount of alum, 1.4 percent, for example, 1 g of fibers in the beater and chest is associated with 35 ml of water containing 0.014 g of alum. This concentration is over three times as great as that of the strongest solution of alum referred to in the preceding section, which contained 10 times the amount of alum calculated on the basis of no retention, for extraction conditions of paper sample 13 of table 1. Thus, the amount of aluminum retained under these papermaking conditions may be expected to be large.

On the basis of the foregoing experiments, such large amounts of alum would be expected to result in much lower values for pH-cold than those of table 1. In the foregoing experiments, however, distilled water was used,whereas the papers of table 1 were made, as usual, with tap water of pH=7.6, to which much more alum must be added than to distilled water for a given resultant pH. For example, 70 ml of tap water containing 0.028 g of alum and 70 ml of distilled water containing 0.0091 g of alum both have a pH=4.5.

The proportions in a typical papermaking run were simulated with rag and with soda-sulfite paper fibers. One-gram portions of fibers were added to 35-ml portions of tap water containing 0.014 g of alum each. After 1 hour at room temperature, the mixtures were filtered on a Büchner funnel and allowed to remain thereon until the pads contained 1.5 g of liquid,[12] which corresponds to the moisture content of the paper sheet before it reaches the dryer. The pads were then mixed with 68.5 ml of distilled water, to simulate extraction conditions, and the pH-cold was determined after 1 hour at room temperature. The mixtures were then heated for 1 hour at 100° C, cooled, and the pH-hot was determined. The results are given in table 6, systems 2 and 3, and show that paper extraction conditions for unsized papers were thus reproduced, in that both the pH-cold and the change in pH upon heating were within the normal range.

TABLE 6.—pH *relationships under papermaking and extraction conditions*

System	pH values [a] of fibers	
	No. 11, rag	No. 22, soda-sulfite mixture
(1) 1 g of fibers+35 ml of tap water containing 0.014 g of alum	4.6	5.0
(2) Fibers filtered, retaining 1.5 g of liquid; 68.5 ml of distilled water added to fibers	5.0	5.8
(3) System (2) heated for 1 hour at 100° C, then cooled	4.4	5.0
(4) 1.5 g of original solution of 0.014 g of alum in 35 ml of tap water, added to 68.5 ml of distilled water containing 1 g of fibers	6.4	6.5
(5) System (4) heated for 1 hour at 100° C, then cooled	6.4	6.1

[a] All pH values measured at 25° C.

The retention of aluminum ion under papermaking conditions was found to be considerable, as shown by the data in table 7, whereas that of sulfate ion was small, if it occurred at all. The amounts of aluminum and sulfate (see footnote 10) remaining in the fibers after exposure to tap water and to tap water containing alum were determined after igniting the materials. The ignition of the materials for sulfate analysis required special care. The materials were soaked in an excess of calcium chloride solution, and the mixture was evaporated to dryness and then ignited at 950° C, at which temperature $CaSO_4$ is stable. Blanks were run on all reagents. The presence of aluminum in the form of clay was again avoided by the use of the basic rag material from which sample 11 was made. The two last columns show that from one-third to almost one-half of the aluminum added to the beater is selectively retained, even in the absence of rosin size, whereas 96 percent of the aluminum would remain with the machine water if no selective retention occurred.

[12] Concentration of alum solution due to evaporation under these conditions was found to be negligible, since prolonging the time of the operation from the usual minute or so required to 2 minutes did not change the weight of the moist pad to an important extent; less than 5 percent of water was thereby lost.

TABLE 7.—*Retention phenomena under papermaking conditions*

Fibers	Gain for 1 g of fibers exposed [a] to 35 ml of tap water containing 0.014 g of alum [b]		Gain for 1 g of fibers exposed [a] to 35 ml of tap water. No alum		Gain, net, due to alum		Gain, if no retention occurred, calculated from weight of solution [a] in fibers after filtration		Proportion of substances removed from alum solution by fibers	
	Al	SO_4	Al	SO_4	Al	SO_4	Al	SO_4	Al	SO_4
	mg [c]	*mg*	*mg*	*mg*	*mg*	*mg*	*mg*	*mg*	*Percent*	*Percent*
A. New rags, half stuff	0.45 ±0.01	0.5 ±0.1	0.06 ±0.01	0.1 ±0.1	0.39 ±0.01	0.4 ±0.1	0.05	0.3	33	6
B. Soda-sulfite No. 22	.64 ±0.01	.5 ±0.1	.10 ±0.01	.1 ±0.1	.54 ±0.01	.4 ±0.1	.05	.3	45	6

[a] Fibers remained in the solution 1 hour with constant stirring and were then filtered with suction until 1.5 g of solution remained with each gram of fibers.
[b] 0.014 g of alum=1.19 mg of aluminum and 6.3 mg of sulfate.
[c] The experiments were actually performed with 2.5 g of fibers and corresponding amounts of liquid, for which the analytical precision was 0.02 and 0.2 mg for aluminum and sulfate, respectively.

It was of interest to determine the pH relationships if no retention were allowed to take place. This was done as follows. 1.5 g of the original tap water-alum solution was directly added to 68.5 ml of distilled water containing 1 g of fibers. This amount of alum would be the same as that in solution in the 1.5 g of liquid in the fibers, if retention of aluminum-ion by the fibers had not occurred. It was found, however, that not only was the pH of the mixtures made up by direct addition of alum solution much higher, but also the change in pH upon heating was much smaller, than in the mixture made up in the previous manner, by allowing 1.5 g of liquid to remain with the fibers. The results are given in the remainder of table 6.

VI. EFFECT OF ROSIN UPON pH RELATIONSHIPS

It has already been pointed out that the addition of rosin decreases not only the acidity of a paper, but also decreases the change in hydrogen-ion concentration upon heating the paper-water mixture, for papers made with 2 percent or more of alum. Since alum is always used in excess over the amount necessary to precipitate the rosin completely, this appears to be due to a reduction in the amount of available alum, presumably by the formation of insoluble aluminum resinate, as the following experiments show. Typical paper-water mixtures, referred to in table 1, were filtered after they had stood for 1 hour at room temperature. These filtrates were then heated for 1 hour at 100° C and then cooled. The pH was determined before and after heating. A decrease in pH was found only for the filtrates from papers made with relatively large quantities of alum. The results are given in column 10 of table 1. The effect of rosin upon the amount of alum leaving the paper fibers and dissolving into cold water is seen in the sample pairs 1 and 2, 3 and 4, and 12 and 13.

Other effects of rosin upon the pH and pH changes during heating may, of course, occur, for no attempt has been made to extend the investigation to cover this point. It is to be observed, however, that if such effects exist, they are small, since no systematic difference between the behavior of sized and unsized papers in table 1 is noticeable, from the standpoint of pH. The decreasing effect upon the

acidity and acidity changes during heating, by increasing the amount of size used, is obviously not a direct function of the weakly acidic character of rosin itself.

VII. FUNDAMENTAL BASIS FOR CHOOSING BETWEEN HOT EXTRACTION AND COLD EXTRACTION

It has been shown that the effect of hot extraction is to hydrolyze further the aluminum salts in the papers, thereby producing as much as 3 to 4 times the amount of hydrogen ion originally found in the cold extract. These large amounts of acid resulting from the hydrolysis of the aluminum salts obscure the presence of smaller amounts of other acids which may result from cooking or bleaching operations, or which may be present owing to acidic atmosphere.

Hot extraction has a further serious drawback. The aluminum salts in the papers may undergo partial hydrolysis, with the liberation of harmful acid, when they are stored or shipped under warm, humid conditions, or when the drying or other manufacturing processes were faulty. The amount of this acid cannot be measured by the method of hot extraction, since the heating process causes extensive further hydrolysis, irrespective of any partial hydrolysis which may already have occurred. The method of cold extraction, on the other hand, gives pH values corresponding to the hydrolysis equilibrium at room temperature; thus, any displacement of this equilibrium by previous higher temperatures will be measured. If the alum was already partially hydrolyzed by faulty storage or manufacturing conditions, the acid thus liberated should be and is measured in the unheated extract.

If the acidity of a paper, as it exists under conditions of use, can be employed as a measure of its permanence, and it appears that this is true, then the method of cold extraction gives a much closer measure of the significant pH values of papers than do the more complicated methods now in general use.

WASHINGTON, October 20, 1939.

U. S. DEPARTMENT OF COMMERCE NATIONAL BUREAU OF STANDARDS

RESEARCH PAPER RP1263

Part of Journal of Research of the National Bureau of Standards, Volume 23, December 1939

POLAR STRUCTURE OF SOME BENZEIN INDICATORS

By Myron A. Elliott* and S. F. Acree

ABSTRACT

In the study of electronic effects associated with changes of color of indicators, the approximate electric moments have been measured for α-naphtholbenzein and thymolbenzein in benzene solution. The values obtained were 4.3×10^{-18} and 6.8×10^{-18} esu, respectively. These values are much lower than those predicted for the benzein type of molecule on the basis of the static dipolar structure shown in figure 2. They are compatible, however, with the quinone-phenolate resonance theory and indicate that these molecules are predominantly in the structure shown as A_1, figure 1, with very little of the resonant dipolar form A_2.

CONTENTS

		Page
I.	Introduction	675
II.	Apparatus and method	677
III.	Data and calculations	678
IV.	Sources of error	680
V.	Conclusions	680
VI.	References	681

I. INTRODUCTION

In investigations of the effects of hydrogen ions and various types of salts on indicators, the need of more information about the dipole moments of the indicators has been felt. Some preliminary data on the dielectric constants of α-naphtholbenzein and thymolbenzein in benzene solutions are given in this paper. From these data the dipole moments of the molecules have been calculated and some interpretations made.

The dipole moment, which is a measure of the electrical asymmetry of a molecule, gives important information concerning molecular structure. Here we shall attempt to correlate the measured dipole moments of some benzein indicators with those predicted by each of two conflicting theories for the structure and origin of color of these indicators. One of these theories [1],[1] the quinone-phenolate theory, attributes the weak color of the benzeins in their free state to a resonance within the quinone group (*A*, fig. 1) and the intense color of the ionized molecule to a resonance in the quinone-phenolate anion (*B*, fig. 1). The other theory [2] attributes the color of the free benzein and the highly colored form respectively to a fixed dipolar structure (*C*, fig. 2) and to a charged, fixed dipolar structure (*D*, fig. 2).

*Research Associate at the National Bureau of Standards, representing the Florida Citrus Commission.

[1] Figures in brackets indicate the literature references at the end of this paper.

In *A*, the resonance which affects the visible frequencies occurs within the typical quinone group alone, two extreme resonating structures being shown by A_1 and A_2, although several intermediate ones can be expected also. In *B*, resonance occurs in the whole quinone-phenolate anion; each $C_{10}H_6O$ group being thought of as changing alternately between modified quinone and phenolate ion structures [1].

The second theory postulates a trivalent central carbon atom carrying a unit positive charge with a negative charge on the oxygen. This gives the static structures *C* and *D*, respectively, in place of *A* and *B*.

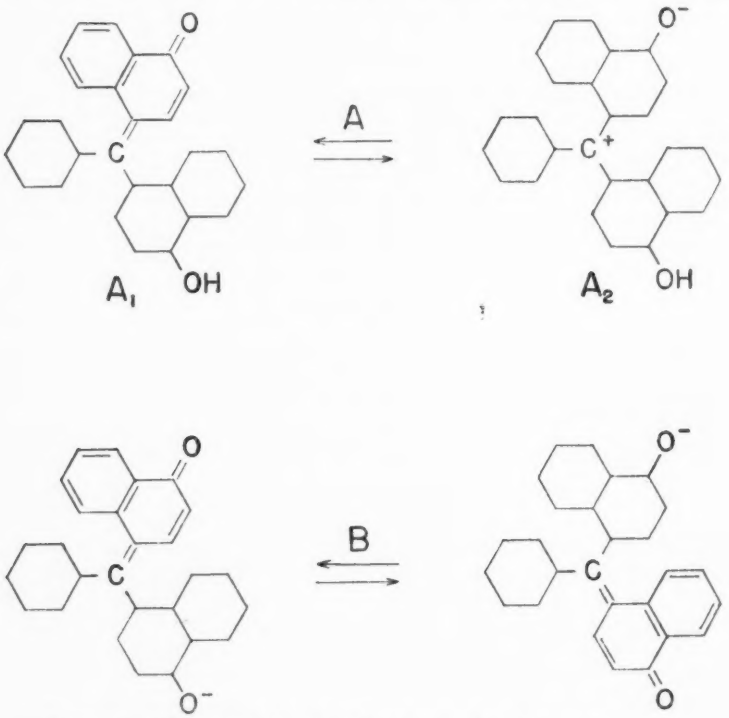

FIGURE 1.—*Resonant quinoid and quinone-phenolate structures for α-naphtholbenzein.*

A, Weakly colored quinoid; *B*, Intensely colored quinone-phenolate anion.

On the basis of the quinone-phenolate theory, *C* or *D* is one of the resonance structures of *A* or *B*, respectively. It should be emphasized, therefore, that one cannot decide against the quinone-phenolate resonance theory by finding chemical reactions in agreement with structures *C* and *D*. On the other hand, one could obtain evidence against the fixed dipolar structures (*C* and *D*) by finding chemical reactions of a quinone. One cannot, however, at present rule out a static dipolar structure on the basis of chemical reactions alone. This can be done by a measurement of the dipole moment, since, as is evident from structures *A* and *C*, the two theories predict widely different dipole moments for the benzein in its free state or in benzene

solution. That the benzein has the same form in benzene solution as in its free state, as would be expected from the low dielectric constant of benzene, is shown by the fact that the color is red in both cases, whereas the aqueous alkaline solution containing the ionized molecules is blue.

A simple calculation shows that a molecule having structure *C* would have a dipole moment close to 27 Debye units ($D=10^{-18}$ esu). From structures *A*, on the other hand, one can predict a value somewhere between 3.9 and 27 *D*, depending upon the relative probabilities of A_1 and A_2. The smaller the value of the measured dipole moment, the less is the contribution of structure A_2. From the measured dipole moments to be given later, a rough estimation could be made of the

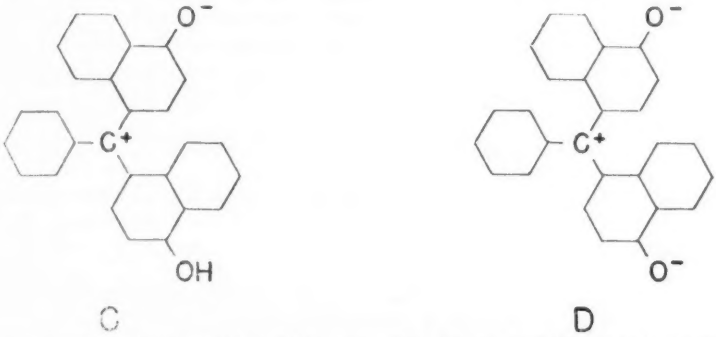

C D

FIGURE 2.—*Postulated static dipolar structures for the weakly and the intensely colored forms of α-naphtholbenzein.*

relative probabilities of A_1 and A_2, if one neglects the intermediate structures which occur to some extent.

II. APPARATUS AND METHOD

The above-mentioned moments were calculated from measurements of their dielectric constants, made at 25° C with a resonance apparatus of a modified Wyman type placed in an air thermostat [3]. The cell consisted of three concentric platinum cylinders 5 cm long. The diameter of the central one was 2 cm, and the three cylinders were spaced 1.5 mm apart. They were mounted in a glass jacket. One heavy straight lead was attached to both the outer and inner cylinders and another to the intermediate cylinder. External inductors of various sizes could be connected across these leads. The resonance frequency of this electric circuit was determined by its interaction with a variable high-frequency oscillator. The interaction was detected by a sudden change in the plate current of the oscillator when its frequency was tuned to the resonance frequency of the nearby cell. The cell was calibrated with standard known solutions of nitrobenzene in benzene and a curve made of frequency against dielectric constant for each of the inductors. The dielectric constants of the solutions were very nearly inversely proportional to the squares of the respective resonance frequencies for a given external inductance. Theoretically, the proportionality should be exact [3] if the solution

encompassed the total electrostatic field in and about the cell. The frequency of the variable oscillator was checked before and after each measurement by beating it against the higher harmonics of a standard piezoelectric oscillator. This apparatus was built for studying the dielectric constants of solutions of the amino acids and proteins found in citrus juices and is not ideally suited to the type of measurements described here. The values obtained may be considered good enough, however, for use in testing the very different predictions of the two structural theories outlined above. In the range studied, the molar polarization of these benzein indicators in benzene decreased with decreasing concentrations, so it was necessary to extrapolate to infinite dilution to obtain a proper value to use for calculating the electric moments. Because of the low solubility at 25° C of thymolbenzein in benzene, it was not possible to obtain satisfactory points to make an extrapolation to infinite dilution. Some tentative values were obtained by assuming the slope of the curve for the short thymolbenzein extrapolation to be the same as that for the α-naphtholbenzein.

III. DATA AND CALCULATIONS

Table 1 contains the data used in calculating the electric moments of α-naphtholbenzein and thymolbenzein. The terms used in this table are defined.

TABLE 1.—*Data on dielectric constants and molar polarizations of α-naphtholbenzein and thymolbenzein at various concentrations in benzene*

f_1	ϵ	P_1/f_1	P_{12}	P_1	Frequency
α-NAPHTHOLBENZEIN					
					Mc
0.00499	2.442	26.646	29.439	560	11.3
.00248	2.358	26.713	28.057	543	11.3
.00123	2.318	26.748	27.387	518	11.3
.000615	2.299	26.764	27.065	499	11.3
.00499	2.435	26.646	29.346	542	13.3
.00248	2.347	26.713	27.900	480	13.3
.00123	2.312	26.748	27.298	446	13.3
.00442	2.396	26.660	28.700	460	39.4
.00218	2.333	26.721	27.653	427	39.4
Values extrapolated to infinite dilution				467	11.3
				416	13.3
				348	39.4
THYMOLBENZEIN					
0.000557	2.321	26.765	27.373	1092	11.3
.000279	2.298	26.773	27.034	936	11.3
.000557	2.319	26.765	27.347	1045	13.3
.000279	2.300	26.773	27.056	1015	13.3
.00235	2.443	26.720	29.111	1019	39.4
.00133	2.368	26.740	28.010	957	39.4
Values extrapolated to infinite dilution				1080	11.3
				1020	13.3
				910	39.4

The molar polarization (P_{12}) of a binary mixture may be expressed [4, p. 44] by the equation

$$\frac{\epsilon-1}{\epsilon+2}\cdot\frac{M_1f_1+M_2f_2}{\rho}=P_1f_1+P_2f_2=P_{12}, \quad (1)$$

where ϵ=dielectric constant of the solution;
ρ=density of the solution;
M_1=molecular weight of component 1;
M_2=molecular weight of component 2;
f_1=mole fraction of component 1;
f_2=mole fraction of component 2;
P_1=molar polarization of component 1;
P_2=molar polarization of component 2;
P_{12}=molar polarization of the mixture;

In this case the solvent benzene is taken as component 1. The constant P_1 is obtained from eq 1 by letting $f_1=1$, $f_2=0$, and substituting the proper constants for benzene,

$$P_1=\frac{\epsilon-1}{\epsilon+2}\cdot\frac{M_1}{\rho_1}=\frac{2.283-1}{2.283+2}\cdot\frac{78.05}{0.873}=26.778. \quad (2)$$

The total polarization, P, of a molecule is the sum of its electronic, atomic, and orientation polarizations. The sum of the electronic and atomic polarizations will be designated as P_0, the polarization due to deformation of the molecule. The desired orientation polarization will then be $P-P_0$. The total polarization, P, can be obtained from table 1 and is equal to the value of P_2 at infinite dilution. The deformation polarization, P_0, can usually be approximated from measurements of the refractive index, but, because of absorption bands in the visible spectrum, such data could not be obtained here. This P_0 could also be calculated if another value of the dielectric constant of the solutions were obtained at a frequency in the infrared region that was too great for orientation to occur but low enough for the electronic and atomic deformations to occur. Since it was not feasible in the course of this work to obtain dielectric constant or refractive index data at frequencies in the infrared region, the value of P_0 was obtained by use of the following approximation:

It may be expected that at frequencies in the infrared the polarization per unit volume for benzene solutions of the benzein indicators will be somewhat greater than that of pure benzene. This is because of the greater possibility for atomic polarization in the large benzein molecules than could occur with pure benzene. For molecules having large moments, however, this difference between the polarization per unit volume of the solution and that of the pure solvent at infrared frequencies will be very small compared with the corresponding difference at radio frequencies, where the orientation polarization gives its full effect. This is particularly true if the solute and solvent are composed largely of the same kinds of atoms and groups. Let the approximation be made that the polarization per unit volume of these indicator solutions is equal to that of pure benzene at infrared frequencies. Then it can be calculated that for α-naphtholbenzein

P_0=93 cm³ and for thymolbenzein P_0=116 cm³. The dipole moment μ, [4, p. 42] of a molecule is given by the formula

$$\mu=0.0127\times10^{-18}\sqrt{(P-P_0)\times T}\text{ esu,} \quad (3)$$

where T is the absolute temperature. The use of eq 3 and values of P obtained from the data of table 1, of P_0 as calculated and given above, and of 298.1 (25° C) for T gives 4.3 D and 6.8 D for the dipole moments of α-naphtholbenzein and thymolbenzein, respectively.

IV. SOURCES OF ERROR

Careful consideration will show that P_0 calculated with the above approximation will likely be too small for these particular systems. This means that μ may, therefore, be a little too large. This fact does not interfere with arguments given here on the polar structure of benzein indicators, since these deductions depend on the moments being below and not above certain limits. Another source of difficulty in working with molecules of this size at high frequencies is that due to the anomalous dispersion of the dielectric constant [4, chap. 5]. This dispersion or variation arises because the molecules may be too large for their orientations to keep pace with the rapid changes in the electric field. If they lag behind these field changes, the dielectric constant, and hence the molar polarization, are diminished relatively to the values at low frequencies. Table 1 shows that the molar polarization of α-naphtholbenzein was 348 at 39.4 Mc and 467 at 11.3 Mc. To explain this difference one might suspect some colloidal material to be present, but it was found that the solution would readily diffuse through a rubber membrane, so that possibility was discarded. Calculations based on the size of the benzein molecules and the viscosity of the solvent show that the frequency range 7.5 to 27 m (40 to 11 Mc) is near or perhaps out of the dispersion region on the low frequency side. Wyman in his work on amino acids and related compounds [5] with molecular weights as high as 150 found no evidence of anomalous dispersion at wave lengths down to 2.5 m (120 Mc). The molecular weights of the benzein derivatives discussed in this paper are between 350 and 400, but the lowest frequencies used (27 m or 11 Mc) are less than one-tenth of those just mentioned. This leads to the belief that at 11 Mc the frequency should be at least near the lower limit of the region of anomalous dispersion if not out of it. Until further work can be done at lower frequencies, the values obtained at 11 Mc are the best available. Any corrections necessary because of anomalous dispersion will tend to increase the electric moments reported herein. These corrections, if later found to be necessary, will not seriously affect the conclusions concerning the structure of the indicators presented here unless these corrections should exceed 100 percent.

V. CONCLUSIONS

The dipole moment of 4.3 D obtained for α-naphtholbenzein is only slightly larger than the minimum of 3.9 D calculated for structure A_1. This shows that highly polar states are present only a very small fraction of the time.

The higher moment of 6.8 *D* obtained for thymolbenzein indicates that this molecule is in highly polar states somewhat more of the time than α-naphtholbenzein.

None of these facts is inconsistent with a structural theory based on the resonance concept, whereas the observed electric moments are not sufficiently large to justify the assumption of the static dipolar structure. Such a dipolar structure can at most exist as only one of many transient states formed during resonance. The theoretical calculations of Pauling [6], Mulliken [7], and Sklar [8] are in accord with a resonance phenomenon for the basis of the origin of color in the conjugated double bond type of molecule. In harmony with this concept, preliminary measurements of the electric moment of phenol blue indicate that resonance between conventional and dipole structures may be associated with the intense color of this indicator, indigoes, oxazones, and similar dyes.

$$\text{O: } C_6H_4\text{: N–}C_5H_4N(CH_3)_2 \rightleftarrows \overline{\text{O}}\text{–}C_6H_4\text{–N: } C_6H_4\text{: } N^+(CH_3)_2,$$

Knowledge of the polar structure of indicators is important in devising equations for expressing the effects of H-ions and salts on their color changes. The equations expressing the corrections for the effects of surrounding salts on a highly polar or amphoteric compound are different from those used in the case of an ordinary ion or molecule [9]. Further measurements of dielectric constants and refractive indices at various temperatures and frequencies and also in ionizing solvents will be necessary. Spectrophotometric data in the infrared should also be obtained to give further information about the bonding in these molecules. Measurements should also be made on similar molecules having the OH groups replaced by methoxy or acetate radicles so that there can be no hydrogen bond formation [10]. The accumulation and interpretation of such data will aid in perfecting the theory and technique of the indicator method.

We are indebted to J. R. Johnson, of Cornell University, for supplying a number of benzein compounds and to A. L. Sklar, of this laboratory, for many suggestions on the theoretical aspects of this paper.

VI. REFERENCES

[1] E. A. Slagle and S. F. Acree, Am. Chem. J. **39,** 531 (1908); **42,** 129 (1909). See also R. T. Birge and S. F. Acree, J. Am. Chem. Soc. **41,** 1048 (1919), and Am. Chem. J. **38,** 1 (1907), for earlier references and mathematical treatments of tautomerism of indicators.
[2] H. Lund, Math-fysik. Med. Dansk. **11,** 6 (1931).
[3] J. Wyman, Jr., Phys. Rev. **35,** 623 (1930).
[4] P. Debye, Polar Molecules (Reinhold Publishing Corp., Inc., New York, N. Y., 1929).
[5] J. Wyman, Jr., Chem. Rev. **19,** 213 (1936).
[6] L. Pauling in H. Gilman's Organic Chemistry, **2,** 1888–89. (John Wiley & Sons, Inc., New York, N. Y., 1938).
[7] R. S. Mulliken, J. Chem. Phys. **7,** 20, 121, 364 (1939).
[8] A. L. Sklar, J. Chem. Phys. **5,** 669 (1937).
[9] G. Scatchard and J. G. Kirkwood, Physik. Z. **33,** 297 (1932).
[10] W. M. Latimer and W. H. Rodebush, J. Am. Chem. Soc. **42,** 1419 (1920). W. H. Rodebush and A. M. Buswell, J. Phys. Chem. **43,** 219 (1939).

WASHINGTON, October 10, 1939.

U. S. Department of Commerce National Bureau of Standards

RESEARCH PAPER RP1264

Part of Journal of Research of the National Bureau of Standards, Volume 23, December 1939

ZEEMAN EFFECT IN THE SECOND AND THIRD SPECTRA OF XENON

By Curtis J. Humphreys, William F. Meggers, and T. L. deBruin*

ABSTRACT

The Zeeman effect in the spectra of singly and doubly ionized xenon has been observed in the laboratory "Physica" in Amsterdam and at the National Bureau of Standards. The source used in the case of the former observations was a Back lamp consisting of a spark between metal electrodes operated in an atmosphere of the gas, whereas at the National Bureau of Standards a Geissler tube placed transversely between the poles of the magnet was employed. Measurable patterns were obtained for 130 lines of Xe II and 62 of Xe III. Reasonably good agreement between the observations from the two laboratories was obtained.

Analysis of observed patterns has permitted computation of 61 g values associated with levels of Xe II and 34 of Xe III.

Most of the patterns are only partially resolved. Use of the formulas of Shenstone and Blair to set up observation equations which were adjusted by the method of least squares has permitted calculation of a fairly consistent set of g values. The g-sum rule was tested where possible and was found to be satisfied very closely in case of two different electron configurations in Xe^+. Observed g values depart considerably from those calculated by the Landé formula in most instances. A vector coupling scheme intermediate between LS and Jj is indicated for both Xe^+ and Xe^{++}.

The analysis of Xe II has not required important changes as a result of the Zeeman-effect observations. No changes of J values are indicated. In two instances, pairs of levels are interchanged in the term tables. In Xe III, the revisions are confined mostly to the group of levels of ^2D parentage from the $s^2p^3.6p$ configuration. Changes in the assignment of J values are required in five instances.

CONTENTS

		Page
I.	Introduction	683
II.	Observations	684
III.	Calculation and interpretation of the g factors	685
IV.	Xe II—data and results	687
V.	Xe III—data and results	695
VI.	References	699

I. INTRODUCTION

A series of papers dealing with the analyses of the spectra originating in singly and in doubly ionized xenon have been published jointly or separately by the authors of this paper. A partial analysis of Xe II was published in 1931 [1].[1] In a recent paper [2] this analysis is revised and extended so that nearly all conspicuous lines of Xe II are accounted for. DeBruin announced the first-observed regularities in Xe III in 1935 [3]. Humphreys [4], in 1936, extended the analysis to

* Professor of Physics, Laboratory "Physica," University of Amsterdam, Amsterdam, Holland.

[1] Numbers in brackets indicate the literature references at the end of this paper.

192170—39——4

account for most of the observed lines. Portions of these spectra in the Schumann region have been observed and analyzed by Boyce [5].

The second, third, and probably higher spectra of xenon are excited simultaneously in the sources commonly used, such as the electrodeless discharge or a Geissler tube operated in a circuit containing a spark gap and condensers. Methods of identifying a particular spectrum or of favoring its production are discussed in the literature referred to. Lines of the third, or higher, spectra appearing in the Geissler-tube source are weakened or suppressed, by inserting suitable amounts of inductance in the discharge circuit.

The earlier work of the authors, as well as that of Bloch, Bloch, and Déjardin [6, 7] has made it possible to classify almost all xenon lines according to the ions in which they originate.

A few Zeeman patterns in Xe III were available to deBruin when he published his paper on the Spectral Structure of the Doubly Ionized Noble Gases [3]. These had been observed by C. J. Bakker at the laboratory "Physica" in Amsterdam, but the results had not been published. The other investigations of the structure of Xe II and Xe III were carried out without the aid of the Zeeman effect.

II. OBSERVATIONS

Early in 1938 deBruin communicated to the other authors of this paper a set of Zeeman effect observations in xenon spectra in the region between 3400 and 5600 A. These observations included about 60 patterns for Xe II and 20 for Xe III. A number of additional patterns were indicated as "provisional." These have been incorporated into the tables in cases where interpretation of the patterns gave results consistent with other observations.

A year later, Zeeman effect observations in Xe II and Xe III were made at the National Bureau of Standards. These observations duplicated in part the earlier work but extended farther into the red to about 7000 A, and yielded measurable patterns of several intense low-level lines of Xe II not observed by deBruin. Ninety-seven patterns of Xe II and 62 of Xe III were measured. Most of the patterns were recorded more than once, a few as many as four times. A 30,000-line/inch grating was used for all the observations at the National Bureau of Standards. The ultraviolet lines were observed in both the first and second order spectra, whereas first order observations only were available for lines of wave length greater than 4250 A. The essential difference between the Amsterdam and Washington observations was in the sources employed. DeBruin used a Back lamp [8], which consists of a chamber containing the noble gas at low pressure mounted between the magnetic poles. A metallic spark is passed through the narrow space between the pole pieces. The spectra of the gas are excited along with the spectrum from the electrodes. This type of source probably yields sharper patterns but has the disadvantage of low intensity, making it necessary to maintain the magnet in operation for very long periods of time.

Geissler-tube sources were used in all of the observations at the National Bureau of Standards, the intensities of these sources permitted satisfactory spectrograms to be obtained in exposure times ranging from 30 to 60 minutes but the tubes, mounted with the capillary portion between the pole pieces and at right angles to the field, quickly became unserviceable because the discharge, driven

against the capillary wall by the magnetic field darkened or caused disintegration of the tube wall. Tubes designed to be inserted in bored pole pieces to permit passage of the discharge parallel to the field were not used, because, according to Back [8], it is not possible to get a uniform field in the region of observation between bored pole pieces. A current of 150 amperes was maintained in the magnet windings by means of a motor generator. The applied electromotive force was about 100 volts. The field strength calculated from standard patterns of sodium, zinc, magnesium, and aluminum amounted to very nearly 36,000 gausses.

The greatest disadvantage of the use of condensed discharges from Geissler tubes is that the lines are not very sharp. Only in case of transitions between levels of small J values, ½ to ½ or ½ to 1½ in a spectrum of even multiplicity, such as Xe II, are completely resolved patterns obtainable. Resolution of the parallel components was obtained in only a few instances.

III. CALCULATION AND INTERPRETATION OF THE *g* FACTORS

The theoretical interpretation of the so-called anomalous Zeeman effect is too well known to require any extended discussion. The observed pattern results from the combination of levels, one or both of which are separated into a number of components by a magnetic field. These level displacements are accounted for by the acquisition of quantized amounts of energy $Mg\mathbf{L}$ in which M, the magnetic quantum number, stands for the quantized values of the projection of the vector J upon the vector H. There are $2J+1$ values of M, increasing by steps of one from $-J$ to $+J$. At the very beginning of the development of the quantum theory, Landé [9] set up a formula for the g factor. It was later shown that this g was the ratio of the magnetic to the mechanical angular momentum of the atom. $\mathbf{L}$ is the Lorentz unit[1] given by $He/4\pi mc^2$. It expresses the splitting which occurs in the normal Zeeman triplet. It is customary to specify all patterns in terms of these units of normal Zeeman splitting. The displacements of the components of a level are given then by the various products, Mg, where M takes all permitted values.

In cases where the coupling between the quantum vectors is of the *LS* type, a completely resolved Zeeman pattern may be analyzed to yield the quantum numbers, J, L, and S, associated with each of the combining levels.

It becomes apparent, therefore, that Zeeman-effect observations are extremely helpful in the assignment of quantum numbers to the levels of a spectrum. Complete tables of theoretical Zeeman patterns of the Landé type have been prepared by Kiess and Meggers [10] for transitions between levels belonging to terms of all multiplicities which may be expected to occur. Identification of any pattern by aid of the tables establishes the term transition responsible for the line as well as the g factor for each level.

If the coupling is not of the *LS* type, the splitting factors, or g values, may still be derived from observed patterns if the J's of the combining levels are known. If more than one pattern involving the same level is observed, it is generally possible to determine an un-

[1] The symbol m in this expression refers to the mass of the electron. It is not used in this sense elsewhere in this paper.

known J. Characteristic distributions of intensities of components in the pattern are shown, depending on whether the combining J's are equal or unequal. These features are easily recognized by the experienced observer. The solution of simultaneous linear equations involving the g's and magnetic quantum numbers of combining levels was first illustrated by Back [11] and is also discussed in the paper by Kiess and Meggers just referred to [10].

Theoretical g values may be calculated by the following formula, in cases of Jj-coupling:

$$g=g_i\frac{J(J+1)+j_i(j_i+1)-J_p(J_p+1)}{2J(J+1)}+g_p\frac{J(J+1)+J_p(J_p+1)-j_i(j_i+1)}{2J(J+1)}$$

The subscripts i and p refer, respectively, to the added electron and the parent configuration. It is not always possible to select the values of j_i and J_p which combine to give J for a particular level. One can, however, tabulate the complete set, calculate the g's and then make the most reasonable correlation with the observed g's. One is required to make some assumption regarding g_p. If the parent level has LS coupling, it is found at once from the Landé formula. This assumption has been made in our calculations, because the parent levels are the lowest in doubly ionized xenon. Zeeman effects cannot be observed for lines involving these levels, because they appear in the extreme-ultraviolet region, but in spectra where g values have been determined for the lowest states, they are always of the Landé type. Other possibilities are that the parent level may have pure Jj coupling, or some type of intermediate coupling. The g values for s^2p^4, on the assumption of pure Jj coupling are the same as for s^2p^2 and may be obtained by the above formula using the J's for two p electrons. Calculation of g's, on the assumption of pure Jj coupling for the parent levels, were made for some of the levels of Xe II but are not included in the tables, because the results indicated this assumption to be less probable than that of LS coupling for the normal configuration of the Xe^{++} ion. It is probable that the coupling is actually of intermediate type as is to be expected in spectra of heavier noble gases. The matter will be discussed further, when the results are treated in detail. Other observers have had considerable success in the calculation of g's for cases of intermediate coupling, and in the interpretation of observed patterns. An excellent example is the work of Green on the first spectra of noble gases [12].

Determination of a complete set of g values, for the levels arising from a given electron configuration, permits the application of the g-sum rule [13]. According to this rule, the sum of the g's, associated with levels from a particular configuration, which have the same J value, is independent of the coupling scheme. This sum may be obtained, of course, by adding the Landé g's for the levels of given J predicted by the Hund theory for that configuration. Application of the rule is extremely useful in determining parentages and electron configurations associated with the levels of a spectrum.

In the present investigation, the problem of determining g values was of considerable difficulty because not only was the vector coupling not of the LS type, but most of the patterns were only partially

resolved. Fortunately, the previous analysis of Xe II and Xe III had given a generally correct assignment of J values. For the calculation of g values of partially resolved patterns, one must resort to the formulas of Shenstone and Blair [14]. These formulas are based on the theoretical distribution of intensities of components calculated by Hönl [15], and express the displacement of the center of intensity of an unresolved group of components in terms of the g's and J's of the combining levels. The formulas are of comparatively simple form. It turns out that, where $\Delta M=1$, the center of intensity of an unresolved group of n components is one-fourth the distance from the strongest to the weakest component. Where $\Delta M=0$, the pattern of n components is symmetrical about its own center, so that twice the measured displacement of an unresolved n component gives directly the sum of the two g's. Shenstone and Blair remark that the use of their formulas is most satisfactory for term transitions involving nearly equal g's, especially in cases where the pattern is rather compact, and far from complete resolution. It is apparent, of course, that such formulas can be correct only to the extent that the actual intensity distribution in the pattern is the same as that theoretically predicted. We assume this to be true in employing the formulas, although the rather large departure from LS coupling in these spectra may result in intensity distributions among the Zeeman components somewhat different from those given by the Hönl formulas. In the analysis of nearly resolved open patterns, it is sometimes best to assume that the measured positions of the components are the actual positions of the strongest components.

The Shenstone and Blair formulas may be applied if one of the g's is known and if we have the distance of the center of intensity of either the n or p components from the undisplaced line position, or if both p and n components are partially resolved, giving two equations involving the respective g's. In the latter case, it is necessary to decide which g to assign to its respective level, if both are previously unknown. Usually a given level appears in a considerable number of transitions. This makes possible the writing of systems of simultaneous equations involving several observed patterns. Using the methods of least-squares adjustments, these observation equations may be transformed into normal equations and be solved to give the most probable set of g's. It is quite possible to adjust the entire set of observations in one normal solution. Because of the length and complexity of such an operation, it was found simpler in this investigation to make several small adjustments, each involving not more than about six observation equations.

IV. Xe II—DATA AND RESULTS

All observed patterns in Xe II which were satisfactory for measurement are listed in table 1. Here are shown in successive columns the wave lengths, wave numbers, term combinations, Zeeman patterns observed by Humphreys and Meggers, Zeeman patterns observed by deBruin, and the Zeeman patterns, calculated from the set of g values, which appeared to be most consistent from the data as a whole.

TABLE 1.—*Zeeman patterns in* Xe II

Wave length (air)	Wave number (vac)	Term combination	Observed Zeeman pattern Humphreys-Meggers	Observed Zeeman pattern deBruin	Calculated Zeeman pattern
A	cm^{-1}				
3500.36	28560.35	$(^3P)6s\ ^4P_{2\frac{1}{2}}-(^3P)6p\ ^4S^0_{1\frac{1}{2}}$	(0.00) 1.80		**(0.14,** 0.42) 1.14, 142, 1.70, **1.98**
3506.56	28509.85	$(^3P)6s\ ^4P_{0\frac{1}{2}}-(^1D)6p\ ^2P^0_{1\frac{1}{2}}$		(0.51) ——	(0.50) **0.87,** 1.87
3508.88	28491.00	$(^3P)6s\ ^2P_{0\frac{1}{2}}-(^1D)6p\ ^2P^0_{0\frac{1}{2}}$		(0.00) 0.64	(0.00) 0.64
3564.30	28048.02	$(^3P)6s\ ^4P_{1\frac{1}{2}}-(^3P)6p\ ^2D^0_{2\frac{1}{2}}$	(0.00) 1.46		**(0.01,** 0.03) 1.38, 1.40, 1.42, 1.44
3612.37	27674.79	$(^3P)5d\ ^4D_{3\frac{1}{2}}-(^3P)6p\ ^3D^0_{2\frac{1}{2}}$	(0.00) 1.39	(0.00) 1.42	**(0.01,** 0.02, 0.09) **1.38,** 1.39, 1.40, 1.41, 1.42, 1.43
3644.91	27427.75	$(^3P)5d\ ^2P_{1\frac{1}{2}}-(^1D)\ 6p\ ^2P^0_{0\frac{1}{2}}$		(0.22) 0.92, **1.36**	**(0.22)** 0.93, **1.35**
3672.57	27221.16	$(^3P)5d\ ^4D_{1\frac{1}{2}}-(^3P)6p\ ^2P^0_{1\frac{1}{2}}$	(0.00) 1.33		(0.11, **0.33**) 1.06, **1.28,** 1.50
3711.64	26934.63	$(^3P)6p\ ^4P^0_{1\frac{1}{2}}-20_{0\frac{1}{2}}$		(0.00) 1.53	(0.15) **1.46,** 1.75
3717.20	26894.35	$(^3P)5d\ ^2P_{1\frac{1}{2}}-(^1D)6p\ ^2D^0_{2\frac{1}{2}}$	(0.00) 1.25		**(0.01,** 0.03) 1.19, 1.21, 1.23, **1.25**
3720.80	26868.33	$(^3P)6s\ ^2P_{1\frac{1}{2}}-(^1D)6p\ ^2P^0_{1\frac{1}{2}}$	(0.00) 1.47	(0.25) 1.50	(0.10, **0.31**) 1.26, **1.47, 1.68**
3731.18	26793.58	$(^3P)5d\ ^2P_{0\frac{1}{2}}-(^1D)6p\ ^2P^0_{0\frac{1}{2}}$		(0.34) 1.04	(0.33) 1.05
3763.37	26564.41	$(^3P)6s\ ^4P_{1\frac{1}{2}}-(^3P)6p\ ^4S^0_{1\frac{1}{2}}$	(0.00) 1.30		(0.05, **0.16**) 1.22, **1.33, 1.44**
3811.05	26232.07	$(^1D)6s\ ^3D_{1\frac{1}{2}}-7i_{1\frac{1}{2}}$	(0.00) 1.41		**(0.03,** 0.09) 1.25, **1.31, 1.37,** 1.43
3858.53	25909.29	$sp^6\ ^2S_{0\frac{1}{2}}-(^3P)6p\ ^4D^0_{1\frac{1}{2}}$		(0.36) 1.06	(0.32) **1.04,** 1.68
3869.63	25834.97	$(^3P)5d\ ^4P_{0\frac{1}{2}}-(^1D)6p\ ^2P^0_{0\frac{1}{2}}$		(0.54) 1.24	(0.53) 1.25
3907.91	25581.91	$(^3P)6p\ ^4D^0_{3\frac{1}{2}}-(^3P)6d\ ^4F_{2\frac{1}{2}}$		(0.17) 1.22	(0.05, 0.15, 0.23) 0.99, 1.09, 1.19, 1.29, 1.39
3954.53	25279.05	$(^1D)5d\ ^2F_{2\frac{1}{2}}-15^0_{2\frac{1}{2}}$		(0.00) 1.08	(0.00) 1.08
3972.58	25165.46	$(^1D)6p\ ^2F^0_{2\frac{1}{2}}-(^1D)6d\ ^2F_{2\frac{1}{2}}$		0.85(0.39) (0.19) 1.03	
3990.33	25053.52	$(^3P)6p\ ^4P^0_{2\frac{1}{2}}-20_{0\frac{1}{2}}$		(0.18) 1.68	(0.20) 1.69
4002.35	24978.29	$(^1S)5d\ ^2D_{1\frac{1}{2}}-35^0_{2\frac{1}{2}}$		(0.00) 1.00	
4025.19	24836.55	$(^3P)5d\ ^2D_{1\frac{1}{2}}-(^1D)6p\ ^2P^0_{0\frac{1}{2}}$	(——) 1.41	**(0.24)** 1.00, **1.47**	**(0.23)** 0.94, **1.39**
4037.29	24762.12	$(^3P)6p\ ^4P^0_{1\frac{1}{2}}-18_{0\frac{1}{2}}$		(0.33) 1.27, **1.92**	(0.33) **1.27, 1.93**
4037.59	24760.28	$(^3P)6p\ ^2S^0_{0\frac{1}{2}}-(^3P)6d\ ^2D_{1\frac{1}{2}}$		(——) 0.53	(0.53) **0.46,** 1.53
4044.64	24717.12	$(^3P)6p\ ^4P^0_{1\frac{1}{2}}-16_{1\frac{1}{2}}$		(0.19) 1.64	(**0.04, 0.12**) 1.56, **1.64, 1.72**
4098.89	24389.99	$(^3P)6p\ ^4P^0_{2\frac{1}{2}}-12_{1\frac{1}{2}}$		(0.23) 0.79	(0.23) **0.79,** 1.25
4100.34	24381.37	$(^3P)5d\ ^4D_{1\frac{1}{2}}-(^3P)6p\ ^4D^0_{0\frac{1}{2}}$	(——) 1.35		(0.27) 0.90, **1.44**
4104.95	24353.98	$(^3P)5d\ ^2P_{1\frac{1}{2}}-(^1D)6p\ ^2P^0_{1\frac{1}{2}}$	(0.00) 1.28	(0.40) 1.26	(0.08, **0.25**) 1.11, **1.28,** 1.45
4131.01	24200.35	$(^1D)6s\ ^3D_{2\frac{1}{2}}-(^1D)6p\ ^2D^0_{2\frac{1}{2}}$	(——) **1.36**		(**0.01,** 0.03, 0.05) **1.19,** 1.21, 1.23, **1.25, 1.27**
4158.04	24043.04	$(^3P)6p\ ^2S^0_{0\frac{1}{2}}-(^3P)6d\ ^2P_{0\frac{1}{2}}$		(0.84) 1.23	(0.84) 1.23
4162.16	24019.24	$(^3P)5d\ ^2D_{1\frac{1}{2}}-(^1D)6p\ ^2D^0_{1\frac{1}{2}}$	(—*d*) 1.05	(0.45) ——	(0.10, **0.31**) 0.84, **1.05,** 1.26
4193.15	23841.72			(0.00) 0.92	
4208.48	23754.88	$(^3P)6p\ ^4P^0_{1\frac{1}{2}}-(^3P)6d\ ^4D_{2\frac{1}{2}}$	(0.00) 1.39	(0.00) 0.90	(**0.09,** 0.28) 1.15, 134, 153, 172
4209.47	23749.29	$(^3P)6p\ ^4P^0_{2\frac{1}{2}}-(^3P)6d\ ^4D_{1\frac{1}{2}}$	(——) 1.36	(0.00) 1.58	(0.08, 0.24) 1.24, 1.40, 1.56, 1.72
4213.72	23725.34	$(^3P)6p\ ^4D^0_{3\frac{1}{2}}-(^3P)6d\ ^4P_{1\frac{1}{2}}$	(0.00) 1.07	(0.00) 0.82	(0.17) 0.80, 1.15
4214.69	23719.88	$(^3P)5d\ ^2P_{0\frac{1}{2}}-(^1D)6p\ ^2P^0_{1\frac{1}{2}}$		(0.00) 1.41	(0.01) 1.39, 1.41
4215.60	23714.76	$(^3P)6s\ ^4P_{2\frac{1}{2}}-(^3P)6p\ ^4D^0_{1\frac{1}{2}}$	(0.00) 1.72	(0.00) 1.73	(**0.09,** 0.27) 1.29, **1.47,** 1.65, **1.83**
4223.00	23673.20	$(^3P)6p\ ^2P^0_{1\frac{1}{2}}-14_{2\frac{1}{2}}$		(0.14) 0.52	
4238.25	23588.02	$(^3P)6p\ ^4P^0_{2\frac{1}{2}}-(^3P)6d\ ^4D_{2\frac{1}{2}}$	(0.00) 1.41*H*	(0.34) 1.38	(**0.02,** 0.07, **0.12**) **1.35,** 1.40, 1.45, **1.50,** 1.55
4244.41	23553.79	$(^3P)5d\ ^2P_{1\frac{1}{2}}-(^3P)6p\ ^2F^0_{2\frac{1}{2}}$	(0.00) 1.71		(**0.14,** 0.42) 0.80, 0.78, 1.06, 1.34
4245.38	23548.41	$(^3P)6p\ ^4P^0_{1\frac{1}{2}}-(^3P)6d\ ^4D_{3\frac{1}{2}}$	(0.00) 1.27*h*	(0.00) 1.12	(**0.06,** 0.18, 0.30) **1.06,** 1.18, 1.30, 1.42, 1.54, 1.66
4251.57	23514.12	$(^3P)6p\ ^2P^0_{0\frac{1}{2}}-(^1D)6d\ ^2D_{1\frac{1}{2}}$		)0.00) 1.05	(0.02) **1.04,** 1.10
4263.44	23448.66		(——) 1.32		
4269.84	23413.51	$(^3P)6s\ ^4P_{0\frac{1}{2}}-(^3P)6p\ ^2P^0_{1\frac{1}{2}}$	(—*d*) 1.86		(0.66) 1.79
4296.40	23268.78	$(^3P)6p\ ^4P^0_{1\frac{1}{2}}-(^3P)7s\ ^4P_{0\frac{1}{2}}$	(—*h*) 1.51	(0.21) 1.36, 1.77	(0.22) **1.40,** 1.87
4310.51	23192.61	$(^3P)6p\ ^2D^0_{2\frac{1}{2}}-(^1D)7s\ ^2D_{2\frac{1}{2}}$		(0.22) 1.44	(0.05, 0.16, **0.27**) 1.22, 1.33, 1.44, 1.55, 1.66
4321.82	23131.92	$(^3P)6s\ ^4P_{0\frac{1}{2}}-(^3P)6p\ ^2D^0_{1\frac{1}{2}}$	(—*d*) 0.85		(0.54) **0.83,** 1.91
4330.52	23085.45	$(^3P)6p\ ^4D^0_{3\frac{1}{2}}-(^3P)6d\ ^4F_{3\frac{1}{2}}$	(0.00) 0.99*H*	(0.00) 0.90	
4367.05	22892.34	$(^3P)6p\ ^4D^0_{2\frac{1}{2}}-(^3P)6d\ ^4F_{2\frac{1}{2}}$	(——) 1.53		(0.13, 0.39, 0.65, **0.91**) 0.48, 0.74, **1.00, 1.26,** 1.52, **1.78,** 2.04

TABLE 1.—*Zeeman patterns in* Xe II—Continued

Wave length (air)	Wave number (vac)	Term combination	Observed Zeeman pattern Humphreys-Meggers	Observed Zeeman pattern deBruin	Calculated Zeeman pattern
A	cm^{-1}				
4369.20	22881.08	$(^3P)6p\ ^4P^0_{1/2}-18g_{1/2}$	(——) 1.32	(0.22) 1.23	(0.28) 1.22
4384.93	22799.00	$sp^6\ ^2S_{1/2}-(^3P)6p\ ^4P^0_{1/2}$	(0.00) 1.77	(0.28) 1.71	(0.24) 1.76
4393.20	22756.08	$(^3P)6p\ ^4S^0_{1/2}-(^3P)6d\ ^2D_{3/2}$		(0.00) 1.13	(**0.02**, 0.06) **1.13**, 1.17, 1.21, 1.25
4395.77	22742.77	$(^1D)5d\ ^2F_{3/2}-43g_{1/2}$		(0.00) 1.04	(**0.01**, 0.03, 0.05) **1.01**, 1.03, 1.05, 1.07, 1.09, 1.11
4414.84	22644.54	$(^3P)5d\ ^2D_{3/2}-(^1D)6p\ ^2D^0_{3/2}$	(0.29) **1.28**	(0.27) 1.24	(0.06, 0.18, **0.30**) 1.04, 1.16, **1.28**, 1.40, 1.52
4448.13	22475.07		(0.00) 1.14*III*	(0.00) 1.09	
4462.19	22404.25		(0.00) 1.06*III*	(0.00) 1.07	
4470.90	22360.61	$(^3P)5d\ ^3D_{2/2}-(^1D)6p\ ^3D^0_{1/2}$	(0.00) 1.79*h*		(**0.19**, 0.58) 0.75, 1.14, 1.53, **1.92**
4480.86	22310.90	$(^3P)6p\ ^4D^0_{1/2}-(^3P)6d\ ^4F_{3/2}$		(0.00) 0.88	(**0.11**, 0.34) **0.78**, 1.01, 1.24, 1.47
4524.21	22097.13	$(^3P)6s\ ^4P_{5/2}-(^2P)6p\ ^2P^0_{1/2}$	(**0.58**) **0.79**, 1.92	(**0.54**) **0.74**, 1.83	(**0.53**) **0.86**, 1.92
4532.49	22056.76	$(^1D)6s\ ^2D_{2/2}-(^1D)6p\ ^2F^0_{3/2}$	(0.00) 1.12	(0.00) 1.06	(**0.03**, 0.09, 0.15) **1.03**, 1.09, 1.15, 1.21, 1.27, 1.33
4540.89	22015.96	$(^3P)6p\ ^2D^0_{3/2}-(^1D)7s\ ^2D_{3/2}$	(0.00) 1.22	(0.00) 1.23	(**0.03**, 0.10) **1.19**, 1.26, 1.33, **1.40**
4545.23	21994.94	$(^3P)6p\ ^4D^0_{3/2}-(^3P)6d\ ^4D_{3/2}$	(0.00) 1.62	(0.00) 1.47	(**0.05**, 0.16, 0.27) 1.08, 1.19, 1.30, 1.41, 1.52, **1.63**
4555.94	21943.24	$(^2P)6p\ ^4D^0_{1/2}-20g_{1/2}$		(0.23) 1.13	(0.26) **1.09**, 1.62
4577.06	21841.98	$(^3P)6p\ ^4D^0_{3/2}-(^3P)6d\ ^4D_{3/2}$	(0.00) 1.29		(**0.02**, 0.06, 0.10) **1.29**, 1.33, 1.37, 1.41, 1.45, 1.49
4585.48	21801.88	$(^3P)6p\ ^4D^0_{5/2}-(^3P)6d\ ^4D_{3/2}$	(0.00) 1.33	(0.16) 1.37	(0.01, 0.04, 0.07, **0.10**) 1.28, 1.31, 1.34, **1.37**, 1.40, 1.43, 1.46
4592.05	21770.69	$(^3P)6p\ ^4S^0_{1/2}-(^3P)6d\ ^4P_{3/2}$		(0.00) 1.06	(**0.04**, 0.12) **1.03**, 1.11, 1.19, 1.27
4603.03	21718.76	$(^3P)6s\ ^4P_{1/2}-(^3P)6p\ ^4D^0_{1/2}$	(0.00) 1.39	(0.00) 1.35	(0.00, **0.01**) 1.38, **1.39**, 1.40
4615.50	21660.08	$(^1D)6s\ ^2D_{2/2}-(^1D)6p\ ^2P^0_{1/2}$	(0.00) 1.15	(0.00) 1.04	(**0.07**, 0.20) **1.05**, 1.18, 1.31, 1.44
4633.30	21576.87	$(^3P)5d\ ^4F_{3/2}-(^3P)6p\ ^2D^0_{3/2}$	(——) 0.75		
4651.94	21490.41	$(^3P)6s\ ^2P_{1/2}-(^3P)6p\ ^2D^0_{3/2}$	(0.00) 1.52	(0.39) 1.41	(0.10, **0.31**) 1.27, **1.48**, 1.69
4668.49	21414.23	$(^1D)5d\ ^2D_{1/2}-(^1D)6p\ ^2P^0_{1/2}$	(—*II*) 1.42	(0.26) 0.98, **1.50**	(0.26) 0.98, **1.50**
4674.56	21386.42	$(^3P)5d\ ^4D_{3/2}-(^3P)6p\ ^4D^0_{1/2}$	(——) 1.28		(**0.02**, 0.06) **1.28**, 132, 1.36, 1.40
4698.01	21279.67	$(^3P)6p\ ^4D^0_{1/2}-12g_{1/2}$	(——) 1.18		(0.20, **0.59**) 0.79, **1.18**, 1.57
4712.63	21213.66		(——) 1.44		
4769.05	20962.69	$(^3P)5d\ ^2D_{1/2}-(^1D)6p\ ^2F^0_{1/2}$	(—*II*) 0.61		(**0.12**, 0.36) **0.56**, 0.80, 1.04, 1.28
4779.18	20918.26	$sp^6\ ^2S_{0/2}-(^3P)6p\ ^4P^0_{1/2}$	(——) 1.48		(0.19) **1.43**, 1.81
4787.77	20880.73	$(^1D)5d\ ^2D_{1/2}-(^1D)6p\ ^2D^0_{3/2}$	(0.00) 1.20		(**0.01**, 0.03) **1.19**, 1.21, 1.23, 1.25
4818.02	20749.63	$(^3P)5d\ ^4D_{1/2}-(^3P)6p\ ^4D^0_{1/2}$	(——) 1.30		(0.10, **0.31**) 1.07, **1.28**, 1.49
4823.35	20726.70	$(^3P)6p\ ^4P^0_{1/2}-(^3P)7s\ ^4P_{1/2}$	(——) 1.39*H*		(**0.04**, 0.13) **1.39**, 1.48, 1.57, 1.66
4823.41	20726.45				
4844.33	20636.94	$(^3P)6s\ ^4P_{3/2}-(^3P)6p\ ^4D^0_{3/2}$	(0.00) 1.22	(0.00) 1.04	(**0.08**, 0.25, 0.42) **0.97** 1.14, 1.31, 1.48, 1.65, 1.82
4853.77	20596.81	$(^1D)5d\ ^2D_{1/2}-(^1D)6p\ ^2D^0_{1/2}$	(——) 1.23		(0.15, **0.44**) 0.81, **1.10**, 1.39
4862.45	20560.04	$(^3P)6p\ ^4P^0_{3/2}-(^3P)7s\ ^4P_{3/2}$	(——) 1.53	(0.00) 1.50	(0.02, 0.07, **0.12**) 1.41, 1.46, **1.51**, 1.56, 1.61
4862.54	20559.66				
4876.50	20500.80	$(^3P)5d\ ^2D_{2/2}-(^1D)6p\ ^2F^0_{3/2}$	(0.00) 0.96	(0.00) 0.89	(**0.08**, 0.24, 0.40) **0.78**, 0.94, 1.10, 1.26, 1.42, 1.58
4883.53	20471.29	$(^3P)6s\ ^4P_{5/2}-(^3P)6p\ ^4S^0_{3/2}$	(0.58) **0.70**, 1.83	(——) 0.61	(0.58) **0.70**, 1.86
4887.30	20455.50	$(^3P)6s\ ^2P_{1/2}-(^3P)6p\ ^2P^0_{1/2}$	(0.00*II*) 1.50	(0.37) 1.44	(0.10, **0.29**) 1.30, **1.49**, 1.68
4890.09	20443.83	$(^3P)6s\ ^4P_{3/2}-(^3P)6p\ ^4D^0_{3/2}$	(0.76) 1.40*H*		(0.15, 0.46, **0.77**) 0.78, 1.09, **1.40**, **1.71**, 2.02
4919.66	20320.95	$(^3P)6s\ ^2P_{3/2}-(^3P)6p\ ^2P^0_{1/2}$	(——) 0.88		(0.28) 0.84
4921.48	20313.44	$(^3P)6s\ ^2P_{1/2}-(^3P)6p\ ^2D^0_{3/2}$	(0.00) 1.25	(0.00) 1.21	(**0.08**, 0.25) **1.15**, 1.32, 1.49, 1.66
4972.71	20104.17	$(^3P)5d^4\ D_{2/2}-(^1D)6p\ ^2P^0_{1/2}$	(0.00) 1.30	(0.00) 1.23	(**0.01**, 0.04) **1.29**, **1.32**, **1.35**, **1.38**

TABLE 1.—*Zeeman patterns in* Xe II—Continued

Wave length (air)	Wave number (vac)	Term combination	Observed Zeeman pattern Humphreys-Meggers	Observed Zeeman pattern deBruin	Calculated Zeeman pattern
A	cm^{-1}				
4988.77	20039.45	$(^3P)6s\ ^3P_{0\frac{1}{2}}-(^3P)6p\ ^2D^1_{1\frac{1}{2}}$	(——) 1.72		(0.40) 0.96, 1.77
5044.92	19816.41	$(^1D)6s\ ^3D_{1\frac{1}{2}}-(^1D)6p\ ^2P^0_{0\frac{1}{2}}$		(0.09) 1.02	(0.13) 0.84, 1.10
5080.62	19677.17	$(^3P)6p\ ^4D^1_{3\frac{1}{2}}-(^3P)7s\ ^4P_{1\frac{1}{2}}$		(0.00) 1.10	(0.10, 0.30) 0.94, 1.14, 1.34, 1.54
5191.37	19257.39	$(^3P)6s\ ^4P_{0\frac{1}{2}}-(^3P)6p\ ^4D^1_{0\frac{1}{2}}$	(0.82) 1.45	(0.86) 1.43	(0.91) 1.54
5260.44	19004.54	$(^3P)6s\ ^2P_{0\frac{1}{2}}-(^3P)6p\ ^2P^1_{1\frac{1}{2}}$	(0.00) 1.76	(0.35) 1.55	(0.42) 0.98, 1.81
5261.95	18999.09	$(^1D)6s\ ^3D_{1\frac{1}{2}}-(^1D)6p\ ^2D^1_{1\frac{1}{2}}$	(0.00) 0.94	(0.07) 0.92	(0.01, 0.04) 0.91, 0.94, 0.97
5292.22	18890.42	$(^3P)6s\ ^4P_{2\frac{1}{2}}-(^3P)6p\ ^4P^1_{2\frac{1}{2}}$	(0.00) 1.52	(0.20) 1.48	(0.04, 0.12, 0.20) 1.36, 1.44, 1.52, 1.60, 1.68
5309.27	18829.76	$(^3P)6s\ ^2P_{1\frac{1}{2}}-(^3P)6p\ ^4S^1_{1\frac{1}{2}}$	(0.41) 1.42		(0.15, 0.45) 1.13, 1.43, 1.73
5313.87	18813.46	$(^3P)6p\ ^4D^2_{3\frac{1}{2}}-(^3P)7s\ ^4P_{2\frac{1}{2}}$		(0.00) 0.80	(0.07, 0.21, 0.35) 1.04, 1.18, 1.32, 1.46, 1.60, 1.74
5339.35	18723.67	$(^3P)6s\ ^4P_{2\frac{1}{2}}-(^3P)6p\ ^4P^1_{1\frac{1}{2}}$	(0.00) 1.52	(0.00) 1.50	(0.03, 0.09) 1.47, 1.53, 1.59, 1.65
5372.39	18608.53	$(^3P)6s\ ^4P_{1\frac{1}{2}}-(^3P)6p\ ^4P^0_{0\frac{1}{2}}$	(0.00) 1.37	(0.00) 1.32	(0.06) 1.33, 1.45
5419.15	18447.96	$(^3P)6s\ ^4P_{1\frac{1}{2}}-(^3P)6p\ ^4D^1_{2\frac{1}{2}}$	(0.00) 1.14	(0.00) 1.06	(0.07, 0.21) 1.04, 1.18, 1.32, 1.46
5438.96	18380.77	$(^3P)6s\ ^2P_{1\frac{1}{2}}-(^3P)6p\ ^2S^1_{0\frac{1}{2}}$	(0.24) 1.32, 1.80	(0.27) 1.25	(0.24) 1.34, 1.82
5460.39	18308.63	$(^3P)5d\ ^4D_{3\frac{1}{2}}-(^3P)6p\ ^4D^1_{3\frac{1}{2}}$	(0.00) 1.45		(0.02, 0.07, 0.12) 1.26, 1.31, 1.36, 1.41, 1.46, 1.51
5472.61	18267.75	$(^3P)5d\ ^4D_{3\frac{1}{2}}-(^3P)6p\ ^4D^1_{2\frac{1}{2}}$	(0.00) 1.39		(0.00, 0.01, 0.02, 0.03) 1.36, 1.37, 1.38, 1.39, 1.40, 1.41, 1.42
5531.07	18074.68	$(^3P)5d\ ^4D_{3\frac{1}{2}}-(^3P)6p\ ^4D^1_{3\frac{1}{2}}$	(0.00) 1.60		(0.07, 0.22, 0.37) 1.02, 1.17, 1.32, 1.47, 1.62, 1.77
5581.93	17909.99			(0.15) 1.00	
5616.67	17799.21	$(^3P)5d\ ^2P_{1\frac{1}{2}}-(^3P)6p\ ^2D^1_{2\frac{1}{2}}$	(0.00) 1.54		(0.10, 0.31) 1.10, 1.31, 1.52, 1.73
5659.38	17664.89	$(^3P)5d\ ^4P_{0\frac{1}{2}}-(^3P)6p\ ^4P^1_{0\frac{1}{2}}$	(0.36) 1.46		(0.36) 1.46
5667.56	17639.39	$(^3P)5d\ ^4D_{1\frac{1}{2}}-(^3P)6p\ ^4P^1_{0\frac{1}{2}}$	(0.15) 1.05		(0.17) 1.00, 1.34
5719.61	17478.87	$(^3P)5d\ ^4D_{1\frac{1}{2}}-(^3P)6p\ ^4D^1_{2\frac{1}{2}}$	(0.00) 1.32		(0.04, 0.12) 1.13, 1.21, 1.29, 1.37
5726.91	17456.59	$(^1D)5d\ ^3F_{2\frac{1}{2}}-(^1D)6p\ ^2D^1_{2\frac{1}{2}}$	(0.00) 1.15		(0.07, 0.21, 0.35) 0.87, 1.01, 1.15, 1.29, 1.43
5751.03	17383.38	$(^3P)5d\ ^4P_{0\frac{1}{2}}-(^3P)6p\ ^2D^1_{1\frac{1}{2}}$	(0.00) 1.22		(0.22) 1.15, 1.60
5758.65	17360.38	$(^1D)5d\ ^3D_{3\frac{1}{2}}-(^1D)6p\ ^3F^1_{3\frac{1}{2}}$	(0.00) 1.27		(0.03, 0.10, 0.17) 1.00, 1.07, 1.14, 1.21, 1.28, 1.35
5776.39	17307.06	$(^3P)5d\ ^2P_{0\frac{1}{2}}-(^3P)6p\ ^2P^1_{1\frac{1}{2}}$	(0.00) 1.33		(0.01) 1.39
5905.13	16929.75	$(^3P)6s\ ^2P_{0\frac{1}{2}}-(^3P)6p\ ^2S^1_{0\frac{1}{2}}$	(0.77) 1.31		(0.75) 1.31
5945.53	16814.71	$(^3P)5d\ ^4D_{0\frac{1}{2}}-(^3P)6p\ ^4P^0_{0\frac{1}{2}}$	(0.46) 0.96		(0.50) 1.00
5976.46	16727.69	$(^3P)6s\ ^4P_{1\frac{1}{2}}-(^3P)6p\ ^4P^1_{1\frac{1}{2}}$	(0.30) 1.50		(0.11, 0.34) 1.27, 1.50, 1.73
6036.20	16562.14	$(^3P)5d\ ^4D_{2\frac{1}{2}}-(^3P)6p\ ^4P^1_{2\frac{1}{2}}$	(0.27) 1.41		(0.07, 0.21, 0.35) 1.13, 1.27, 1.41, 1.55, 1.69
6051.15	16521.22	$(^3P)5d\ ^4D_{3\frac{1}{2}}-(^3P)6p\ ^4P^1_{2\frac{1}{2}}$	(0.00) 1.29		(0.04, 0.12, 0.20) 1.20, 1.28, 1.36, 1.44, 1.52, 1.60
6097.59	16395.39	$(^3P)5d\ ^4D_{2\frac{1}{2}}-(^3P)6p\ ^4P^1_{1\frac{1}{2}}$	(0.37) 1.07		(0.14, 0.42) 0.92, 1.20, 1.48, 1.66
6101.43	16385.07	$(^3P)5d\ ^2D_{1\frac{1}{2}}-(^3P)6p\ ^2D^1_{1\frac{1}{2}}$	(0.00) 1.26		(0.10, 0.31) 1.05, 1.26, 1.47
6270.82	15942.48	$(^1D)6s\ ^3D_{1\frac{1}{2}}-(^1D)6p\ ^3F^1_{2\frac{1}{2}}$	(0.00) 0.92		(0.00) 0.92
6277.54	15925.41	$(^3P)5d\ ^4D_{1\frac{1}{2}}-(^3P)6p\ ^4P^1_{2\frac{1}{2}}$	(0.00) 1.70		(0.15, 0.46) 1.01, 1.32, 1.63, 1.94
6300.86	15866.47	$(^3P)5d\ ^2P_{1\frac{1}{2}}-(^3P)6p\ ^2S^1_{0\frac{1}{2}}$	(0.51)——		(0.43) 0.77, 1.63
6343.96	15758.68	$(^3P)5d\ ^4D_{1\frac{1}{2}}-(^3P)6p\ ^4P^1_{1\frac{1}{2}}$	(0.63) 1.00, 1.57		(0.22, 0.67) 0.95, 1.40, 1.85
6512.83	15350.07	$(^3P)5d\ ^2D_{1\frac{1}{2}}-(^3P)6p\ ^2P^1_{1\frac{1}{2}}$	(0.00) 1.23		(0.12, 0.35) 1.04, 1.27, 1.40
6595.01	15158.80		(0.00) 1.02		
6805.74	14689.43	$(^3P)5d\ ^4F_{3\frac{1}{2}}-(^3P)6p\ ^4D^1_{3\frac{1}{2}}$	(0.00) 0.85		(0.09, 0.27, 0.45) 0.62, 0.80, 0.98, 1.16, 1.34, 1.52
6990.88	14300.41	$(^3P)5d\ ^4F_{4\frac{1}{2}}-(^3P)6p\ ^4D^1_{3\frac{1}{2}}$	(0.00) 1.10		(0.05, 0.15, 0.25, 0.35) 0.94, 1.04, 1.14, 1.24, 1.34, 1.44, 1.54, 1.64

As the two sets of data were obtained in different laboratories and by different observers using techniques not exactly the same, it has been decided to make a separate tabulation. In general, reasonably good agreement has been obtained from lines involving levels of low J value which have relatively simple patterns. In a majority of instances both deBruin's displacement of components and g values are somewhat lower than those observed at the NBS. No very plausible reason for the discrepancy has been found. The field strengths in the case of the Washington observations were calculated partly from patterns obtained with metallic spark sources and partly from the sodium lines appearing in the tube discharge. No appreciable discrepancies were found for the resulting field strengths calculated from patterns yielded by these different types of sources when both were operated during the same run of the magnet.

The calculated Zeeman patterns appearing in the final column of table 1 were obtained from the g values derived from the observations by Humphreys and Meggers, where such observed g's were available. The remaining calculated patterns, some 20 in all, were computed from g values derived from deBruin's data. In some cases the g value could be established only from deBruin's observations. The best instance is that of the level $(^1D)6p\ ^2P^\circ_{0\frac{1}{2}}$, which was observed by deBruin in several combinations giving well-resolved patterns, whereas the same lines were too weak to appear on our plates with the exposures used.

Observed and calculated g values in Xe II are listed in table 2 with the corresponding level values and designations. In successive columns are shown parentages, electron configurations, quantum designations, and numerical values of the various levels. These are followed in order by the appropriate g values, observed by Humphreys and Meggers, observed by deBruin, calculated by the Landé formula, and calculated for Jj coupling. The term table does not list all known levels but is complete as far as the levels due to $6s$, $6p$, or $5d$ are concerned. That is, a place is assigned to all such levels in the table, even though some of them are still unknown. This was done in order that complete theoretical calculations might be shown. Only those levels of higher n value are listed for which g values have been determined from observations. A few levels are given a different designation from that indicated in the earlier publication, although all J values have been retained. These changes are discussed in succeeding paragraphs. Previous assignments [2] are listed in the final column of table 2. The theoretical calculation of g's for Jj coupling is correct for the groups as a whole, because it can be verified by the g-sum rule. Individual correlations of levels for LS and Jj coupling are necessarily somewhat arbitrary, since it is not certain how series-forming terms approach their limits in spectra of noble-gas type. The correlations are based largely on evidence from observed g's. It is apparent that in a spectrum showing higher series numbers, if successive members of the same series yielded the same observed g values, in other words, if Preston's law were obeyed, these g values might assist in determining how the levels of a multiple limit are approached. This statement applies only to cases where the valence electron is added in Jj fashion or very nearly so.

TABLE 2.—*g values*—Xe II *levels*

Xe II levels			Observed g, Humphreys and Meggers	Observed g, deBruin	Calculated g, Landé formula	Calculated g, Jj coupling	Previous designation, RP1164
Origin	Designation	Magnitude					
$5s\,5p^5$	$^2S_{0\frac{1}{2}}$	80194. 57	2. 00	2. 00	2. 00	2. 00	
$5s^2\,5p^4\,(^3P)6s$	$^4P_{2\frac{1}{2}}$	78000. 00	1. 56	1. 53	1. 60	1. 60	
	$^4P_{1\frac{1}{2}}$	76004. 06	1. 39	——	1. 73	1. 40	
	$^4P_{0\frac{1}{2}}$	69910. 89	2. 45	2. 37	2. 67	2. 00	
	$^2P_{1\frac{1}{2}}$	68269. 34	1 58	1. 58	1. 33	1. 67	
	$^2P_{0\frac{1}{2}}$	66818. 34	0. 56	0. 58	0. 67	1. 33	
$5s^2\,5p^4(^1D)6s$	$^2D_{2\frac{1}{2}}$	63061. 15	1. 24	1. 19	1. 20	1. 20	$5s^2\,5p^4\,(^3P)5d\,^2D_{2\frac{1}{2}}$
	$^2D_{1\frac{1}{2}}$	58143. 70	0. 92	0. 97	0. 80	0. 80	
$5s^2\,5p^4\,(^1S)6s$	$^2S_{0\frac{1}{2}}$	46998. 31	——	——	2. 00	2. 00	
$5s^4\,5p^4\,(^3P)5d$	$^4F_{4\frac{1}{2}}$	71663. 50	1. 29	——	1. 33	1. 33	
	$^4F_{3\frac{1}{2}}$	72245. 54	1. 07	——	1. 24	1. 29	
	$^4F_{2\frac{1}{2}}$	69532. 75	——	——	1. 03	1. 20	
	$^4F_{1\frac{1}{2}}$	——	——	——	0. 40	0. 99	
	$^4D_{3\frac{1}{2}}$	75630. 80	1. 40	——	1. 43	1. 32	
	$^4D_{2\frac{1}{2}}$	75671. 72	1. 34	——	1. 37	1. 30	
	$^4D_{1\frac{1}{2}}$	75034. 96	1. 17	——	1. 20	1. 24	
	$^4D_{0\frac{1}{2}}$	74210. 26	0. 50	——	0. 00	0. 33	
	$^4P_{2\frac{1}{2}}$	64593. 23	——	——	1. 60	1. 24	
	$^4P_{1\frac{1}{2}}$	63686. 65	——	——	1. 73	1. 36	
	$^4P_{0\frac{1}{2}}$	64162. 29	1. 82	1. 79	2. 67	2. 20	$5s^2\,5p^4\,(^3P)5d\,^2P_{0\frac{1}{2}}$
	$^2F_{3\frac{1}{2}}$	——	——	——	1. 14	1. 20	
	$^2F_{2\frac{1}{2}}$	——	——	——	0. 86	1. 08	
	$^2D_{2\frac{1}{2}}$	61505. 25	1. 34	1. 31	1. 20	1. 23	$5s^2\,5p^4\,(^1D)6s\,^2D_{2\frac{1}{2}}$
	$^2D_{1\frac{1}{2}}$	63163. 90	1. 16	1. 23	0. 80	0. 80	
	$^2P_{1\frac{1}{2}}$	65755. 07	1. 20	1. 14	1. 33	1. 08	
	$^2P_{0\frac{1}{2}}$	65120. 86	——	1. 38	0. 67	0. 80	$5s^2\,5p^4\,(^3P)5d\,^4P_{0\frac{1}{2}}$
$5s^2\,5p^4\,(^1D)5d$	$^2G_{4\frac{1}{2}}$	——	——	——	1. 11	1. 11	
	$^2G_{3\frac{1}{2}}$	——	——	——	0. 89	0. 91	
	$^2F_{3\frac{1}{2}}$	56154. 44	——	——	1. 14	1. 11	
	$^2F_{2\frac{1}{2}}$	56317. 32	1. 08	——	0. 86	0. 93	
	$^2D_{2\frac{1}{2}}$	58364. 82	1. 11	——	1. 20	1. 13	
	$^2D_{1\frac{1}{2}}$	59741. 47	1. 24	1. 24	0. 80	0. 96	
	$^2P_{1\frac{1}{2}}$	43541. 0	——	——	1. 33	1. 17	
	$^2P_{0\frac{1}{2}}$	44057. 7	——	——	0. 67	1. 20	
	$^2S_{0\frac{1}{2}}$	41819. 9	——	——	2. 00	1. 47	
$5s^2\,5p^4\,(^1S)5d$	$^2D_{2\frac{1}{2}}$	51982. 90	——	——	1. 20	1. 20	
	$^2D_{1\frac{1}{2}}$	46766. 22	——	——	0. 80	0. 80	
$5s^2\,5p^4\,(^3P)6p$ --	$^4D^o_{3\frac{1}{2}}$	57363. 07	1. 39	1. 39	1. 43	1. 43	
	$^4D^o_{2\frac{1}{2}}$	57556. 11	1. 24	1. 24	1. 37	1. 33	
	$^4D^o_{1\frac{1}{2}}$	54285. 29	1. 38	1. 36	1. 20	1. 47	
	$^4D^o_{0\frac{1}{2}}$	50653. 53	0. 63	——	0. 00	0. 67	
	$^4P^o_{2\frac{1}{2}}$	59109. 56	1. 48	1. 45	1. 60	1. 44	
	$^4P^o_{1\frac{1}{2}}$	59276. 32	1. 62	1. 60	1. 73	1. 67	
	$^4P^o_{0\frac{1}{2}}$	57395. 55	1. 51	1. 49	2. 67	1. 67	
	$^4S^o_{1\frac{1}{2}}$	49439. 60	1. 28	1. 23	2. 00	1. 33	
	$^2D^o_{2\frac{1}{2}}$	47955. 90	1. 41	1. 39	1. 20	1. 40	
	$^2D^o_{1\frac{1}{2}}$	46778. 90	1. 37	1. 27	0. 80	1. 22	
	$^2P^o_{1\frac{1}{2}}$	47813. 79	1. 39	1. 30	1. 33	1. 38	
	$^2P^o_{0\frac{1}{2}}$	46497. 38	1. 13	——	0. 67	1. 22	
	$^2S^o_{0\frac{1}{2}}$	49888. 58	2. 06	2. 07	2. 00	1. 78	

TABLE 2.—*g values*—Xe II *levels*—Continued

Xe II levels			Observed g, Humphreys and Meggers	Observed g, deBruin	Calculated g, Landé formula	Calculated g, Jj coupling	Previous designation, RP1164
Origin	Designation	Magnitude					
$5s^2\,5p^4\,(^1D)6p$--	$^2F^o_{3½}$	41004. 37	1. 18	1. 13	1. 14	1. 14	
	$^2F^o_{2½}$	42201. 21	0. 92	——	0. 86	0. 93	
	$^2D^o_{2½}$	38860. 72	1. 22	1. 17	1. 20	1. 12	
	$^2D^o_{1½}$	39144. 64	0. 95	——	0. 80	1. 07	
	$^2P^o_{1½}$	41401. 03	1. 37	1. 40	1. 33	1. 07	
	$^2P^o_{0½}$	38327. 31	——	0. 71	0. 67	0. 67	
$5s^2\,5p^4\,(^1S)6p$--	$^2P^o_{1½}$	30858. 18	——	——	1. 33	1. 33	
	$^2P^o_{0½}$	——	——	——	0. 67	0. 67	
$5s^2\,5p^4\,(^3P)7s$--	$^4P_{2½}$	38549. 7	1. 53	1. 52	1. 60	1. 60	
	$^4P_{1½}$	37879. 2	——	1. 45	1. 73	1. 40	
	$^4P_{0½}$	36007. 5	2. 06	1. 98	2. 67	2. 00	
$5s^2\,5p^4\,(^1D)7s$--	$^2D_{2½}$	24763. 0	1. 30	1. 50	1. 20	1. 20	
	$^2D_{1½}$	21266. 0	——	——	0. 80	0. 80	
$5s^2\,5p^4\,(^3P)6d$--	$^4F_{4½}$	——	——	——	1. 33	1. 33	
	$^4F_{3½}$	34470. 7	1. 13	1. 10	1. 24	1. 29	
	$^4F_{2½}$	31974. 3	——	1. 13	1. 03	1. 20	
	$^4F_{1½}$	——	——	——	0. 40	0. 99	
	$^4D_{3½}$	35561. 2	1. 36	1. 34	1. 43	1. 32	
	$^4D_{2½}$	35521. 4	1. 43	1. 26	1. 37	1. 30	
	$^4D_{1½}$	35360. 2	1. 64	1. 35	1. 20	1. 24	
	$^4D_{0½}$	——	——	——	0. 00	0. 33	
	$^4P_{2½}$	27669. 0	——	1. 15	1. 60	1. 24	
	$^4P_{1½}$	26928. 2	0. 98	0. 78	1. 73	1. 36	
	$^4P_{0½}$	30185. 0	——	——	2. 67	2. 20	
	$^2D_{2½}$	26683. 4	——	1. 19	1. 20	1. 23	
	$^2D_{1½}$	25128. 3	——	1. 00	0. 80	0. 80	
	$^2P_{1½}$	——	——	——	1. 33	1. 08	
	$^2P_{0½}$	25845. 7	——	0. 38	0. 67	0. 80	
$5s^2\,5p^4\,(^1D)6d$--	$^2D_{2½}$	21371. 1	——	——	1. 20	1. 13	
	$^2D_{1½}$	22983. 2	——	1. 07	0. 80	0. 96	
	$12_{1½}$	33005. 6	0. 99	1. 02			
	$14_{2½}$	24140. 6	——	0. 98			
	$16_{1½}$	34559. 15	——	1. 68			
	$18_{0½}$	34514. 23	——	0. 94			
	$20_{0½}$	32342. 0	——	1. 89			$5s^2\,5p^4\,(^3P)6d\,^4D_{0½}$
	$43^3_{1½}$	33574. 65	——	1. 06			
	$15^3_{2½}$	31038. 29	——	1. 08			

Table 3 shows the application of the g-sum rule to the $6s$ and $6p$ levels of Xe II. The essentially satisfactory manner in which the rule is obeyed, in spite of the fact that a high degree of precision cannot be claimed for our measurements, confirms the assignments of quantum numbers and electron configurations indicated in the previous publication [2]. In cases where only a single observed g is needed to complete the sum, a value is given, in parentheses, which will satisfy the rule. Differences of one or two units in the last place in the sums of theoretical g's are due to rounding off the g's to two places of decimals. In the final columns are listed the values of the quantities substituted in the formula for g in case of Jj coupling.

TABLE 3.—*Application of the g-sum rule in* Xe II

Configuration	Level designation		Observed g	Calculated g, Landé formula	Calculated g, Jj coupling	J_p	j_i	g_p	g_i
$5s^2\ 5p^4\ 6s$	$(^3P)\ {}^4P_{2\frac{1}{2}}$		1. 56	1. 60	1. 60	2	½	3/2	2
	$(^1D)\ {}^2D_{2\frac{1}{2}}$		1. 24	1. 20	1. 20	2	½	1	2
		Sum	2. 80	2. 80	2. 80				
	$(^3P)\ {}^4P_{1\frac{1}{2}}$		1. 39	1. 73	1. 40	2	½	3/2	2
	$(^3P)\ {}^2P_{1\frac{1}{2}}$		1. 58	1. 33	1. 67	1	½	3/2	2
	$(^1D)\ {}^2D_{1\frac{1}{2}}$		0. 92	0. 80	0. 80	2	½	1	2
		Sum	3. 89	3. 86	3. 87				
	$(^3P)\ {}^2P_{0\frac{1}{2}}$		0. 56	0. 67	1. 33	1	½	3/2	2
	$(^3P)\ {}^4P_{0\frac{1}{2}}$		2. 45	2. 67	2. 00	0	½	0/0	2
	$(^1S)\ {}^2S_{0\frac{1}{2}}$		(2. 32)	2. 00	2. 00	0	½	1	2
		Sum	(5. 33)	5. 34	5. 33				
$5s^2\ 5p^4\ 6p$	$(^2P)\ {}^4D^\circ_{3\frac{1}{2}}$		1. 39	1. 43	1. 43	2	3/2	3/2	1/3
	$(^1D)\ {}^2F^\circ_{3\frac{1}{2}}$		1. 18	1. 14	1. 14	2	3/2	1	1/3
		Sum	2. 57	2. 57	2. 57				
	$(^3P)\ {}^4P^\circ_{2\frac{1}{2}}$		1. 48	1. 60	1. 44	2	3/2	3/2	1/3
	$(^3P)\ {}^4D^\circ_{2\frac{1}{2}}$		1. 24	1. 37	1. 33	2	1/2	3/2	2/3
	$(^3P)\ {}^2D^\circ_{2\frac{1}{2}}$		1. 41	1. 20	1. 40	1	3/2	3/2	1/3
	$(^1D)\ {}^2D^\circ_{2\frac{1}{2}}$		1. 22	1. 20	1. 12	2	3/2	1	1/3
	$(^1D)\ {}^2F^\circ_{2\frac{1}{2}}$		0. 92	0. 86	0. 93	2	½	1	2/3
		Sum	6. 27	6. 23	6. 22				
	$(^3P)\ {}^4D^\circ_{1\frac{1}{2}}$		1. 38	1. 20	1. 47	2	3/2	3/2	1/3
	$(^3P)\ {}^4P^\circ_{1\frac{1}{2}}$		1. 62	1. 73	1. 67	2	1/2	3/2	2/3
	$(^3P)\ P^\circ_{1\frac{1}{2}}$		1. 39	1. 33	1. 38	1	3/2	3/2	1/3
	$(^3P)\ {}^2D^\circ_{1\frac{1}{2}}$		1. 37	0. 80	1. 22	1	1/2	3/2	2/3
	$(^3P)\ {}^2S^\circ_{1\frac{1}{2}}$		1. 28	2. 00	1. 33	0	3/2	0/0	1/3
	$(^1D)\ {}^2P^\circ_{1\frac{1}{2}}$		1. 37	1. 33	1. 07	2	3/2	1	1/3
	$(^1D)\ {}^2D^\circ_{1\frac{1}{2}}$		0. 95	0. 80	1. 07	2	1/2	1	2/3
	$(^1S)\ {}^2P^\circ_{1\frac{1}{2}}$		(1. 17)	1. 33	1. 33	0	3/2	1	1/3
		Sum	(10. 53)	10. 52	10. 54				
	$(^3P)\ {}^4P^\circ_{0\frac{1}{2}}$		1. 51	2. 67	1. 67	2	3/2	3/2	1/3
	$(^3P)\ {}^2P^\circ_{0\frac{1}{2}}$		1. 13	0. 67	1. 22	1	3/2	3/2	2/3
	$(^3P)\ {}^2S^\circ_{0\frac{1}{2}}$		2. 06	2. 00	1. 78	1	1/2	3/2	2/3
	$(^3P)\ {}^4D^\circ_{0\frac{1}{2}}$		0. 63	0. 00	0. 67	0	1/2	0/0	2/3
	$(^1D)\ {}^2P^\circ_{0\frac{1}{2}}$		0. 71	0. 67	0. 67	2	3/2	1	1/3
	$(^1S)\ {}^2P^\circ_{0\frac{1}{2}}$		(0. 64)	0. 67	0. 67	0	1/2	1	3/3
		Sum	(0. 68)	6. 68	6. 68				

Application of the g-sum rule has shown the need of a few changes of assignment of quantum numbers. The designations of levels 61505.25 and 63061.15 are interchanged, also 64162.29 and 65120.86. In the earlier work there was no basis for distinguishing such levels, which showed similar combining properties.

The level 32342.0, previously designated (^{3}P) 6*d* $^4D_{0½}$, has a *g* value, 1.89, which makes that designation untenable. In the present paper, it is simply assigned a number, $20_{0½}$.

Tables 1 and 2 incorporate the revisions in classifications, resulting from new designations of certain levels, which are required to bring the corresponding tables of RP1164 [2] up to date, to the extent permitted by the limitation of table 1 to the list of lines for which Zeeman patterns have been observed. These changes will necessarily affect the classifications of a number of other lines, involving newly designated levels, for which Zeeman effects have not been observed.

Zeeman patterns have been observed for several unclassified lines. The line at 4037.29 A exhibits a sextet pattern, indicating a transition $J=½$ to $J=1½$. There is a little evidence that it is a combination of a new level, 34514.23 with the known level 59276.32.

A multiplet array of newly classified lines is shown in table 4. Support for the classifications is furnished by the distribution of line intensities in the group, by the repeated appearance of "constant frequency" differences, and by Zeeman patterns for the three strongest lines. It is probable that the suggested new levels are attributable to *f*-electron binding.

TABLE 4.—*New multiplet in* Xe II

New level	Suggested designation	$^2F_{2½}$ 56317.32	$^2F_{3½}$ 56154.44
		(500*Hl*)	(2*h*)
		4395. 77	4427. 52
33574. 65	$^2F_{3½}$	22742. 77	22579. 69
		(150*Hl*)	(500*H*)
		4416. 07	4448. 13
33679. 22	$^2F_{2½}$	22638. 24	22475. 07
			(1000*H*)
			4462. 19
33750. 19	$^2G_{4½}$		22404. 25

V. Xe III—DATA AND RESULTS

The third spectrum of xenon, which appears along with the second in condensed spark discharges, exhibits its most intense lines, barring the extreme ultraviolet lines involving the normal state, in the region between 3000 and 4000 A. This region is rather favorable for the observation of the Zeeman effect since most gratings and photographic emulsions perform best in this range. Among these intense lines the most conspicuous are combinations of levels of the $5s^25p^3$ (^{4}S°)6*s* group with those of the $5s^2$ $5p^3$ (^{4}S°)6*p* configuration. Next to these in intensity are the combinations of levels from the same configurations in the (^{2}D°) family. These two types of transitions supply almost all our Zeeman patterns, inasmuch as the (^{2}P°) family of levels gives combinations of considerably less intensity.

The observed and calculated Zeeman patterns in Xe III are given in table 5 along with the wave lengths, wave numbers, and appropriate designations of the respective lines. Table 5 is constructed according

to the same plan as table 1 for Xe II. In cases where evidence afforded by this investigation indicates a different classification for a line, the revised designations appear in the table. These revisions are taken up in detail in the following discussion.

TABLE 5.—*Zeeman patterns in* Xe III

Wage length (air)	Wave number (vac)	Term combination	Observed Zeeman pattern Humphreys and Meggers	Observed Zeeman pattern deBruin	Calculated Zeeman pattern
A	cm^{-1}				
3331.65	30006.56	$4[1\frac{1}{2}]-(^3D)6p\ ^1D_2$	(0.00) 1.32		(0.00, 0.32, 0.64) 0.58, 0.90, 1.22, 1.54, 1.86
3444.23	29025.78	$(^3D)6s\ ^3D[1]-(^1D)6p\ ^3D_2$	(0.00) 1.57		(0.00, 0.79) 0.38, 1.17, 1.96
3454.25	28941.58	$(^3D)6s\ ^1D[2]-(^3D)6p\ ^1D_2$	(0.00) 1.01	(0.16) 1.03	(0.12, 0.24) 0.84, 0.96, 1.08, 1.20
3458.71	28904.26		(0.83) 1.47		
3467.20	28833.49	$(^3D)5d\ ^3D[1]-(^3D)6p\ ^1D_2$	(0.00) 1.37	(0.00) 1.29	(0.00, 0.14, 0.28) 0.94, 1.08, 1.22, 1.36, 1.50
3468.19	28825.26	$(^4S)6s\ ^4S[1\frac{1}{2}]-(^4S)6p\ ^3P_1$	(0.00) 2.13		(0.00, 0.36) 1.59, 1.95, 2.31
3509.78	28483.69		(0.00) 1.30		
3542.33	28221.97	$(^3D)6s\ ^3D[1]-(^3D)6p\ ^3P_2$	(0.00) 1.28	(0.00) 1.31	(0.00, 0.05, 0.10) 1.23, 1.28, 1.33, 1.38, 1.43
3552.13	28144.11	$4[1\frac{1}{2}]-4_1$	(0.00) 1.12	(0.00) 1.07	(0.00, 0.48) 0.42, 0.90, 1.38
3561.38	28071.01	$4[1\frac{1}{2}]-(^3D)6p\ ^1F_3$	(0.00) 1.28		(0.00, 0.19, 0.38) 0.71, 0.90, 1.09, 1.28, 1.47
3565.18	28041.10		(0.00) 1.25		
3579.69	27927.44	$(^3D)6s\ ^3D[3]-(^3D)6p\ ^3F_3$	(0.00) 1.09	(0.00) 1.04	(0.00, 0.10, 0.20) 0.88, 0.98, 1.08, 1.18, 1.28
3583.64	27896.65	$(^3D)6s\ ^3D[3]-(^3D)6p\ ^3F_4$	(0.00) 1.19	(0.00) 1.10	(0.00, 0.05, 0.10, 0.15) 1.13, 1.18, 1.23, 1.28, 1.33, 1.38, 1.43
3596.60	27796.14		(0.00) 0.72	(0.00) 0.69	
3607.01	27715.91	$(^3D)6s\ ^3D[3]-(^3D)6p\ ^3D_3$	(0.00) 1.27		(0.11, 0.22, 0.33) 1.00, 1.11, 1.22, 1.33, 1.44, 1.55
3609.44	27697.26	$(^3D)6s\ ^3D[3]-6_4$	(0.00) 1.28		(0.00, 0.02, 0.04, 0.06) 1.25, 1.27, 1.29, 1.31, 1.33, 1.35, 1.37
3623.13	27592.61	$(^3D)6s\ ^3D[2]-(^3D)6p\ ^3D_2$	(0.00) 1.18	(0.00) 1.20	(0.01, 0.02) 1.16, 1.17, 1.18, 1.19
3624.05	27585.60	$(^4S)6s\ ^4S[1\frac{1}{2}]-(^4S)6p\ ^3P_2$	(0.00) 1.18	(0.00) 1.07	(0.00, 0.38, 0.76) 0.81, 1.19, 1.57, 1.95, 2.33
3632.14	27524.16	$(^3P)6s\ ^3P[2]-26_1$	(0.00) 1.51	(0.00) 1.38	(0.00) 1.51
3641.00	27457.19	$(^3D)6s\ ^3D[2]-(^3D)6p\ ^3F_2$	(0.00) 1.06		(0-00, 0.46) 0.38, 0.84, 1.30
3649.56	27392.79		(0.00) 1.35		
3654.63	27354.79	$(^3D)5d\ ^3S[1]-(^3D)6p\ ^3P_1$	(0.00) 1.43	(0.00) 1.50	(0.26) 1.30, 1.56
3676.63	27191.10	$(^4S)6s\ ^3S[1]-(^4S)6p\ ^3P_0$	(0.00) 1.76	(0.00) 1.74	(0.00) 1.77
3745.72	26689.58	$(^3D)5d\ ^1D[2]-(^3D)6p\ ^1D_2$	(0.53) 0.96	(0.38) ——	(0.27, 0.54) 0.54, 0.81, 1.08, 1.35
3762.26	26572.24		(0.00) 1.41	(0.00) 1.39	
3765.85	26546.91	$(^3P)6s\ ^3P[1]-26_1$	(0.00) 1.49		(0.04) 1.47, 1.51
3772.53	26499.91	$25[1]-36_1$	(0.00) 1.15	(0.28) 1.11	
3776.30	27473.45	$(^3P)6s\ ^3P[1]-(^3P)6p\ ^3D_2$	(0.00) 1.03	(0.00) 0.97	(0.00, 0.29) 0.89, 1.18, 1.47
3780.98	26440.69	$(^4S)6s\ ^3S[1]-(^4S)6p\ ^3P_2$	(0.00) 1.36	(0.00) 1.29	(0.00, 0.27) 1.23, 1.50, 1.77
3841.52	26024.01	$(^3D)6s\ ^3D[1]-(^3D)6p\ ^3F_2$	(0.62) 1.00		(0.34, 0.68) 0.50, 0.84, 1.18, 1.52
3861.05	25892.37	$4[1\frac{1}{2}]-(^3D)6p\ ^3D_2$	(0.00) 1.04		(0.27, 0.54) 0.63, 0.90, 1.77, 1.44
3877.80	25780.54	$(^3D)6s\ ^3D[1]-(^3D)6p\ ^1F_3$	(0.47) 1.20		(0.24, 0.48, 0.72) 0.61, 0.85, 1.09, 1.33, 1.57, 1.81
3880.46	25762.86	$(^3D)6s\ ^3D[1]-(^3D)6p\ ^3D_1$	(0.00) 0.92		
3895.03	25666.50		(0.00) 1.12		
3922.53	25486.56	$(^4S)6s\ ^4S[1]-(^4S)6p\ ^3P_2$	(0.44) 1.84	(0.48) 1.74	(0.25, 0.50) 1.45, 1.70, 1.95, 2.20
3950.56	25305.73	$(^4S)6s\ ^4S[1]-(^4S)6p\ ^3P_1$	(0.00) 1.79		(0.00, 0.33) 1.62, 1.95, 2.28
3985.96	25080.99	$23[1]-32_1$	(——) 1.44H		
3992.85	25037.71	$(^3D)6s\ ^1D[2]-(^3D)6p\ ^3P_1$	(——) 0.79		(0.00, 0.34) 0.62, 0.96, 1.30
4028.58	24815.65	$(^3D)5d\ ^3D[1]-(^3D)6p\ ^3P_2$	(——) 1.33		(0.26, 0.52) 0.86, 1.12, 1.38, 1.64
4043.21	24725.86	$(^3P)6s\ ^3P[1]-(^3P)6p\ ^3D_1$	(——) 0.65		(0.00) 0.65
4050.05	24684.10	$(^4S)6s\ ^3S[1]-(^4S)6p\ ^3P_1$	(0.00) 1.68	(0.18) 1.68	(0.18) 1.59, 1.77
4060.43	24621.00	$25[1]-32_1$	(0.00) 1.01	(0.00) 0.94	
4109.07	24329.56	$(^3D)6s\ ^3D[1]-(^3D)6p\ ^3D_1$	(0.00) 1.37		
4142.01	24136.08	$(^3P)6s\ ^3P[1]-26_1$	(——) 1.25		
4145.73	24114.43	$(^3D)5d\ ^3D[1]-(^3D)6p\ ^3D_2$	(0.00) 1.50		(0.00, 0.67) 0.50, 1.17, 1.84
4176.53	23936.60	$(^3D)6s\ ^3D[1]-(^3D)6p\ ^3F_2$	(——) 1.18		(0.25, 0.50, 0.75) 0.58, 0.83, 1.08, 1.33, 1.58, 1.83
4203.92	23780.65	$(^3D)5d\ ^3S[1]-4_1$	(——) 1.36h		
4226.96	23651.03		(——) 1.52		
4240.24	23576.95	$17[\frac{1}{2}]-(^1D)6p\ ^1D_2]$	(0.00) 1.25?		

TABLE 5.—*Zeeman patterns in* Xe III—Continued

Wave length (air)	Wave number (vac)	Term combination	Observed Zeeman pattern Humphreys and Meggers	Observed Zeeman pattern deBruin	Calculated Zeeman pattern
A	*cm*$^{-1}$				
4272.60	23398.39	$(^3D)5d\ ^3D_3^1-(^3D)6p\ ^3F_4$	(0.00) 1.36		(0.00, 0.06, 0.12, 0.18) 1.10, 1.16, 1.22, 1.28, 1.34, 1.40, **1.46**
4285.89	23325.84	$(^3D)6s\ ^1D_2^1-(^3D)6p\ ^3D_3$	(0.00) 1.48		(0.00, 0.26, 0.52) 0.70, 0.96, 1.22, 1.48, **1.74**
4308.00	23206.12	$23_2^1-28_1$	(——) 1.12		
4309.33	23198.96	$(^3D)5d\ ^3D_3^1-6_4$	(——) 1.43		(0.00, 0.09, 0.18, 0.27) 1.04, 1.13, 1.22, 1.31, 1.40, 1.49, **1.58**
4434.16	22545.88	$(^3D)5d\ ^3D_1^1-(^3D)6p\ ^3F_2$	(0.00) 1.01		(0.00, 0.34) 0.50, 0.84, 1.18
4453.61	22447.41	$(^3D)5d\ ^3D_2^1-4_1$	(——) 1.36?		(0.00, 0.70) 0.42, 1.12, **1.82**
4503.46	22198.94	$27_2^1-32_1$	(——) 1.18		
4537.33	22033.24	$(^3D)6s\ ^3D_2^1-(^3D)6p\ ^3F_2$	(——) 2.00H		(0.00, 0.49, 0.98) 0.35, 0.84, 1.33, 1.82, **2.31**
4657.78	21463.46	$(^3D)6s\ ^1D_2^1-4_1$	(——) 1.24		(0.00, 0.54) 0.42, 0.96, **1.50**
4673.66	21390.54	$(^3D)6s\ ^1D_2^1-(^3D)6p\ ^1F_3$	(——) 1.28		(0.00, 0.13, 0.26) 0.83, 0.96, 1.09, 1.22, **1.35**
4683.53	21345.46	$(^4S)6s\ ^3S_1^1-(^4S)6p\ ^3P_2$	(0.00) 1.66		(0.00, 0.07) **1.63**, 1.70, 1.77
4748.92	21051.55	———	(——) 1.10		
4869.47	20530.40	$(^3D)5d\ ^3D_2^1-(^3D)6p\ ^3F_3$	(——) 1.26		(0.00, 0.04, 0.08) 1.00, 1.04, 1.08, 1.12, 1.16

deBruin's Zeeman patterns for the lines arising from combinations of levels of the (^{4}S°) family are quoted from his publication on the spectral structure of doubly ionized noble gases [3].

The earlier analysis of Xe III [4] accounted for the majority of the lines clearly attributable to this spectrum and the number of energy levels found was nearly equal to the number which could be accounted for on the basis of configurations which might reasonably be expected. In many cases, however, the assignment of quantum numbers was limited to the *J*-value, and in others the complete designation was given with reservations. The reasons for this somewhat unsatisfactory state of the analysis are nonconformity with the *LS* coupling scheme, which prevents appearance of multiplets of regular intensities and intervals; very wide level separations, as great or greater than the term separations; and mutual perturbations of levels from the same or different configurations which result in the appearance of several pairs of levels which are essentially alike as to combining properties. The usual notation for spectral terms probably means little in this kind of spectrum, but from the standpoint of simplicity, there seems to be some advantage in using it even though the coupling is not *LS*. It was expected that the Zeeman observations would permit confirmation or revision of a number of levels which were designated in somewhat arbitrary fashion. This expectation has been realized in regard to several levels which are involved in intense combinations. The outstanding line combinations among the (^{4}S°) family of terms yield patterns which clearly confirm the original classification [3].

Table 6 contains a list of levels for which *g* values have been observed, together with observed and calculated *g*'s. The calculation of *g's* for *Jj* coupling is made on the assumption of *LS* coupling for the parent level. The justification for this procedure is the same in this case as it was in connection with the calculation of *g's* in Xe II. The designations at the left of the table are those at present regarded as most probable. A column at the extreme right gives the earlier [4] designations in cases where they differ. Discussion of these revisions follows.

TABLE 6.—*g-values*—Xe III *levels*

Xe III levels			Observed g, Humphreys and Meggers	Observed g, de Bruin	Calculated g, Landé formula	Calculated g, Jj coupling	Former designation, RP898
Origin	Designation	Magnitude					
$5s^2\ 5p^3\ (^4S°)6s$	$^5S_2^\circ$	137613.00	1.95	1.87	2.00	2.00	
	$^3S_1^\circ$	133471.80	1.77	1.76	2.00	2.00	
$5s^2\ 5p^3(^2D°)6s$	$^3D_1^\circ$	125854.72	0.38		0.50	0.50	
	$^3D_2^\circ$	124421.51	1.18		1.17	1.10	
	$^3D_3^\circ$	120430.72	1.33		1.33	1.33	
	$^1D_2^\circ$	116040.63	0.96	0.98	1.00	1.07	
$5s^2\ 5p^3\ (^2P°)6s$	$^3P_0^\circ$	108583.55	0.00	0.00	%	%	
	$^3P_1^\circ$	107606.40	1.47		1.50	1.33	
$5s^2\ 5p^3\ (^2D°)5d$	$4[1\frac{1}{2}]_2^\circ$	122721.35	0.90				$^1P_1^\circ$
	$^3S_1^\circ$	118357.77	1.56		2.00		
	$^3D_1^\circ$	120943.39	0.50		0.50		
	$^3D_2^\circ$	117024.51	1.12		1.17		
	$^3D_3^\circ$	115932.46	1.22	1.19	1.33		
	$^1D_2^\circ$	113788.61	0.81		1.00		
$5s^2\ 5p^3\ (^4S°)6p$	$^5P_1$	112307.29	2.28		2.50	2.33	
	$^5P_2$	112126.40	1.70	1.61	1.83	1.67	
	$^5P_3$	110027.40	1.57	1.47	1.67	1.67	
	$^3P_0$	106280.64	0.00	0.00	%	%	
	$^3P_1$	108787.71	1.59	1.59	1.50	1.67	
	$^3P_2$	107031.06	1.50	1.45	1.50	1.67	
$5s^2\ 5p^3\ (^2D°)6p$	$^3F_2$	98397.50	0.84		0.67	0.77	$^3D_2$
	$^3F_3$	96494.07	1.08		1.08	1.11	$^3D_3$
	$^3D_2$	96828.90	1.17		1.17	1.21	$^3F_2$
	$^1F_3$	94650.20	1.09		1.00	1.07	2_2
	4_1	94577.18	0.42				4_1 $^1P_1$
	6_4	92733.48	1.31				6_2 $^1F_3$
	$^3D_3$	92714.78	1.22		1.33	1.24	8_2
	$^3F_4$	92534.05	1.28	1.24	1.25	1.25	10_3 $^3F_3$
	$^3P_2$	92208.79	1.38	1.35	1.50	1.29	12_2
	$^3P_1$	91002.85	1.30		1.50	1.10	14_1 $^3P_1$
	$^1D_2$	87099.00	1.08	1.08	1.00	1.07	
$5s^2\ 5p^3\ (^2P°)6p$	$^3D_1$	83857.65	0.65		0.50	0.67	
	$^3D_2$	81132.93	1.18		1.17	1.17	
	26_1	81059.42	1.51	1.38			

The only important changes in designations of levels of Xe III have been made among the group belonging to the $5s^2\ 5p^3 \cdot 6p$ configuration and of (^{2}D°) parentage. These levels are now capable of a much clearer interpretation. Levels previously [4] designated 2_2 and 8_2 must have their J values increased from 2 to 3. The former value, 2_2, is now called $^1F_3$ and 8_2 becomes $^3D_3$. Similarly, the inner quantum numbers of 6_3 and 10_3, as listed in the earlier paper, both become 4. After this change has been made, it seems probable that the level formerly called 10_3 can now be identified as the missing level, (^{2}D°)$6p$ $^3F_4$. There can be only one level with this inner quantum number from the $6p$ configuration. Accordingly, 6_4 must be accounted for by another configuration. It may belong to a term caused by the binding of an f-electron. The following changes of designation with

retention of the same J values are suggested for other levels of the same group by the observed g values: $6p\ ^3D_2$ to $6p\ ^3F_2$, $6p\ ^3D_3$ to $6p\ ^3F_3$, $6p\ ^3F_2$ to $6p\ ^3D_2$, 12_2 to $6p\ ^3P_2$, and 14_1 to $6p\ ^3P_1$. The alternative designation, $6p\ ^1P_1$ for 4_1, is abandoned on account of the low g value, 0.42, obtained for this level.

The level at 122721.35, formerly called $(^2D^\circ)\ 5d\ ^1P_1^\circ$, should have a j value, 2. This rules out the former designation, so we simply give the level a number, 41_2. Since the same level combines with 92793.33, designated $(^2D^\circ)6p\ ^3P_0$, the j value of the latter must be increased from 0 to 1, invalidating the former classification.

Mainly on account of relative weakness of combinations within the $(^2P^\circ)$ family, an insufficient number of patterns are available to test the g-sum rule. The g value of the level $(^2D^\circ)6s\ ^3D_3^\circ$ is taken to be 1.33, according to the g-sum rule, because it is the only level from this configuration having a J value, 3. The g value is, therefore, that given by the Landé formula.

Calculation of the g's for Jj coupling in the manner explained gives values in many cases identical with the Landé g's, in several others differing from the Landé g's by a relatively small amount. In the absence of a more complete set of Zeeman effect observations for Xe III, it is rather difficult to draw final conclusions regarding the coupling of the quantum vectors. The g values for the lowest levels observed are fairly close to those given by the Landé formula, whereas the majority of the intermediate levels yield g's more closely approximating those associated with Jj coupling.

S. A. Goudsmit communicated some valuable suggestions in regard to the probable vector-coupling schemes in these spectra and the methods of calculating theoretical g values, which the authors gratefully acknowledge.

VI. REFERENCES

[1] C. J. Humphreys, T. L. deBruin, and W. F. Meggers, BS J. Research **6,** 287 (1931) RP275.
[2] C. J. Humphreys, J. Research NBS **22,** 19 (1939) RP1164.
[3] T. L. deBruin, Zeeman Verhandelingen, p. 413–423 (1935).
[4] C. J. Humphreys, J. Research NBS **16,** 639 (1936) RP898.
[5] J. C. Boyce, Phys. Rev. **49,** 730 (1936).
[6] L. Bloch, E. Bloch, and G. Déjardin, Ann. phys. [10] **2,** 461 (1924).
[7] G. Déjardin, Ann. phys. [10] **13,** 82 (1930).
[8] E. Back and A. Landé, Zeemaneffekt und Multiplettstrukten der Spektrallinien, chap. 7 (Julius Springer, Berlin, 1925).
[9] A. Landé, Z. Physik **5,** 231 (1921).
[10] C. C. Kiess and W. F. Meggers, BS J. Research **1,** 641 (1928) RP23.
[11] E. Back, Z. Physik **15,** 206 (1923).
[12] J. B. Green, Phys. Rev. **52,** 736 (1937).
[13] W. Pauli, Z. Physik **16,** 155 (1923).
[14] A. G. Shenstone and H. A. Blair, Phil. Mag. [7] **8,** 765 (1929).
[15] H. Hönl, Z. Physik **31,** 340 (1925).

WASHINGTON, November 3, 1939.

U. S. Department of Commerce National Bureau of Standards

RESEARCH PAPER RP1265

Part of Journal of Research of the National Bureau of Standards, Volume 23, December 1939

AN IMPROVED ELECTRIC HYGROMETER

By Francis W. Dunmore

ABSTRACT

The psychrometer and hair hygrometer are common means of determining the moisture content of air. There are, however, many circumstances to which these are not well adapted, especially in the measurement of upper-air humidities by means of the radio sonde, where marked and sudden changes of humidity are encountered. In fact, when humidity readings are to be made or recorded graphically, remote from the point of measurement, or where humidity must be determined rapidly or in confined spaces or at low temperatures, these methods are not practical.

This paper describes a type of electric hygrometer which better fulfills the above requirements. It covers improvements made in an earlier type of electric hygrometer previously described by the author. The improved unit consists of an 0.01-inch-wall aluminum tube $1\frac{1}{16}$ inches long coated with polystyrene resin and wound with a bifilar winding comprising 20 turns (of each wire) per inch of No. 38 AWG bare palladium wire. The unit is then coated with a thin film of partially hydrolyzed polyvinyl acetate with the addition of a small amount of lithium chloride, the amount depending upon the humidity range to be covered by the unit. The electric resistance of the film between the two coils is a function of humidity.

The thin-walled aluminum tube enables the unit to assume quickly the temperature of the air, as it must if measuring relative humidity. The use of palladium wire eliminated a continuous aging effect or increase in resistance caused by a film which continued to form on the surface of all other wires previously used. The polystyrene resin forms an excellent water-resistant surface of high electric resistance for the wire and water-sensitive film. This construction eliminated hysteresis effects previously experienced, caused by the adsorption of water by glass and other materials used as bases.

The polyvinyl acetate forms a porous binder for the lithium chloride, which not only gives stability and uniformity to the units but also greatly reduces polarization effects previously experienced when using the electric hygrometer in the d-c radio-sonde circuit.

Methods of construction, coating, aging, and using the units in both a-c and d-c circuits are given.

A method is provided which makes possible the measurement of relative humidity from 10 to 100 percent by using several units of different sensitivities in parallel, with resistors in series with each.

The humidity-resistance characteristics are given for individual units coated with different percentages of lithium chloride and for three- and five-element composite units.

A calibration of a three-element unit used in the radio-sonde circuit serves as an example of measurements over a temperature range from $+30°$ to $-60°$ C.

Electric-hygrometer units have been made which have not varied more than 2 or 3 percent over a period of several months.

CONTENTS

	Page
I. Introduction	702
II. Improvements over earlier device	703
1. Prevention of long-period aging	703
2. Elimination of short-period aging	704
3. Use of partially hydrolyzed polyvinyl-acetate film	705
(a) Use as a binder for the lithium chloride	705
(b) Homogeneous film	705
(c) Reduction of polarization	705
4. Method of making the hygrometer units	706
(a) Constructional details	706
(b) Coating procedure	706
(c) Aging	706
5. Special design for covering the full humidity range without switching means	707
III. Operating characteristics in d-c radio-sonde circuits	707
1. Three-element unit	708
2. Frequency-humidity characteristic	709
3. Temperature correction	709
IV. Operating characteristics in a-c measuring circuits	710
1. Circuit arrangement	710
2. Humidity-resistance characteristics	711
(a) Single-unit characteristics	711
(b) Composite-unit arrangement	712
V. Designs for special uses	712
1. Design for use where a-c power is available	712
2. Battery-operated unit	712
3. Multiscale unit for conditions of wide temperature variations	713

I. INTRODUCTION

The psychrometer method of measuring humidity has long been a common means of determining the moisture content of air. There are, however, many conditions for which this method is not well adapted, a particular case being the measurement of upper-air humidities by means of the radio sonde. When remote indications or recording of the humidity is required, or when measurements must be made in small confined spaces or at low temperatures, the psychrometer method is not practical. The hair-type hygrometer is now generally used, but its slow rate of response and other peculiarities have made its use undesirable in many instances. In radio meteorography the large time lag in response of the hair hygrometer introduces serious errors, since sudden humidity changes are often encountered by a rapidly ascending balloon. This lag increases with decreasing temperature, with the result that the accuracy of this type of hygrometer becomes progressively less at increasing altitude.

In a previous paper,[1] an electric type of hygrometer was described for use with the radio sonde, which, subject to certain precautions, gave some promise of satisfying the requirements for a remote humidity-indicating device without moving parts or appreciable lag. It consisted of two fine tinned copper wires spirally wound simultaneously on a thin-walled etched glass tube so as to form 20 bifilar turns per inch. After the glass tube was wound, it was coated with a dilute solution of lithium chloride in water. The lithium salt, with the moisture which it takes up from the air, formed an electrolytic conductor on the glass surface between the two wires. The resistance of this conducting film varied greatly with the moisture content of the air, so

[1] F. W. Dunmore, *An electric hygrometer and its application to radio meteorography*, J. Research NBS **20**, 723–744 (1938) RP1102.

that the resistance of the unit could be expressed in terms of percentage of relative humidity. Such a unit gave satisfactory results if certain precautions were observed in its use. These precautions were necessary because of continuous short- and long-period aging effects and a polarization error when the unit was used in d-c circuits. It was also found necessary to switch in two or more units of different sensitivities in order to cover the full humidity scale.

Recent research on this hygrometer has substantially overcome these difficulties, resulting in a unit which now appears to be definitely superior to the hair-type hygrometer, especially for radio-sonde use. It also has advantages over the psychrometer method under many other conditions of measurement. The original features of rapid rate of response and inherent variation in resistance with changes of humidity have been retained.

The present paper describes the improvements made in the original electric hygrometer, the method of construction, the operating characteristics of the new unit in a-c and d-c circuits, and some special applications.

The method of using the electric hygrometer in the radio sonde and results obtained on routine operation are given in a separate paper.[2]

II. IMPROVEMENTS OVER EARLIER DEVICE

The improvements incorporated in the new electric hygrometer may be classified under four headings: (1) Prevention of long-period aging; (2) prevention of a hysteresis effect, or short-period aging; (3) use of partially hydrolyzed polyvinyl-acetate film, (a) lithium-chloride binder, (b) homogeneous film, (c) reduction of polarization; (4) special design for covering the full humidity range without switching means.

1. PREVENTION OF LONG-PERIOD AGING

Early work with the bifilar-coil electric hygrometer showed that the electric resistance of the unit continued to increase from week to week, so that it was necessary to calibrate the device shortly before using. It has since been found that this increase in resistance was caused by a film which gradually formed on the surface of the wire used for the coils. After units were wound with many kinds of wire, it was found that platinum and palladium wire were the only kinds which would eliminate this aging effect. (Recent tests indicate that it may be possible to use gold or gold-plated wire.) As palladium is cheaper than platinum, the former is now used. Units wound with this wire have been found to hold a calibration to within ± 3 percent for 6 months. Twenty bifilar turns per inch of No. 38 AWG gave the best results. A reduction in the number of turns per inch increases the current density at the surface of the wire, which tends to increase the polarization effect in d-c circuits and to decrease the life of the unit in a-c circuits. Fewer turns, however, make a unit which covers a greater range of humidity for a given resistance change. With amplifying means between the unit and indicating instrument, it is possible that fewer turns might be used.

[2] H. Diamond, W. S. Hinman, Jr., and F. W. Dunmore, *An improved radio sonde and its performance*; Publication pending.

2. ELIMINATION OF SHORT-PERIOD AGING

Another phenomenon termed hysteresis, or short-period aging, involving intervals of several hours before becoming apparent, made it necessary to calibrate the units shortly before using, or to store them at a fixed humidity. The cause of this effect was finally traced to the adsorption of water by the etched-glass surface upon which the bifilar coils were wound. As giving up or taking on of water by the glass required several hours, the result was a shift in the calibration curve for the unit to lower values of resistance if the unit had been exposed to a high humidity for several hours, or to higher resistance values if the unit had been exposed to a low humidity for several hours. This behavior of the units was illustrated in the previous paper.

A way of overcoming this effect was to store the units in a fixed humidity chamber until ready for use.

After many water-resistance coatings had been tried on the glass, polystyrene, a thermoplastic resin, was found which overcame this troublesome effect. A coating is applied by dipping the glass tube in a solution of polystyrene.

The construction now preferred consists of a thin-walled aluminum tube in place of the glass tube. The aluminum tubing is dipped in the polystyrene solution, heated to drive off the solvents, and it is then wound with the bifilar coil of palladium wire. The aluminum tubing should be of the commercial hard-tempered type with an outside diameter of ⅝ inch and a wall thickness of 0.01 inch. The thin wall is necessary, as the unit must attain the temperature of the air surrounding it in order to register the true relative humidity. This is especially important in radio-sonde use, where sharp temperature inversions are often encountered. Such a unit is shown in figure 1.

The polystyrene film on the aluminum tube serves as a surface of high electric resistance for the bifilar coil and the moisture-sensitive coating, without adversely influencing the functioning of the device.

In applying this film it is important that the composition of the polystyrene solution be such that the film will dry without cracking or crazing. Any such surface irregularities tend to produce a hysteresis effect, or lag in response of the device. Also, such a surface structure causes nonuniformity of the coating of the moisture-sensitive film which is applied after the unit is wound.

A satisfactory polystyrene solution for coating the aluminum tubing by dipping was found to be as follows:

100.0 g of polystyrene (Resoglaz).
18.4 g of dibutyl phthalate (plasticizer).
90.0 g of ethyl acetate.
133.0 g of butyl acetate.
90.6 g of xylene.
135.0 g of toluene.

The aluminum tubing (with ends closed) was dipped in this solution and immediately withdrawn at a steady rate of approximately 1 inch per 7 seconds. This process was repeated with a drying interval between each coat of 3 hours, until the film of styrene resin was about 0.01 inch thick. After the application of the last coat the unit was heated at 80° C for 18 hours before winding. The polystyrene surface should not be roughened, as such treatments produce units which are not reproducible when coated with the moisture-sensitive film.

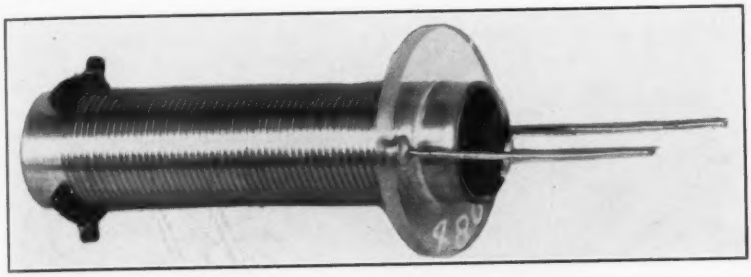

FIGURE 1.—*An electric-hygrometer unit.*

(See p. 706 for approximate dimensions.)

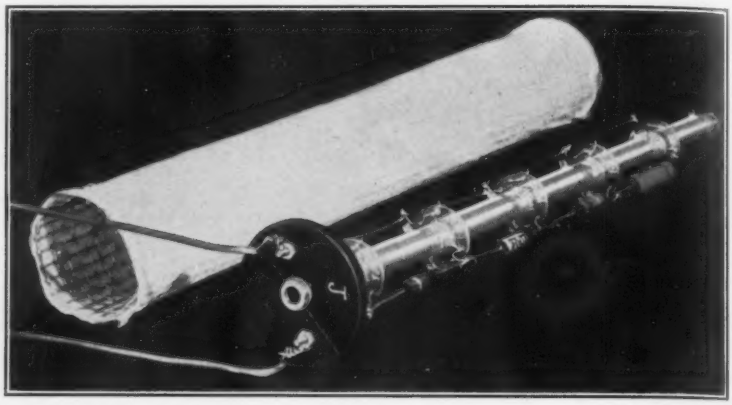

FIGURE 4.—*Five-element electric hygrometer for indicating relative humidities from 10 to 100 percent.*

The five units are connected as shown in figure 3. The cloth-covered housing protects the units from dirt but allows water vapor to reach them.

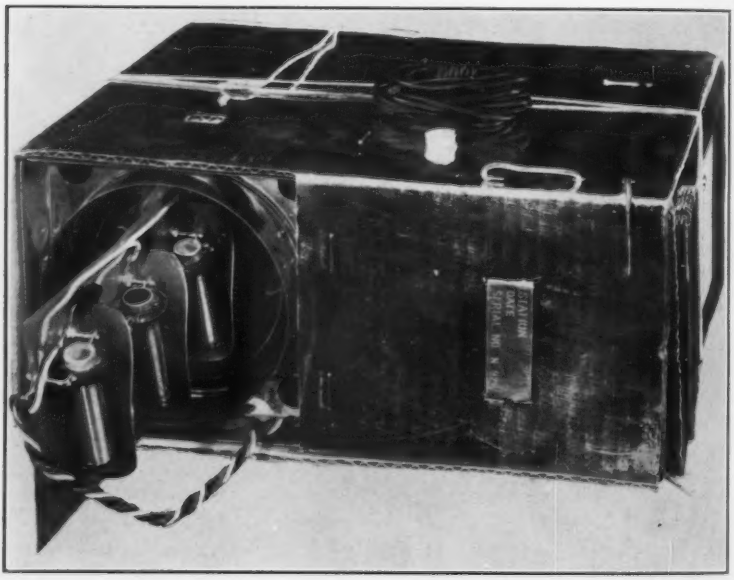

FIGURE 5.—*Three-element electric hygrometer in radio-sonde mounting.*

Bottom (and side) view of radio sonde. The electric-hygrometer mounting is shown withdrawn from the lower end of the sun shield.

3. USE OF PARTIALLY HYDROLYZED POLYVINYL-ACETATE FILM

(a) USE AS A BINDER FOR THE LITHIUM CHLORIDE

The moisture-sensitive material used on the polystyrene surface is a dilute solution of lithium chloride in water. In order to keep the lithium chloride on the smooth polystyrene surface, a suitable binder had to be found which would mix readily with the solution of lithium chloride in water and form a thin film which would readily pass water vapor without producing appreciable lag in the response of the unit.

Early in the work on the electric hygrometer, at the suggestion of T. P. Sager, of the Bureau's Chemistry Division, a partially hydrolyzed polyvinyl acetate called Hydrogel or Solvar was tried as a sensitive hygroscopic coating on shellac, spar varnish, and balata as bases. These combinations were not sufficiently sensitive. However, in later work this material mixed with lithium chloride as the sensitive element proved to be a most satisfactory combination. This partially hydrolyzed polyvinyl acetate (36 percent saponifiable) is sold by the Shawinigan Products Corporation, Empire State Building, New York City, under the name of Solvar—sample 6341 S. O. 1232, W. O. 5356–11. This was furnished in the form of a viscous alcoholic solution containing 25 percent of solid material. A satisfactory dipping mixture consists of 1 part of this solution by volume to 6 parts (by volume) of a mixture of equal parts of water and ethyl alcohol. To this solution the saturated solution of lithium chloride in water (at 21° C) is added in percentages by volume, depending upon the range in the humidity scale to be covered by the unit to be coated. In using this solution, care should be taken to prevent evaporation of the alcohol as this causes the solution to become more concentrated, giving units with a resistance below normal. The percentages of lithium chloride necessary to cover specified ranges of humidity will be discussed under section IV–2 (a).

(b) HOMOGENEOUS FILM

Another advantage in the use of the partially hydrolyzed polyvinyl-acetate–lithium-chloride solution is that it flows evenly on the smooth polystyrene-resin surface, thereby distributing the lithium chloride uniformly. Lithium chloride and water alone form small globules. With the uniform film, units may be duplicated so that about 75 percent of them will agree in their humidity indications to within ±3 percent. A satisfactory method of coating is described under section II–4 (b).

(c) REDUCTION OF POLARIZATION

A third advantage in the use of the partially hydrolyzed polyvinyl-acetate film proved to be a reduction of the polarization, or counter-electromotive force, set up by the direct current flowing through the unit when used with the radio sonde developed by Diamond, Hinman, and Dunmore.[3] In normal use alternating current may be applied to the units when making measurements, in which case polarization errors are not present. However, it is necessary to use the same type of circuit or indicating instrument as was used in calibrating the units, as the resistance of the unit is a function of the current flowing through it. The coating on the unit behaves like an electrolyte.

[3] H. Diamond, W. S. Hinman, Jr., and F. W. Dunmore, *A method for the investigation of upper-air phenomena and its application to radio meteorography*, J. Research *NBS* **20**, 369-392 (1938) RP1082.

The reason for the reduction of polarization by the polyvinyl-acetate film is not fully understood.

4. METHOD OF MAKING THE HYGROMETER UNITS

(a) CONSTRUCTIONAL DETAILS

A typical unit, as shown in figure 1, consists of 32 inches (about 25 bifilar turns) of 38 AWG bare soft-drawn palladium wire having an ultimate tensile strength of 600 grams. This wire is wound 20 bifilar turns per inch on the polystyrene-coated aluminum tube. (See section II–2 for description of polystyrene coatings.) The tubing is about $1\frac{1}{16}$ inches long with an outside diameter of $\frac{3}{8}$ inch and a wall thickness of 0.01 inch. The insulated washer at one end serves to hold the terminal leads while the split washer at the other end serves to anchor the free ends of the bifilar coil. These washers should be made of a highly water-resistant material, such as polystyrene resin, and should be put on over the polystyrene-resin coat and anchored with a drop or two of the polystyrene solution about $\frac{1}{8}$ inch from the end of the tube. This gives a longer leakage path from the terminals to the aluminum tubing. If sufficient rigidity could be obtained with a unit moulded from polystyrene resin with a wall thickness of 0.02 inch, then the whole unit, washers and all, could be moulded in one piece without the need for the aluminum tubing. High temperatures might cause such a unit to lose shape and thereby loosen the winding. This type of construction is still under consideration.

In order to insure a tight winding, the palladium wires should be heated as they go on to the tubes so that they seat just slightly into the polystyrene-resin surface.

(b) COATING PROCEDURE

In order to obtain units with predetermined operating characteristics, it is important that a standard method of applying the polyvinyl-acetate–lithium-chloride coating be followed. A satisfactory procedure is to mount the units with their longest axis vertical. They are quickly immersed up to the terminal washer in the solution and then withdrawn by a motor-driven device at a constant rate of 1 inch in 12 minutes. The surplus liquid clinging to the lower end of the unit is absorbed with a blotter, and the units are allowed to dry in still air.

(c) AGING

After the units are coated, they must go through an aging period of at least 10 to 14 days before they are ready for use. During this time the resistance of the units continues to decrease until it settles down to a final value (for any given humidity) where it remains for 6 months, at least, which is the longest time a unit has been on test. Recent experiments on 19 units seem to indicate that this aging period may be reduced to 2 days by putting the units in a humidity chamber with air at 60-percent relative humidity and 26° C and continually circulating the air gently over the units.

Attempts to age by baking in an oven in still air at 60° C were not successful.

5. SPECIAL DESIGN FOR COVERING THE FULL HUMIDITY RANGE WITHOUT SWITCHING MEANS

If an attempt were made to cover the full humidity range with a single unit such as shown in figure 1, the variation in resistance of the unit would be so extreme that it would extend outside the normal limits of a measuring device. Furthermore, the excessive current from the measuring circuit through the unit at high humidities would be harmful to the unit.

For the radio sonde the resistance variation for a change in humidity from 5 to 100 percent from +30° to −30° C should not vary outside the limits of 3 megohms to 10,000 ohms. When used in an a-c circuit, such as with a Weston model 764 capacity meter (calibrated to read in ohms), the resistance variation for a change from 5- to 100-percent humidity should be confined within the limits from 8 megohms to 75,000 ohms.

In order to make possible this condition for radio-sonde use, a multiple-unit design with different percentages of LiCl coatings on each unit was devised. By arranging three units in parallel with 1-, 2-, and 3-percent LiCl coatings, respectively,[4] with the proper resistors in series with each, as shown in figure 2, it is possible to confine the resistance variation of the composite unit to the required limits.

For use in an a-c circuit a five-element unit as shown in figures 3 and 4 has been found necessary. In such an arrangement, unit A, figure 3, would have a polyvinyl-acetate coating only, B a coating of 0.25 percent of LiCl, C 0.5 percent of LiCl, D 1.0 percent of LiCl, E 2.2 percent of LiCl. R_5 is greater than R_4, R_4 than R_3, etc. At the high humidities, units B, C, D, and E, although practically shorted, are prevented from causing a short at terminals F by resistors R_2, R_3, R_4, and R_5, yet the resultant resistance at F will vary through limits below the values of the parallel circuits of R_2, R_3, R_4, and R_5, since unit A has resistor R_1, only, in series with it. Thus A is the controlling unit at high humidities. On the other hand, at low humidities A, B, C, and D are practically open-circuited, whereas R_1, R_2, R_3, R_4, and R_5 are not sufficiently high to prevent the change in resistance of unit E from affecting the over-all resistance at F. Thus E is the controlling unit at low humidities. In a like manner, units B, C, and D become the controlling units in turn at intermediate humidities. See section IV–2(a).

All materials used for mounting and wiring the units for the parallel arrangements must be highly water-resistant.

III. OPERATING CHARACTERISTICS IN D-C RADIO-SONDE CIRCUITS

As the radio-sonde circuits pass pulsating direct current through the electric hygrometer, the characteristics of the unit in such a circuit differ somewhat from those obtained when it is used in a-c circuits. Some polarization exists in d-c circuits, but it is a fixed factor in a given type of circuit and does not change the calibration of the unit appreciably during the period of a flight. The unit appears to have a higher resistance at a given humidity than if measured with alternating current flowing through it, as described under section IV–1.

[4] In this paper 1-, 2-, and 3-percent LiCl units refer to those coated with solutions in the proportion of 1.01, 2.02, and 3.03 ml, respectively, of a saturated solution of LiCl in water at 21° C; to 100 ml of the polyvinyl-acetate–alcohol-water (Solvar) solution. Similarly for other percentages.

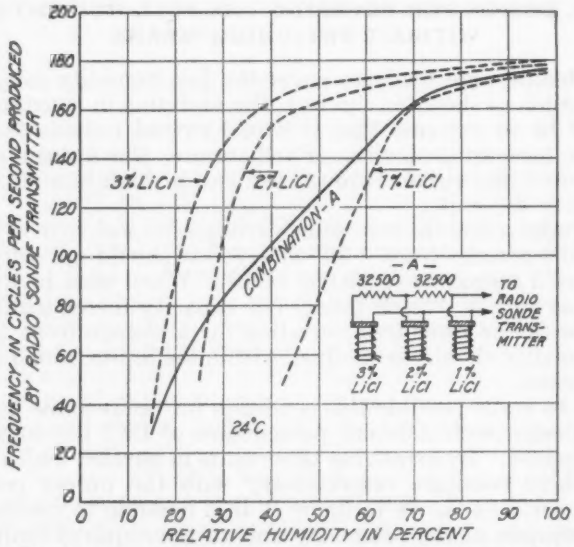

FIGURE 2.—*Circuit arrangement and frequency-humidity characteristics for a three-element electric hygrometer as used in radio sonde.*

Dotted lines show characteristics for individual units. Full line shows characteristic for units connected as shown at *A*.

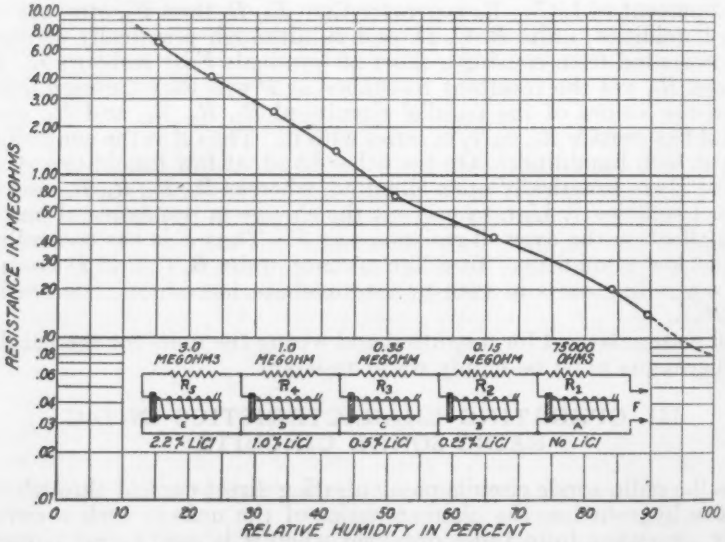

FIGURE 3.—*Five-element electric-hygrometer circuit arrangement with humidity-resistance characteristics (24° C).*

1. THREE-ELEMENT UNIT

For use in the radio-sonde circuit developed for the Navy Department,[5] a three-element unit has been found satisfactory. It consists of three units constructed as outlined under section II–5. Figure 2

[5] See footnote 2, page 703.

shows this circuit arrangement, while figure 5 shows the units mounted on a panel which slides into the sun shield of the radio sonde. The units are coated with a 1-, 2-, and 3-percent lithium-chloride-polyvinyl-acetate solution respectively. The three units are connected in parallel with 32,500 ohms in series with the 2- and 3-percent units.

2. FREQUENCY-HUMIDITY CHARACTERISTIC

In the radio-sonde circuit the variation in resistance of the electric hygrometer alters the audio frequency generated by a special audio oscillator which in turn modulates the carrier-frequency oscillator.

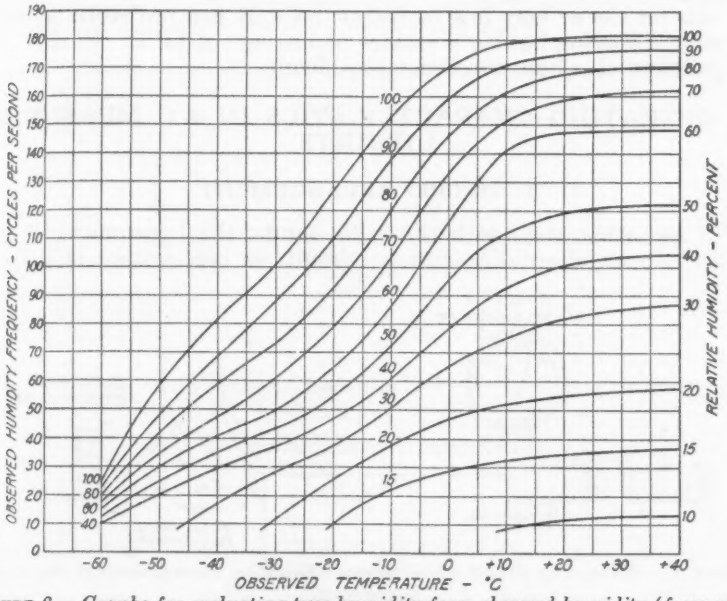

FIGURE 6.—*Graphs for evaluating true humidity from observed humidity (frequency) and temperature.*

This audio note is received on the ground, where it is recorded on a graphical frequency recorder. This record may be interpreted in terms of humidity. In figure 2 are shown in dotted lines the humidity-frequency calibration graphs at 24° C for the individual 1-, 2-, and 3-percent LiCl units when used separately in the radio-sonde circuit. The full-line graph in this figure is for the composite arrangement of the three units at 24° C connected as shown at *A*.

3. TEMPERATURE CORRECTION

The electric hygrometer functions like an electrolyte in that its resistance increases with a decrease in temperature. In radio-sonde use where temperature variations of 100° C are encountered, it is of course necessary to apply a correction to obtain the true humidity. It has not been found possible, even with a composite three-element unit, to cover the full 10- to 100-percent humidity scale, over this extreme temperature range; but it has been feasible, with the composite unit shown in figures 2 and 5 to cover a considerable portion of this range. The family of graphs determined empirically for dif-

ferent temperatures, shown in Figure 6, constitute the standard. These are based on the average of many composite units taken at various low temperatures and having individual units with characteristics at 24° C., as shown in figure 2. Knowing the temperature (as is the case with a radio sonde), the humidity is obtained from the frequency-humidity graph for that temperature.

If the method previously outlined for making and coating the units is carefully followed, it is possible to obtain about 75 percent of the units which will fall within ±3 percent of the standard graph.

For use at varying temperatures other than with the radio sonde, a multiscale indicating instrument may be used—see section V-3.

Units for use at very low temperatures only can probably be made by using a coating having a greater percentage of LiCl. In this case the problem of calibration becomes difficult.

IV. OPERATING CHARACTERISTICS IN A-C MEASURING CIRCUITS

1. CIRCUIT ARRANGEMENT

For use other than with the radio sonde, the hygrometer should be used in an alternating-current circuit, as polarization is thereby

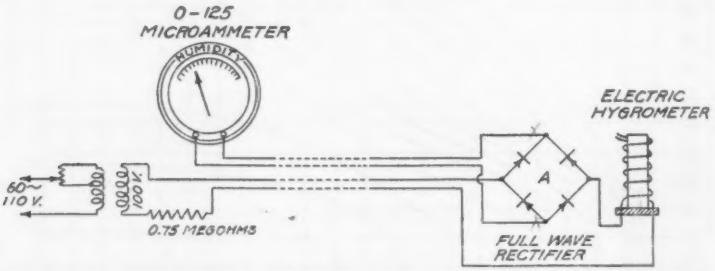

FIGURE 7.—*Measuring circuit which passes alternating current through the electric hygrometer.*

eliminated. For the radio sonde this is not a serious factor, as it does not alter the operation of the hygrometer sufficiently to change the calibration during the period of time (1 hour maximum) in which the unit is used. An a-c circuit arrangement is shown in figure 7. Here the unit is put across about a 100-volt 60-cycle alternating current with 0.75 megohm and the input of a full-wave copper-oxide rectifier in series with it. The d-c output of the rectifier is connected to a microammeter having a scale division of 0 to 125. The microammeter scale may be calibrated in terms of percentage of relative humidity. The voltage impressed on this circuit arrangement should, of course, be kept at 100. The above circuit arrangement is that obtained when using the $C/1{,}000$ scale of a Weston model 764 capacity meter, the electric hygrometer taking the place of the condenser to be measured. This capacity meter may be used as an ohmmeter in this fashion, since it is measuring only ohmic resistance in a nonreactive circuit. This circuit arrangement was adopted because it passes alternating current through the unit, and this current is never greater than 200 microamperes. The current must be kept under this value, as heavy currents would alter the calibration. Information as to the

constancy of calibration of a unit if the current is allowed to flow through it continuously is not yet available, although a current of 100 microamperes flowing through a unit steadily for several days seemed to have little effect. It is safer, until further data are available, to read humidity by allowing current to flow through the unit only for the time necessary to take a reading, or for control purposes a timing switch could connect the unit into circuit only for a time long enough to affect the control mechanism. If this is not feasible, the hygrometer unit could be left in the control circuit continually by placing it in the input circuit of a suitable electron-tube amplifier with the indicating or control device in the output circuit. In such a circuit the current through the unit would be kept within safe limits.

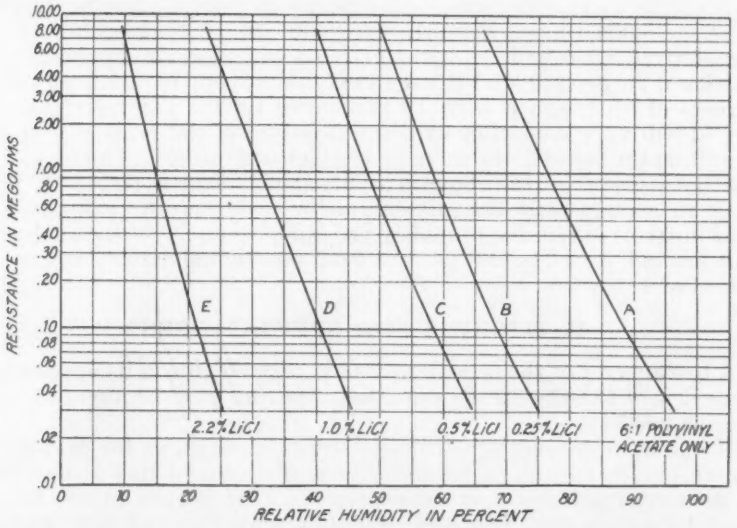

FIGURE 8.—*Humidity-resistance graphs for five individual units (at 24° C) coated as shown and used in the circuit of figure 7 or 10.*

The capacity between the two wires running to the humidity unit should be kept as small as possible by separating them. If appreciable, a circuit arrangement described under section V–1 should be used.

2. HUMIDITY-RESISTANCE CHARACTERISTICS

(a) SINGLE-UNIT CHARACTERISTICS

Using such a circuit arrangement with the capacity meter calibrated to read in ohms instead of microfarads, the humidity-resistance characteristics shown in figure 8 were obtained. Here graphs *B* to *E* are for standard units with a 0.25-, 0.5-, 1-, and 2.2-percent LiCl coating, respectively. Graph *A* is that obtained with the polyvinyl-acetate film alone, without LiCl.

The coatings on these units were so chosen that each unit covers a different range of humidity when varying over the same resistance. Thus, considering a resistance variation from 8 megohms to 75,000 ohms, unit *E* covers from 10 to 22 percent, unit *D* 22 to 42 percent, unit *C* 40 to 60 percent, unit *B* 50 to 70 percent, unit *A* 66 to 91 per-

cent. A percentage of LiCl for B to give less overlap might be 0.10 percent. In this case A might be coated with a somewhat diluted polyvinyl-acetate solution, which should cause the unit to register up to 100 percent.

(b) COMPOSITE-UNIT ARRANGEMENT

While individual units as described above should find some applications (see section V, Design for Special Uses), it is evident from figure 8 that no one unit will cover the full humidity scale. However, by putting the units A to E (fig. 8) in parallel each with its proper series resistor, as shown in figure 3, it is possible to obtain in effect a single unit which covers the humidity range from 10 to 100 percent at room temperatures, with resistance variation confined within the limits of 8 megohms to 75,000 ohms. A satisfactory combination for figure 3 is: R_1=75,000 ohms, R_2=0.15 megohm, R_3=0.35 megohm, R_4=1 megohm, R_5=3 megohms, with A coated with polyvinyl acetate only, B with 0.25 percent of LiCl, C with 0.5 percent of LiCl, D with 1 percent of LiCl, and E with 2.2 percent of LiCl. The resistances required will vary somewhat with the variation in the range of response of different units with the same percentage of coating. The humidity-resistance graph for the above combination is shown in figure 3. With such an arrangement the microammeter scale may be calibrated to read in terms of relative humidity instead of ohms. Such a composite unit has not varied over 3 percent from an original calibration, over a period of 4 months.

V. DESIGNS FOR SPECIAL USES

A hygrometer of the type described is very flexible in its application, since it is of the electrically operated type and may be modified to fit specific needs.

If one is interested in a limited humidity range, as for example in the automatic control of humidity, a single-element unit is desirable, as greater sensitivity may be obtained. (See graphs in fig. 8.) It must be emphasized, however, that information is not yet available as to the life of a unit when the control current is allowed to flow through it continually. An electron-tube amplifier may be used, as described under section IV–1. Replacement units are inexpensive and may be easily plugged into circuit after a given number of hours.

1. DESIGN FOR USE WHERE A-C POWER IS AVAILABLE

Where it is necessary to run long lines from the humidity-indicating device to the humidity unit, it is necessary to locate the full-wave oxide rectifier, A, as shown in figure 7, at the location of the humidity unit and run the d-c output of the rectifier back to the location where the humidity is to be registered. This method is necessary, as the alternating current flowing across the capacity of a long line to the humidity unit would register on the indicating meter.

2. BATTERY-OPERATED UNIT

For portable use and in places remote from a 60-cycle a-c supply a measuring circuit may be used in which the alternating current for operating the unit is obtained from an electron-tube oscillator operating at 60 cycles. It may be powered from small dry cells such as are used in portable radio sets.

3. MULTISCALE UNIT FOR CONDITIONS OF WIDE TEMPERATURE VARIATIONS

For registering humidity under a condition of wide variation in temperature, a multiscale indicator such as shown in figure 9 might be used. Knowing the temperature, the humidity scale for that temperature is used.

A second type of multiscale arrangement for use at room temperatures is shown in figure 10. Here individual units with different sensitivities are connected to the measuring instrument (Weston

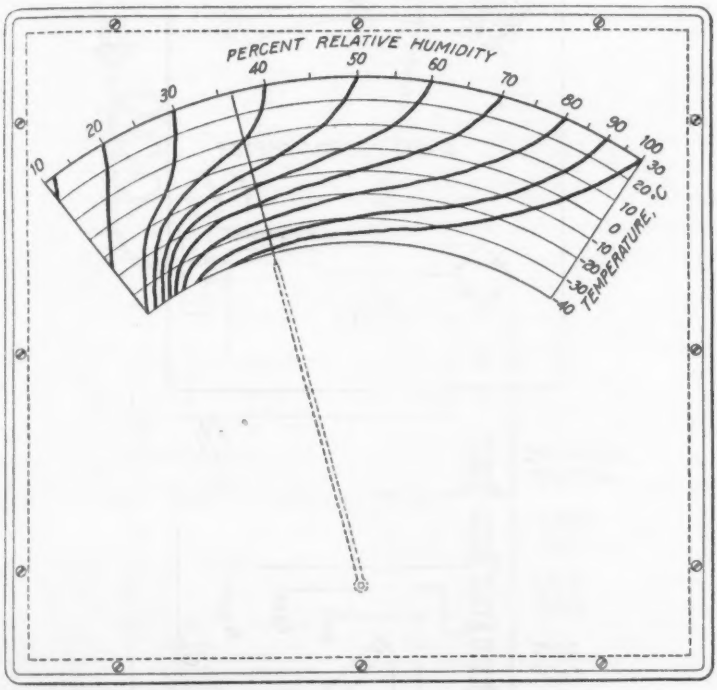

FIGURE 9.—*Proposed scale arrangement for temperature correction.*

model 764 capacity meter set at minimum capacity setting) by means of a five-point switch. Depending upon the humidity, the particular unit may be selected which brings the meter reading within the scale. Thus if the humidity is between 10 and 20 percent, switch contact 1 and scale 1 will be used. This arrangement has the advantage of very open scale, allowing greater precision in humidity readings.

The author expresses his appreciation to Harry Diamond for many helpful suggestions during the progress of this work, to L. L. Hughes for his skillful construction and development of methods of winding the hygrometer units, to W. S. Hinman, Jr., for low-temperature calibrations, to D. N. Craig, of the Electrochemistry Section, for

information and suggestions relative to polarization actions, and to T. P. Sager and E. Wichers, of the Chemistry Division, for information on hygroscopic film-forming materials.

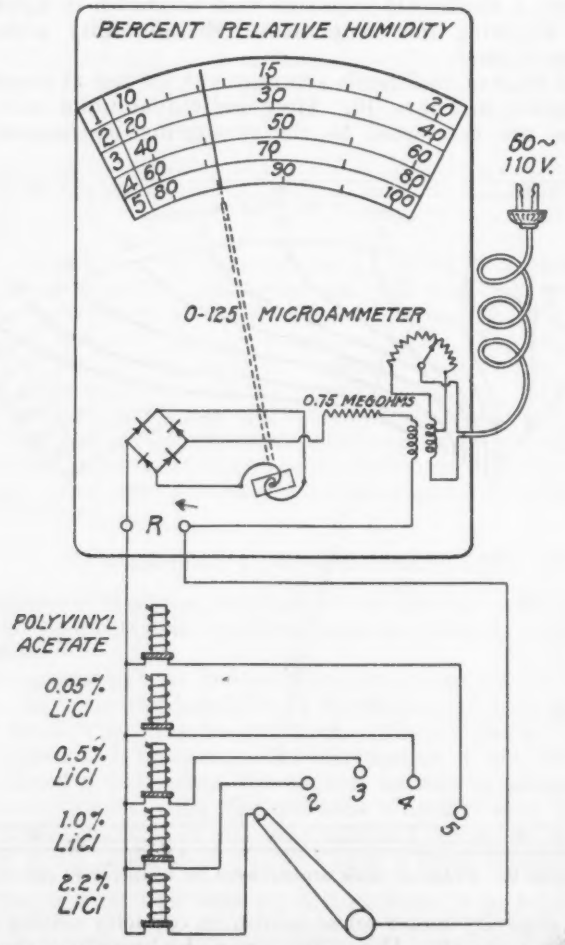

FIGURE 10.—*Multiscale arrangement for use at room temperatures, using five electric-hygrometer units each covering a different humidity range.*

Special acknowledgment is made to R. S. Doyle, of Julien P. Friez and Sons, who, as research associate assigned to the Radio Section of this Bureau for this work, has been of invaluable assistance.

WASHINGTON, October 9, 1939.

INDEX TO VOLUME 23

A

Page

Abrasion of rubber, relation to tensile properties, RP1256 ... 603
Absorption of gamma rays in radium-beryllium neutron sources, RP1257 ... 617
Accelerated aging of paper, RP1241 ... 405
Acree, S. F., Elizabeth E. Hughes and, Quantitative formation of furfural and methylfurfural from pentoses and methylpentoses, RP1233 ... 293
—, *Myron A. Elliott and,* Polar structure of some benzein indicators, RP1263 ... 675
—, *Walter J. Hamer and,* Pentiometric method for the accurate measurement of hydrogen-ion activity, RP1261 ... 647
Adiabatic tensile properties of rubber, RP1256 ... 603
Aggregates, concrete, effect on wear, RP1252 ... 549
Aging, paper, normal and accelerated, RP1241 ... 405
Aircraft, electric hygrometer for, RP1265 ... 701
Air, humidity measurements at high altitudes, RP1265 ... 701
Airplane electric systems, optimum voltage, RP1247 ... 485
Air-setting refractory-bonding mortars of the wet type, RP1219 ... 7
Airship girders, determination of cross-sectional areas, RP1258 ... 621
Alloys, iron-carbon, transformation of austenite on quenching, RP1225 ... 151
Alloys, soil-corrosion, RP1250 ... 515
Alumina crucibles, slip-casting, WP1236 ... 319
Aluminum ion and hydrogen ion, retention in papers, RP1262 ... 663
Analysis of high-purity iron, RP1226 ... 163
Arabinose, formation of furfural from, RP1233 ... 293
Area, cross-sectional, determination, RP1258 ... 621
Astin, Allen V., Leroy L. Stockman, Burrell W. Brown, Leon F. Curtiss and, Cosmic-ray observations in the stratosphere with high-speed counters, RP1254 ... 585
Atmosphere, electric hygrometer for measuring humidity, RP1265 ... 701
Austenite, transformation on quenching iron-carbon alloys, RP1225 ... 151

B

Beek, John Jr., and Arnold M. Sookne, Electrophoresis of collagen, RP1230 ... 271
Bekkedahl, Norman, Chauncey G. Peters, Lawrence A. Wood and, Application of the interferometer to the measurement of dimensional changes in rubber, RP1253 ... 571
Bennett, Erert G., Raymond L. Sanford and, An apparatus for magnetic testing at magnetizing forces up to 5,000 oersteds, RP1242 ... 415
Beryllia crucibles, slip-casting of, RP1236 ... 319
Beryllium-radium neutron sources, internal absorption of gamma rays, RP1257 ... 617
Bishop, Dana L., Particle size and plasticity of lime, RP1232 ... 285
Boron oxide, lead oxide, silica phase equilibria, RP1231 ... 275
Brass, soil corrosion, RP1250 ... 515
Brenner, Abner, Dropping tests for measuring the thickness of zinc and cadmium coatings on steel, RP1240 ... 387
Bright, H. A., Determination of carbon, sulfur, phosphorus, and copper, RP1226 (appendix) ... 175
Brooks, Donald B., Frank L. Howard, and Hugh C. Crafton, Jr., Physical properties of purified 2,2,3-trimethylpentane, RP1259 ... 637
Brown, Burrell W., Allen V. Astin, Leroy L. Stockman, Leon F. Curtiss and, Cosmic-ray observations in the stratosphere with high-speed counters, RP1254 ... 585
Bunting, E. N., R. F. Geller and, The system PbO-B_2O_3-SiO_2, RP1231 ... 275
—, *Howard F. McMurdie and,* X-ray studies of compounds in the system PbO-SiO_2, RP1251 ... 543

C

Page

Cadmium coatings, measurement of thickness, RP1240 ... 387
Calorimeter for specific and latent heats, RP1228 ... 197
Calorimetry of ice, RP1260 ... 643
Cast iron, soil corrosion, RP1250 ... 515
Cement-asbestos pipe, soil corrosion, RP1250 ... 515
Cement mortars, air-setting refractory-bonding of the wet type, RP1219 ... 7
Cements, effect on wear resistance, RP1252 ... 549
Charts, contour, of stresses in rigid frame, RP1224 ... 145
Chemicals and drugs, color names, RP1239 ... 355
Chlorine spectrum and its structure, RP1244 ... 443
Clark, George L., Siegfried T. Gross, and W. Harold Smith, X-ray diffraction patterns of Hevea, Manihot, and other rubbers, RP1218 ... 1
Clay, length changes and endothermic and exothermic effects during heating, RP1243 ... 427
Cleaves, Harold E., John G. Thompson and, Preparation of high-purity iron, RP1226 ... 163
Coatings on steel, measurement of thickness, RP1240 ... 387
Collagen, electrophoresis and isoelectric point, RP1230 ... 271
Color-Council system of color designations, RP1239 ... 355
Color designations, RP1239 ... 355
Colors, interference, of oxide films, rate of oxidation of steels as determined from, RP1221 ... 63
Concrete floors, wear resistance, RP1252 ... 549
Contraction of clays during heating, RP1243 ... 427
Copper, soil corrosion, RP1250 ... 515
Corrosion-resistant materials, RP1250 ... 515
Cosmic rays in the stratosphere, RP1254 ... 585
Crafton, Hugh C., Jr., Frank L. Howard, Donald B. Brooks and, Physical properties of purified 2,2,3-trimethylpentane, RP1259 ... 637
Cross-sectional areas, determination by volumetric methods, RP1258 ... 621
Crucibles, slip-casting from special refractories, RP1236 ... 319
Curtiss, Leon F., Allen V. Astin, Leroy L. Stockman, and Burrell W. Brown, Cosmic-ray observations in the stratosphere with high-speed counters, RP1254 ... 585
—, Detection of radioactive contamination, using Geiger-Müller counters, RP1223 ... 137
—, Internal absorption of gamma rays in radium-beryllium neutron sources, RP1257 ... 617
—, Radium exposure meter, RP1246 ... 479
Cystine in wool, photochemical decomposition, RP1255 ... 597

D

De Bruin, T. L., C. C. Kiess and, Second spectrum of chlorine and its structure, RP1244 ... 443
—, *William F. Meggers, Curtis J. Humphreys and,* Zeeman effect in the second and third spectra of xenon, RP1264 ... 683
Debye-Hückel equation for use in hydrogen-ion activity measurements, RP1261 ... 647
Decomposition, photochemical, of cystine in wool, RP1255 ... 597
Definition of pH, RP1261 ... 647
Detector for radioactive contamination, RP1223 ... 137
Deterioration of paper on aging, RP1241 ... 405
Diamond indenter, RP1220 ... 39
Differences, central, RP1235 ... 309
Diffraction patterns of some natural rubbers, RP1218 ... 1
Digges, Thomas G., Transformation of austenite on quenching high-purity iron-carbon alloys, RP1225 ... 151
Dimensional changes in rubber, interferometric measurements, RP1253 ... 571
Dipole moments of pH indicators, RP1263 ... 675
Dispersion of the dielectric constant, RP1263 ... 675

192170—39——6

Page

Distillation columns, reflux regulator and head for, RP1249 509
Distribution of stress in rigid frame, RP1224 145
Dropping test, thickness measurements of zinc and cadmium coatings by, RP1240 387
Drugs and pharmaceuticals, color names, RP1239 355
Dunmore, Francis W., An improved electric hygrometer, RP1265 701
Dusting, concrete floors, RP1252 549

E

Eiseman, John H., Francis A. Smith and, Saturation of gases by laboratory wet test meters, RP1238 345
Elasticity of enamels, effects of humidity and composition, RP1237 329
Electric hygrometer for measuring humidity at high altitudes, RP1265 701
Electric systems for airplanes, optimum voltage, RP1247 485
Electrophoresis and isoelectric point of wool, RP1245 471
Electrophoresis of collagen, RP1230 271
Electrophoresis of fibroin, sericin, and silk, RP1234 299
Electroplated zinc coatings, measurement of thickness, RP1240 387
Elliott, Myron A., and S. F. Acree, Polar structure of some benzein indicators, RP1263 675
Emerson, Walter B., Chauncey G. Peters, Frederick Knoop and, A sensitive pyramidal-diamond tool for indentation measurements, RP1220 39
Enamels, vitreous, effects of humidity and composition, RP1237 329
Equilibria, phase, PbO-B_2O_3-SiO_2, RP1231 275
Expansion measurements by interferometric methods, RP1227 179
Expansion of clays during heating, RP1243 427
Expansivity of rubber, interferometric measurement, RP1253 571
Exposure meter for radium, RP1246 479

F

Ferrous alloys, soil corrosion, RP1250 515
Fiber-water mixtures, pH changes in heating, RP1262 663
Fibroin, electrophoresis, RP1234 299
Films, oxide, on steels, use in determining rate of oxidation from interference colors, RP1221 63
Floors, concrete, wear tests, RP1252 549
Frame, rigid, stresses, RP1224 145
Frits, enamel, effects of humidity and composition, RP1237 329
Function, approximation to, from a set of mean values, and instantaneous value of, RP1235 309
Furfural, formation from pentoses, RP1233 293

G

Galvanic cell without liquid junction for pH measurements, RP1261 647
Gamma rays in radium-beryllium neutron sources, internal absorption, RP1257 617
Gas, laboratory wet test meters, saturation and tilting errors, RP1238 345
Geiger-Müller counters for cosmic-ray observations in stratosphere, RP1254 585
Geiger-Müller counter for determination of radioactive contamination, RP1223 137
Geil, Glenn W., and Dunlap J. McAdam, Jr., Rate of oxidation of steels as determined from interference colors of oxide films, RP1221 63
Gelatin, isoelectric point, RP1230 271
Geller, R. F., and E. N. Bunting, The system PbO-B_2O_3-SiO_2, RP1231 275
Ginnings, Defoe C., Harold F. Stimson, Nathan S. Osborne and, Measurements of heat capacity and heat of vaporization of water in the range 0° to 100° C, RP1228 197
——, ——, ——, Thermal properties of saturated water and steam, RP1229 261
Girders, aircraft, determination of cross-sectional areas, RP1258 621

Page

Glasgow, Augustus R., Jr., Frederick D. Rossini and, Reflux regulator and head for laboratory rectifying columns, RP1249 509
Glass, expansion, RP1227 179
Grain size of austenite of iron-carbon alloys, RP1225 151
Grant, Vernon H., and Melville F. Peters, Determination of optimum voltage for airplane electric systems, RP1247 485
Greenspan, Martin, Ambrose H. Stang and, Strength of a welded steel rigid frame, RP1224 145
——, Approximation to a function of one variable from a set of its mean values, RP1235 309
Gross, Siegfried T., W. Harold Smith, George L. Clark and, X-ray diffraction patterns of Hevea, Manihot, and other rubbers, RP1218 1

H

Hamer, Walter, J., and S. F. Acree, Potentiometric method for the accurate measurement of hydrogen-ion activity, RP1261 647
Hardenability of iron-carbon alloys, RP1225 151
Hardeners, concrete, tests, RP1252 549
Hardness measurements, RP1220 39
Harris, Milton, Arnold M. Sookne and, Electrophoretic studies of silk, RP1234 299
——, ——, Electrophoretic studies of wool, RP1245 471
——, *Henry A. Rutherford and*, Photochemical decomposition of the cystine in wool, RP1255 597
Harrison, William N., Dwight G. Moore and, Effects of humidity and composition on strength and Young's modulus of enamels, RP1237 329
Head for laboratory rectifying columns, RP1249 509
Heat effects on flint and aluminous clays, RP1243 427
Heat of fusion of ice, RP1260 643
Heindl, Raymond A., and Lewis E. Mong, Length changes and endothermic and exothermic effects during heating of flint and aluminous clays, RP1243 427
——, *and William L. Pendergast*, Properties of air-setting refractory-bonding mortars of the wet type, RP1219 7
Hevea rubber, X-ray diffraction patterns, RP1218 1
High-H permeameter for magnetic testing, RP1242 415
High-speed counters for cosmic-ray observations in the stratosphere, RP1254 585
Hoffman, James I., and G. E. F. Lundell, Separation and colorimetric determination of rhenium and molybdenum, RP1248 497
Holm, Vernon C. F., Determination of oxygen, nitrogen, and hydrogen, RP1226 (appendix) 176
Holt, William L., Frank L. Roth and, Tensile properties of rubber compounds at high rates of stretch, RP1256 603
Hot-dipped zinc coatings, measurement of thickness, RP1240 387
Howard, Frank L., Hugh C., Crafton, Jr., Donald B. Brooks and, Physical properties of purified 2,2,3-trimethylpentane, RP1259 637
Hughes, Elizabeth E., and S. F. Acree, Quantitative formation of furfural and methylfurfural from pentoses and methylpentoses, RP1233 293
Humidity, effect on strength and elasticity of enamels, RP1237 329
Humidity measurements in troposphere, RP1265 701
Humphreys, Curtis J., William F. Meggers, and T. L. deBruin, Zeeman effect in the second and third spectrum of xenon, RP1264 683
——, Pressure displacements in the second spectrum of iron, RP1222 125
Hydrated lime, particle size and plasticity, RP1232 285
Hydrocarbons, paraffin, physical properties of purified, RP1259 637
Hydrogen electrode, preparation and behavior, RP1261 647
Hydrogen-ion activity, potentiometric method for measuring, RP1261 647
Hydrogen ion and aluminum ion, retention in papers, RP1262 663
Hydrogen sulfide, evolution from irradiated wool, RP1255 597

Page

Hygrometer for use in measuring humidity at high altitudes, RP1265 ... 701

I

Ice, heat of fusion, RP1260 ... 643
Indentation tool, RP1220 ... 39
Indicators, pH, polar structure, RP1263 ... 675
Intensity of cosmic rays in the stratosphere, RP1254 ... 585
Interference colors of oxide films, use in determining rate of oxidation of steels, RP1221 ... 63
Interferometric measurement of dimensional changes in rubber, RP1253 ... 571
Interferometric methods and expansion measurements, RP1227 ... 179
Internal absorption of gamma rays in radium-beryllium neutron sources, RP1257 ... 617
Inter-Society Color Council system of color designations, RP1239 ... 355
Ionization potential of Cl^+, RP1244 ... 443
Ionized xenon, Zeeman effects in spectra, RP1264 ... 683
Iron-carbon alloys, hardenability and transformation of austenite on quenching, RP1225 ... 151
Iron, cast, soil corrosion, RP1250 ... 515
Iron, high-purity, preparation, RP1226 ... 163
Iron spectra, pressure displacements, RP1222 ... 125
Isoelectric point of collagen, RP1230 ... 271
Isoelectric point of fibroin, sericin, and silk, RP1234 ... 299

J

Jet test, thickness measurements of zinc and cadmium coatings by, RP1240 ... 387
Judd, Deane B., and Kenneth L. Kelly, Method of designating colors, RP1239 ... 355

K

Kelly, Kenneth L., Deane B. Judd and, Method of designating colors, RP1239 ... 355
Kiess, C. C., and T. L. deBruin, Second spectrum of chlorine and its structure, RP1244 ... 443
Knoop, Frederick, Chauncey G. Peters, and Walter B. Emerson, A sensitive pyramidal-diamond tool for indentation measurements, RP1220 ... 39

L

Launer, Herbert F., Retention of aluminum ion and hydrogen ion in paper, RP1262 ... 663
Lead oxide, borosilicate phase equilibria, RP1231 ... 275
Lead silicates, X-ray studies, RP1251 ... 543
Lime, particle size and distribution, RP1232 ... 285
Logan, Kirk H., Soil-corrosion studies, 1937. Corrosion-resistant materials and special tests, RP1250 ... 515
Lundell, G. E. F., James I. Hoffman and, Separation and colorimetric determination of rhenium and molybdenum, RP1248 ... 497

M

McAdam, Dunlap J., Jr., and Glenn W. Geil, Rate of oxidation of steels as determined from interference colors of oxide films, RP1221 ... 63
McMurdie, Howard F., and Elmer N. Bunting, X-ray studies of compounds in the system $PbO–SiO_2$, RP1251 ... 543
Magnesia crucibles, slip-casting of, RP1236 ... 319
Magnetic methods for measuring thickness of zinc and cadmium coatings, RP1240 ... 387
Magnetic testing apparatus, RP1242 ... 415
Mallett, Manley W., John G. Thompson and, Preparation of crucibles from special refractories by slip-casting, RP1236 ... 319
Manihot, Hevea, and other rubbers, X-ray diffraction patterns, RP1218 ... 1
Mechanical equivalent of heat, RP1228 ... 197
Meggers, William F., T. L. deBruin, Curtis J. Humphreys and, Zeeman effect in the second and third spectrum of xenon, RP1264 ... 683
Meteorography, use of electric hygrometer, RP1265 ... 701
Meter for radium exposure measurements, RP1246 ... 479

Page

Meters, gas, laboratory wet test, saturation and tilting errors, RP1238 ... 345
Methods of analysis of high-purity iron, RP1226 ... 163
Methylfurfural, formation from methylpentoses, RP1233 ... 293
Methylpentoses, formation of methylfurfural from, RP1233 ... 293
Microhardness of transformation products of austenite of iron-carbon alloys, RP1225 ... 151
Microscopic method for measuring thickness of zinc and cadmium coatings, RP1240 ... 387
Miller, James A., Determination of cross-sectional areas of structural members, RP1258 ... 621
Modulus of rupture and elasticity of enamels, RP1237 ... 329
Moisture measurements at high altitudes, RP1265 ... 701
Molecular structure of pH indicators, RP1263 ... 675
Molybdenum, separation from rhenium, RP1248 ... 497
Mong, Lewis E., Raymond A. Heindl and, Length changes and endothermic and exothermic effects during heating of flint and aluminous clays, RP1243 ... 427
Moore, Dwight G., and William N. Harrison, Effects of humidity and composition on strength and Young's modulus of enamels, RP1237 ... 329
Mortars of the wet type, air-setting refractory-bonding, RP1219 ... 7
Mortars, wear tests, RP1252 ... 549

N

α-Naphtholbenzein, polar structure, RP1263 ... 675
Neutron sources, radium-beryllium, absorption of gamma rays in, RP1257 ... 617
Noble gases, spectra, RP1264 ... 683

O

Osborne, Nathan S., Harold F. Stimson, and Defoe C. Ginnings, Measurements of heat capacity and heat of vaporization of water in the range 0° to 100° C, RP1228 ... 197
——, ——, ——, Thermal properties of saturated water and steam, RP1229 ... 261
——, Heat of fusion of ice, RP1260 ... 643
Oxidation of steels, determination from interference colors, RP1221 ... 63

P

Paper, deterioration on aging, RP1241 ... 405
Paper, fiber-water mixtures, pH changes in heating, RP1262 ... 663
Paper, normal and accelerated aging, RP1241 ... 405
Papers, aluminum ion and hydrogen ion retention, RP1262 ... 663
Paraffin hydrocarbons, physical properties of purified, RP1259 ... 637
Particle size and plasticity of lime, RP1232 ... 285
Pendergast, William L., Raymond A. Heindl and, Properties of air-setting refractory-bonding mortars of the wet type, RP1219 ... 7
Pentoses, formation of furfural from, RP1233 ... 293
Permeameter, high-H, for magnetic testing, RP1242 ... 415
Peters, Chauncey G., Walter B. Emerson, Frederick Knoop and, A sensitive pyramidal-diamond tool for indentation measurements, RP1220 ... 39
——, *Norman Bekkedahl, Lawrence A. Wood and*, Application of the interferometer to the measurement of dimensional changes in rubber, RP1253 ... 571
Peters, Melville F., Vernon H. Grant and, Determination of optimum voltage for airplane electric systems, RP1247 ... 485
Pharmaceuticals and drugs, color names, RP1239 ... 355
Phase equilibria $PbO–B_2O_3–SiO_2$, RP1231 ... 275
pH changes when heating paper-water mixtures, RP1262 ... 663
Phenol blue, polar structure, RP1263 ... 675
Photochemical decomposition of cystine in wool, RP1255 ... 597
Plasticity of lime, RP1232 ... 285
Polarization, electronic, atomic, and orientation, RP1263 ... 675

Page

Porcelain enamels, effects of humidity and composition, RP1237 ... 329
Potentiometric method for hydrogen-ion activity, RP1261 ... 647
Potentiometric pH method, RP1261 ... 647
Preparation of high-purity iron, RP1226 ... 163
Pressure effect in iron spectra, RP1222 ... 125
Protective coatings, nonbituminous, for underground use, RP1250 ... 515
Pyramidal-diamond indenter, RP1220 ... 39

Q

Quicklime, particle size and plasticity, RP1232 ... 285
Quinone-phenolate theory of color in pH indicators, RP1263 ... 675

R

Radioactive contamination detector, RP1223 ... 137
Radio meteorograph, electric hygrometer for use with, RP1265 ... 701
Radio recording of cosmic rays in the stratosphere, RP1254 ... 585
Radio sonde, electric hygrometer for use with, RP1265 ... 701
Radium-beryllium neutron sources, internal absorption of gamma rays in, RP1257 ... 617
Radium, detector for determination of contamination, RP1223 ... 137
Radium exposure meter, RP1246 ... 479
Recorder, electric hygrometer for use with, RP1265 ... 701
Record papers, aging, RP1241 ... 405
Rectifying columns, reflux regulator and head for, RP1249 ... 509
Reflux regulator for laboratory rectifying columns, RP1249 ... 509
Refractories, special, slip-casting of crucibles from, RP1236 ... 319
Refractory-bonding mortars of the wet-type, air-setting, RP1219 ... 7
Rhamnose, formation of methylfurfural from, RP1233 ... 293
Rhenium, colorimetric determination, separation from molybdenum, RP1248 ... 497
Rigid frame, stresses, RP1224 ... 145
Rossini, Frederick D., and Augustus R. Glasgow, Jr., Reflux regulator and head for laboratory rectifying columns, RP1249 ... 509
Roth, Frank L., and William L. Holt, Tensile properties of rubber compounds at high rates of stretch, RP1256 ... 603
Rubber, adiabatic tensile properties, RP1256 ... 603
Rubber, interferometric measurement of dimension changes, RP1253 ... 571
Rubber X-ray diffraction patterns, RP1218 ... 1
Rutherford, Henry A., and Milton Harris, Photochemical decomposition of the cystine in wool, RP1255 ... 597

S

Sanford, Raymond L., and Evert G. Bennett, An apparatus for magnetic testing at magnetizing forces up to 5,000 oersteds, RP1242 ... 415
Saunders, James B., Improved interferometric procedure with application to expansion measurements, RP1227 ... 179
Schuman, Louis, and John Tucker, Jr., A portable apparatus for determining the relative wear resistance of concrete floors, RP1252 ... 549
Scribner, B. W., Comparison of accelerated aging of record papers with normal aging for 8 years, RP1241 ... 405
Scribner, Bourdon F., Spectrochemical analysis [of high-purity iron], RP1226 (appendix) ... 174
Second spectrum of iron, RP1222 ... 125
Sedimentation of lime, rate of, RP1232 ... 285
Sericin, electrophoresis and isoelectric point, RP1234 ... 299
Series of Cl II, RP1244 ... 443
Sheridized zinc coatings, measurement of thickness, RP1240 ... 387
Silica, lead borate phase equilibria, RP1231 ... 275
Silicates of lead, X-ray studies, RP1251 ... 543
Silk, degumming, electrophoresis and isoelectric point, RP1234 ... 299

Page

Silver-silver chloride electrodes, preparation and behavior, RP1261 ... 647
Slip-casting process for preparation of crucibles, RP1236 ... 319
Smith, Francis A., and John H. Eiseman, Saturation of gases by laboratory wet test meters, RP1238 ... 345
Smith, W. Harold, Siegfried T. Gross, George L. Clark and, X-ray diffraction patterns of Hevea, Manihot, and other rubbers, RP1218 ... 1
Soil corrosion of metals, alloys, and protective coatings, RP1250 ... 515
Sookne, Arnold M., and John Beck, Jr., Electrophoresis of collagen, RP1230 ... 271
——, *and Milton Harris*, electrophoretic studies of silk, RP1234 ... 299
——, ——, Electrophoretic studies of wool, RP1245 ... 471
Specific surface of lime, RP1232 ... 285
Spectra of ionized xenon, RP1264 ... 683
Spectrum of ionized iron, RP1222 ... 125
Stang, Ambrose H., and Martin Greenspan, Strength of a welded steel rigid frame, RP1224 ... 145
Steam tables, values for use in RP1228 ... 197; RP1229 ... 261
Steel frame, stresses in, RP1224 ... 145
Steel, measurement of zinc and cadmium thicknesses, RP1240 ... 387
Steel, rate of oxidation as determined by interference colors, RP1221 ... 63
Steel, soil corrosion, RP1250 ... 515
Stimson, Harold F., Defoe C. Ginnings, Nathan S. Osborne and, Measurements of heat capacity and heat of vaporization of water in the range 0° to 100° C, RP1228 ... 197
——, ——, ——, Thermal properties of saturated water and steam, RP1229 ... 261
Stockman, Leroy L., Burrell W. Brown, Allen V. Astin, Leon F. Curtiss and, Cosmic-ray observations in the stratosphere with high-speed counters, RP1254 ... 585
Strain in elastic flat plate, RP1235 ... 309
Strain readings on rigid frame, RP1224 ... 145
Stratosphere, cosmic - ray observations, RP1254 ... 585
Strength of enamels, effects of humidity and composition, RP1237 ... 329
Stress distribution in rigid frame, RP1224 ... 145
Stress in tension members containing a circular hole, RP1235 ... 309
Stress-strain curves for rubber, RP1256 ... 603
Structural members, determination of cross-sectional areas, RP1258 ... 621
System PbO–SiO_2, X-ray studies of compounds in, RP1251 ... 543

T

Tensile properties of rubber, RP1256 ... 603
Terms of Cl II, RP1244 ... 443
Thermal expansion measurements by interference methods, RP1227 ... 179
Thermal expansivity of rubber at low temperatures, RP1253 ... 571
Thermal regulator for use at various temperatures, RP1261 ... 647
Thermodynamic properties of water 0° to 100° C, RP1228 ... 197; 0° to 374° C, RP1229 ... 261
Thickness measurements of zinc and cadmium coatings, RP1240 ... 387
Thin-walled sections, determination of cross-sectional areas, RP1258 ... 621
Thompson, John G., and Manley W. Mallett, Preparation of crucibles from special refractories by slip-casting, RP1236 ... 319
——, *and Harold E. Cleaves*, Preparation of high-purity iron, RP1226 ... 163
Thoria, electrically fused, slip-casting of, RP1236 ... 319
Thymolbenzein, pollar structure, RP1263 ... 675
Transitions in rubber, interferometric measurement, RP1253 ... 571
2,2,3-Trimethylpentane, physical properties of purified, RP1259 ... 701
Troposphere, humidity measurements, RP1265 ... 637
Tucker, John, Jr., Louis Schuman and, A portable apparatus for determining the relative wear resistance of concrete floors, RP1252 ... 549

U

Page

Underground corrosion, RP1250 515

V

Vitreous enamels, effects of humidity and composition, RP1237 329
Voltage, optimum, for airplanes, RP1247 485
Volumetric method for cross-sectional area determinations, RP1258 621

W

Water, heat of fusion, RP1260 643
Water, thermodynamic properties { 0° to 100° C RP1228 ... 197; 0° to 374° C RP1229 ... 261
Water-vapor measurements with electric hygrometer, RP1265 701
Water vapor, specific volume, RP1228 197
Wave length changes in ultraviolet lines in second spectrum of iron, RP1222 125
Wave lengths of Cl II, RP1244 443
Wear tests of concrete, RP1252 549
Welded rigid frame, stresses, RP1224 145
Whittemore strain-gage measurements, RP1224 145

Page

Wood, Lawrence A., Norman Bekkedahl, and Chauncey G. Peters, Application of the interferometer to the measurement of dimensional changes in rubber, RP1253 571
Wool, electrophoresis and isoelectric point, RP1245 471
Wool, photochemical decomposition of cystine in, RP1255 597
Wrought iron, soil corrosion, RP1250 515
Wyman resonance apparatus for measurement of dielectric constants, RP1263 675

X

X-ray diffraction patterns of some natural rubbers, RP1218 1
X-ray studies of compounds in the PbO-SiO_2 system, RP1251 543
Xenon, Zeeman effects in spectra, RP1264 683

Z

Zeeman effects in xenon spectra, RP1264 683
Zinc coatings, measurement of thickness, RP1240 387
Zircon, slip-castings, RP1236 319
Zirconia, slip-castings, RP1236 319

○

anal Ol

UNITED STATES DEPARTMENT OF COMMERCE

JAN 22 1940

Journal of Research

of the

National Bureau of Standards

Vol. 23, No. 6 December 1939

CONTENTS

RP	TITLE AND AUTHOR	Page
1259.	Physical properties of purified 2,2,3-trimethylpentane. Donald B. Brooks, Frank L. Howard, and Hugh C. Crafton, Jr. [Price 5c]	637
1260.	Heat of fusion of ice. A revision. Nathan S. Osborne.. [Price 5c]	643
1261.	Potentiometric method for the accurate measurement of hydrogen-ion activity. Walter J. Hamer and S. F. Acree... [Price 5c]	647
1262.	Retention of aluminum ion and hydrogen ion in papers. Herbert F. Launer..... [Price 5c]	663
1263.	Polar structure of some benzein indicators. Myron A. Elliott and S. F. Acree..... [Price 5c]	675
1264.	Zeeman effect in the second and third spectra of xenon. Curtis J. Humphreys, William F. Meggers, and T. L. deBruin. [Price 5c]	683
1265.	An improved electric hygrometer. Francis W. Dunmore. [Price 5c]	701
	Index to volume 23 (July 1939 to December 1939) Research Papers RP1218 to RP1265.....	715

The articles listed may be purchased separately (see cover page II) at the prices stated

A monthly periodical of pure and applied science published by our National Government

Journal of Research

of the

National Bureau of Standards

The July 1939 issue of the Journal of Research of the National Bureau of Standards began the twenty-third semiannual volume of this periodical. Fundamental researches in progress in the Bureau's laboratories are reported in this JOURNAL. If you are interested in new developments in science and technology, you should receive the JOURNAL. If you are not already a subscriber you are invited to send in your subscription.

Technical News Bulletin

This is a monthly publication containing short articles reporting progress of work in the Bureau laboratories, abstracts of papers which appear in the JOURNAL OF RESEARCH, accounts of scientific and technical meetings in which the Bureau has taken part, a list of all publications by members of the staff, and other items within the Bureau's fields. The BULLETIN is designed primarily to give a general and timely review of the activities of the Bureau in brief form. It is a prompt and reliable source of official information. If you have not already subscribed for the BULLETIN, you are invited to do so.

ANNUAL SUBSCRIPTION	Prices	
	United States, Canada, Cuba, Mexico, Newfoundland, Republic of Panama	Other countries
Journal of Research of the National Bureau of Standards:		
12 monthly issues (2 volumes), paper covers	$3.50	$4.50
Bound volume (½ year, 1 volume), blue buckram	3.00	3.50
Technical News Bulletin, 12 monthly issues	.50	.70

Research Papers, reprinted individual articles appearing in the Journal of Research, are available from the Superintendent of Documents shortly after appearance of monthly issue of the JOURNAL.

Address orders only to
Superintendent of Documents, U. S. Government Printing Office,
Washington, D. C.